Characterization and Modelling of Moisture Influence on the Behaviour of Rubberized Fabric Cord

Dissertation

to be awarded the degree

Doctor of Engineering (Dr.-Ing.)

submitted by

M. Sc. Hongying Zhao

from Qingdao, China

approved by the Faculty of Natural and Materials Science

Clausthal University of Technology

Date of oral examination

18.12.2020

Dean

Prof. Dr.-Ing. Karl-Heinz Spitzer

Chairman of Board of Examiners

Prof. Dr. René Wilhelm

Supervising Tutor

Prof. Dr.-Ing. Gerhard Ziegmann

Reviewer

Hon. Prof. Dr. Jorge Lacayo-Pineda

Acknowledgement

My deepest gratitude to Prof. Dr.-Ing. Gerhard Ziegmann, my doctoral supervisor, for his constant guidance and encouragement throughout my work in the last years in the institute. I am very appreciated for having the opportunity to be a scientific co-worker in his group. It is my pleasure to work in a group with family-like atmosphere in Clausthal.

I want to give my thanks to Prof. Dr. Jorge Lacayo-Pineda, my co-supervisor, for his motivation to start my research work in Clausthal and for the help he gives me since the very beginning. Without his help this dissertation would not have been possible.

Thanks to the whole PuK-family, including all the scientific and technical colleagues for your supports on scientific works and daily life. I feel very lucky to be able to work together with all of you.

I also want to say thanks to Thomas Felten, René Krems, Andreas Maibohn, Carole Justine, Manuel Cumbre-Fernandez, Christian Neufeld and other colleagues in the Continental Reifen Deutschland GmbH. for all the concern while helping me with the experiments and for always providing me with the information necessary to comply with all the tasks.

In addition, thanks would like to be given to Prof. Chong Sun and other colleagues from the Key Laboratory of Rubber-plastics, Ministry of Education, Qingdao University of Science and Technology for their support on performing experiments and discussions.

Last but not least, I must express my deep sincere gratitude to my parents for their supports. To my wife Rong Yang for her love, her long-term scarifying for the family and for bringing me my lovely daughter Yahan.

Abstract

Textile cords are important reinforcing materials in rubber technology. They are widely used in rubber products, like tires, transmission and conveyor belts. Due to their microstructure, some textile cords are sensitive to moisture when exposed to it during the product manufacturing process.

In the tyre industry, the textile cords especially the cellulose based cords are well protected before processing. However, it is hard to eliminate the environmental influence on the textile cords. For this reason, it is necessary to have a comprehensive and systematic investigation on this moisture uptake behaviour of textile cords and its influence on their mechanical properties. With this investigation, the influence of moisture on the end product can be reduced by regulating the environment conditions during processing and storage. To achieve the research objectives, different kinds of tyre cords, the rubber matrix and the rubberized textile tyre cords are investigated in this thesis, regarding the following steps:

1. The classical method to determine the moisture content is compared with a new test method. To suit the requirement of the characterization of textile tyre cords, the rubber matrix and the rubberized textile cords, the specific adjustments for the test methods and the corresponding sample preparation are performed.
2. The moisture absorption behaviour of different kinds of tyre cords under different environment conditions is characterized and discussed. The relationship between the environment conditions and the absorbed moisture amount of each cord is investigated. For the rubbers, similar experiments with extended test time are performed to study the influence of different ingredients. The moisture content in rubberized textile cord is determined with special attention to the influence of the open ends. A mathematic model is introduced based on the results of the experiments to predict the moisture uptake behaviour.
3. The influence of absorbed moisture on different mechanical properties is studied. All mechanical tests are performed on both dry samples and samples with different moisture content. The results of moisture absorption are used to build the relationship between environment conditions and the influence on properties. For the rubberized textile cords, the cord-to-rubber adhesion is also investigated with mechanical- and morphological methods.
4. Finally, recommendations are provided based on the research results, so that the tyre industry can reduce the influence of moisture absorbed during storage and processing.

Zusammenfassung

Textilkordeln sind wichtige Verstärkungsmaterialien in Kautschuktechnologie. Ihre Anwendung ist in Gummiprodukten, wie Reifen, Getriebe- und Förderbänder weit verbreitet. Einige Textilkordeln sind aufgrund ihrer Mikrostruktur empfindlich gegenüber Feuchtigkeit, wenn sie während des Produktherstellungsprozesses dieser ausgesetzt werden.

In der Reifenindustrie werden die Textilkordeln, insbesondere die zellulosebasierten Kordeln, vor der Verarbeitung gut geschützt. Die Umwelteinflüsse auf die Textilkordeln lassen sich jedoch nur schwer eliminieren. Aus diesem Grund ist eine umfassende und systematische Untersuchung dieses Feuchteaufnahmeverhaltens von Textilkordeln und dessen Einfluss auf die mechanischen Eigenschaften notwendig. Mit dieser Untersuchung kann der Einfluss der Feuchtigkeit auf das Endprodukt durch Regulierung der Umgebungsbedingungen während der Verarbeitung und Lagerung reduziert werden. Um die Forschungsziele zu erreichen, werden in dieser Arbeit verschiedene Arten von Reifenkordeln, die Gummimatrix und die gummierten textilen Reifenkordeln, hinsichtlich folgender Schritte untersucht:

1. Die klassische Methode zur Bestimmung des Feuchtegehaltes wird mit einer neuen Prüfmethode verglichen. Um den Anforderungen an die Charakterisierung von textilen Reifenkordeln, der Gummimatrix und der gummierten Textilkordeln gerecht zu werden, werden die spezifischen Anpassungen für die Prüfmethoden und die entsprechende Probenvorbereitung vorgenommen.
2. Das Feuchtigkeitsaufnahmeverhalten verschiedener Arten von Reifenkordeln unter unterschiedlichen Umgebungsbedingungen wird charakterisiert und diskutiert. Die Beziehung zwischen den Umgebungsbedingungen und der absorbierten Feuchtigkeitsmenge der einzelnen Kordelarten wird untersucht. Für die Gummis werden ähnliche Experimente mit verlängerter Testzeit durchgeführt, um den Einfluss der verschiedenen Inhaltsstoffe zu untersuchen. Der Feuchtigkeitsgehalt in gummierten Textilkordeln wird mit besonderem Augenmerk auf den Einfluss der offenen Enden bestimmt. Basierend auf den Ergebnissen der Experimente wird ein mathematisches Modell zur Vorhersage des Feuchtigkeitsaufnahmeverhaltens eingeführt.
3. Der Einfluss der absorbierten Feuchtigkeit auf verschiedene mechanische Eigenschaften wird untersucht. Alle mechanischen Untersuchungen werden sowohl an trockenen Proben als auch an Proben mit unterschiedlichem Feuchtigkeitsgehalt durchgeführt. Die Ergebnisse der Feuchtigkeitsaufnahme werden verwendet, um die Beziehung zwischen den Umgebungsbedingungen und dem Einfluss auf die Eigenschaften herzustellen. Für die gummierten Textilkordeln wird auch die Kordel-Gummi-Haftung mit mechanischen und morphologischen Methoden untersucht.

4. Schließlich werden auf der Grundlage der Forschungsergebnisse Empfehlungen gegeben, damit die Reifenindustrie den Einfluss der während der Lagerung und Verarbeitung aufgenommenen Feuchtigkeit reduzieren kann.

Table of Contents

1 Introduction and motivation

1.1 Introduction

Rubber is one of the most versatile materials in technology [1-5]. Nevertheless, the interest on rubber was limited to only a few applications, for example the water proof textiles, because the material becomes soft and tacky under high and brittle at low temperature [6]. This situation lasted until the vulcanisation process was invented by Charles Goodyear in 1844 [7]. Most of the properties of rubber material are enhanced by the vulcanisation in which the crosslinked molecular network is built, so that rubber extended its range to industrial applications [8].

Many rubber types are too weak to be used without reinforcing systems for structural or semi-structural applications. The main principles for reinforcing rubber are either with components containing fillers or fibres in the product assembly phases[9]. The main function of fillers such as carbon black (CB) or silica is to increase the strength and stiffness of rubber materials [10-15]. The fibre-based components can support the rubber product with extra properties to suit the specific purposes.

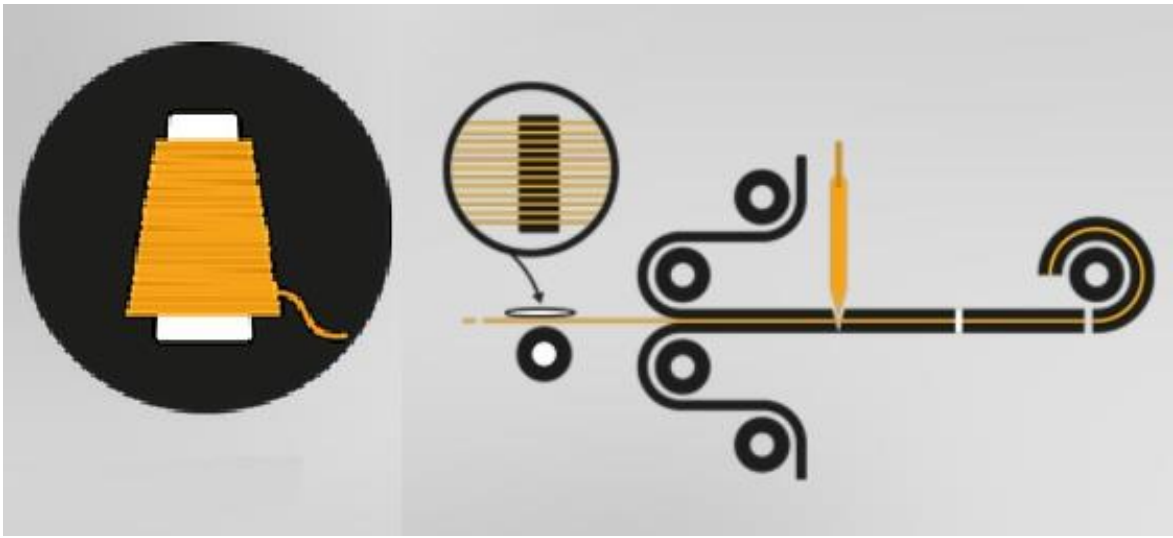

Figure 1.1: Calendering process in tyre manufacturing [16]

Together with the invention of the automobile in the 19th century, the demand of rubber for vehicle tires increased dramatically. Today, rubber is virtually synonymous with pneumatic tyres [17]. To meet the requirements for the usage in automobiles, the tire is reinforced with different types of fibres, used as cord, described as twisted yarns in a continuous shape of cords [18-20]. As shown in Figure 1.1, a multitude of textile tyre cords are fed into the

calender and embedded there between two thin layers of rubber. This continuous sheet is then cut perpendicularly to the travel direction to the desired width and rewound for further processing [16].

The reinforcement of tyre cords is aimed at helping the tire to retain its shape and to support the vehicle weight. Textile cords are used to reinforce tyres since the 1920's. Compared to steel cords, textile cords or a mixture of textile and steel cords have their advantages of having light-weight characteristics and environmentally friendly, and therefore, occupy an important position in tyre reinforcing materials.

The global textile market size for the tire cords was valued at USD 5.5 billion or 2115 Kilotons in 2019. It is expected to grow with a compound annual growth rate (CAGR) of 3.4% from 2020 to 2027. Polyamide tire cord is the largest segment in the global market with a 56.3% revenue share. The growing demand for passenger cars in the developing economies boosts the demand of textile cords. From the perspective of application, round 64% of the market is dominated by the replacement tyre application. The commercial replacement tyres are one of the major factors since they can suit the demand of the vehicles such as trucks and buses carry heavy loads over a long distance. The cord of commercial replacement tyres are generally made of polyamide [21].

The Asia Pacific region is the largest market for textile tyre cords in 2019 with a market share of 47%. It has the largest tyre production in terms of volume at the same time. The main reason is the local availability of major raw materials such as nature rubber, the improving production capabilities as well as the dramatic increasing demand in of vehicles in the Asian area in de past decade. Brazil is expected to be the next region with high expansion speed because of the growing demand of fuel-efficient cars and the increasing of mining and logging activities. Besides, North America and Europe are also the major regions of tyre demands where the countries have more intensive focus on CO_2 emissions [21].

The textile cords are also applied on further rubber applications such as conveyor belts and air springs. However, textile cords especially the cords made of natural fibre or cellulose based fibre are known as moisture sensitive product [22, 23]. Some polymer fibres might absorb moisture from the environment during storage or processing. It is necessary to have a systematic study on the moisture absorption behaviour of the textile cords and the influence of the absorption on the characteristics of the tyre.

1.2 Motivation

Textile cords have been used as reinforcing material since the first pneumatic tyre was developed in 1888, and the number of applications of textile cord has never stopped increasing in the last decades. Different textile cords, from natural fibre such as cotton to the synthetic fibres such as rayon and polyamide, are used to reinforce the tyres with their strength, dimensional stability and abrasion resistance [24, 25]. However, it is known that the textile cords based on natural fibre or cellulose have a significant disadvantage: the moisture sensitivity [26, 27]. The mechanical properties of fibres and fibre reinforced materials can be affected under moisture influence [28]. The water absorption is therefore one of the most important characteristics of natural fibre reinforced composites that determine their end use behaviour in different applications [29].

In the tyre industry, the textile cords especially the cellulose based cords are well protected before processing. However, it is hard to entirely eliminate the environmental influence on the textile cords. For this reason, it is necessary to have a comprehensive and systematic investigation on this moisture uptake behaviour of textile cords and its influence on their mechanical properties. With this investigation, the influence of moisture on the final product can be reduced by regulating the environment condition during processing and storage.

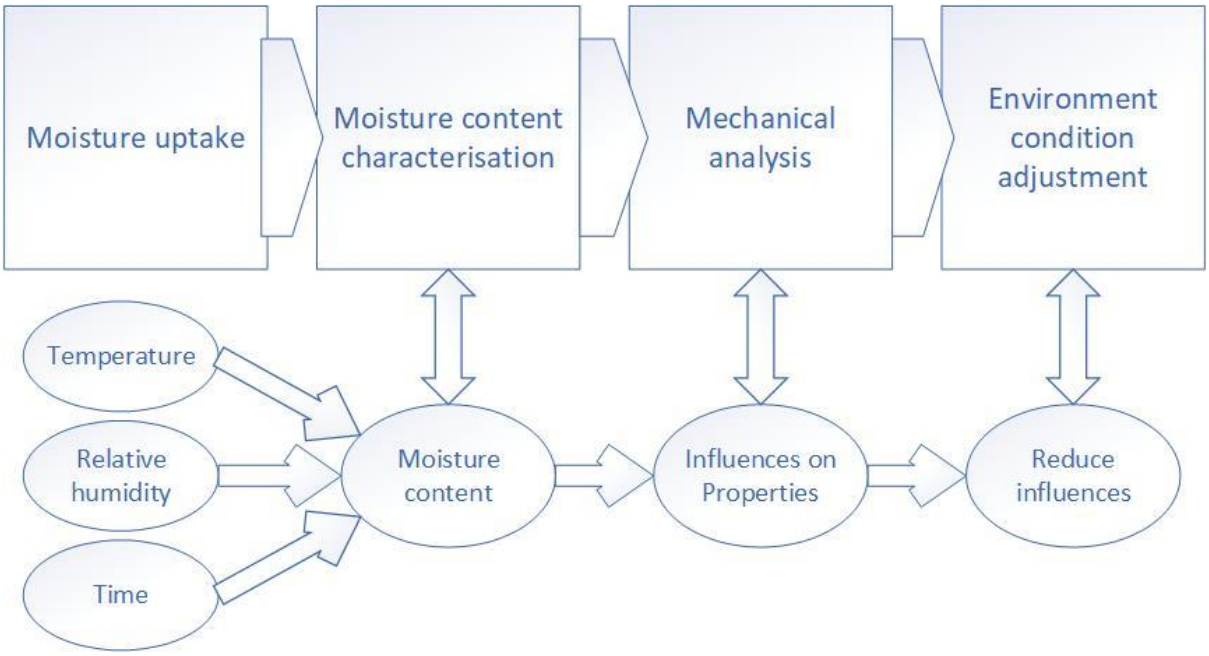

Figure 1.2: Research steps

Most of the studies on moisture uptake behaviour of fibre reinforced rubber have been published before 1980's, and focused on the moisture absorption of cellulose based tyre cords. Due to the limitations of the methodology at that time, measurements were often performed by weighting the sample periodically and manually with a balance. The accuracy

of the measurements for today's requirement cannot be ensured by this method. Secondly, the mass change in the initial stage of the measurement cannot be correctly observed because of the high absorption velocity. It is therefore reasonable to develop a new test method to be able to determine the moisture content in the sample during storage without these disadvantages.

Besides, most of the reports are built on the results from just one or two different environment conditions. To understand the moisture uptake behaviour better and therefore be able to support the production with recommendations to minimize the moisture influence, investigations at different combinations of temperature and relative humidity need to be performed systematically. The relation between moisture absorption and the environment aspects on the mechanical characteristics must be clarified. A databank should be designed based on the results of these measurements so that the tyre industry could utilise this databank to determine the moisture content in the textile cords according to the storage time, temperature and relative humidity.

A mathematic model should be built based on the result of the measurements in order to support the tyre industry as an example to minimize the moisture absorption problem. The moisture uptake behaviour could be predicted with this model. The moisture in the tyre cord could be controlled by adjusting the storage conditions.

It is also important to clarify the relation between moisture content in the textile material and its influence on the product performance. In the past, some investigations often compared the properties of the samples stored under different conditions to determine the influence of moisture on these properties and did not find the meaningful relationship. The relation between moisture amount and its influence on properties should be determined with the support from a databank. This relation can be transformed to the relation between property changes and the environment conditions of storage. Furthermore, this relation can be transferred and utilized by the tyre industry to reduce the influence of moisture on the end product.

1.3 Organization of the dissertation

According to the statement in section 1.2, the research objectives of this study are to provide:

1. A characterization method focusing on monitoring the moisture content i.e. in the tyre cords during storage under certain environment conditions with high accuracy

2. Knowledge on the moisture uptake behaviour based on experimental results. The relation between different aspects and moisture content in the textile cords.

3. A mathematical model based on the experimental results to predict the moisture absorption

4. An experimental approach for measuring the moisture influence on different mechanical properties of the textile tyre cords

5. Knowledge about the relation between moisture content and its influence on different mechanical properties based on the result of mechanical test procedures from point 4

6. Recommendations for the tyre industry to reduce the influence of moisture absorbed during storage and processing.

To achieve the objectives, the solution strategy and detailed study steps of this dissertation are illustrated in Figure 1.3. The whole research can be classified into four steps, namely the methodology development, the characterization of moisture uptake behaviour, the mathematical modelling of moisture absorption and the mechanical characterisations to identify the influence of absorbed moisture.

In chapter 2 the research background is in first step explained in order to clarify some important definitions around the moisture uptake behaviour. The state of the art is then discussed to determine the main research objectives.

In chapter 3 the different materials for the experiments are introduced, followed by the development of the characterization techniques. The classical method to determine the moisture content is compared with a new test method with high reliability. To suit the requirement of the characterization of textile tyre cords, the rubber matrix and the rubberized textile cords, the specific adjustments for the test methods and the corresponding sample preparation are described.

The experimental results of moisture content characterization are discussed in chapter 4. Three kinds of textile cords are measured under different environment conditions. The relationship between the environment conditions and the absorbed moisture amount of each cord is investigated. For the rubbers, similar experiments with extended test time are performed to study the influence of different ingredients. The moisture content in rubberized textile cord is determined with special attention on the influence of the open ends. A mathematical model is introduced in chapter 5 based on the results from chapter 4 to predict the moisture uptake behaviour.

In chapter 6 the influence of absorbed moisture on different mechanical properties is studied. All mechanical tests are performed on both dry sample and samples with different moisture

content. The results of chapter 4 are used to build the relationship between environment conditions and the influence on properties. For the rubberized textile cords, the cord-to-rubber adhesion is also investigated with mechanical- and morphological methods.

In the last chapter, recommendations for reducing the influence of moisture are provided based on the result from chapter 4-6. Finally, the results and contributions of this research are summarized.

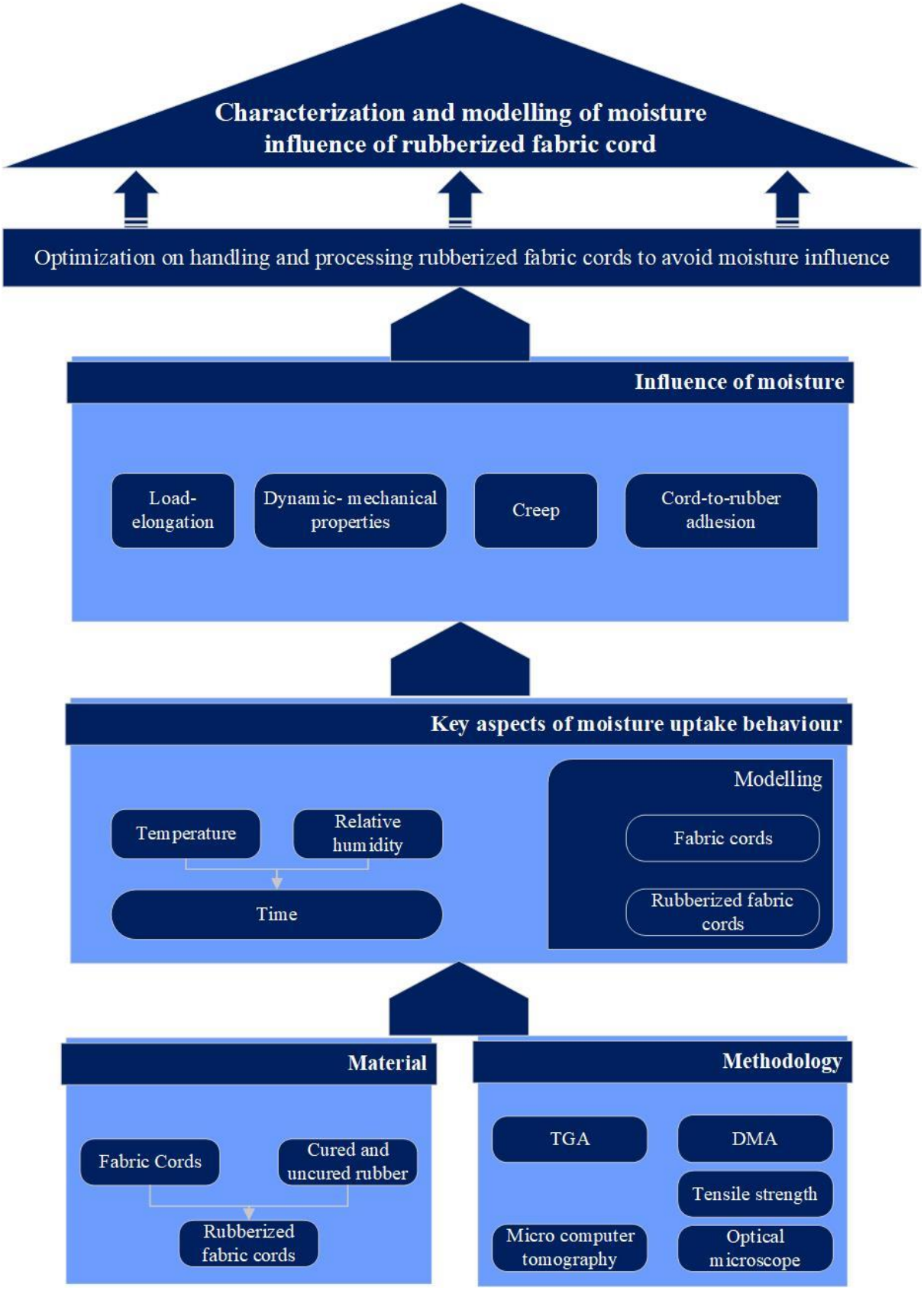

Figure 1.3: Organization of the dissertation

2 Research background and state of the art

In order to clarify the current research status and find out the challenges regarding materials, processing and properties, the literature review concentrated on the key materials, the behaviour of moisture uptake and its influence on different properties is performed.

2.1 Textile reinforcements

2.1.1 Textile reinforcements in tyre industry

Tyres are widely used since last centuries in the transportation industry from bicycles to the aeroplanes. It is a highly complex product and the unique component of a car touching the road. All the forces, vibrations, moments are transferred from the road to the car through it. A modern tyre contains several compounds with diverse ingredients in differing amount in order to meet all the requirements. The compounds, ingredients and their amounts vary by tyre size and tyre type[30].

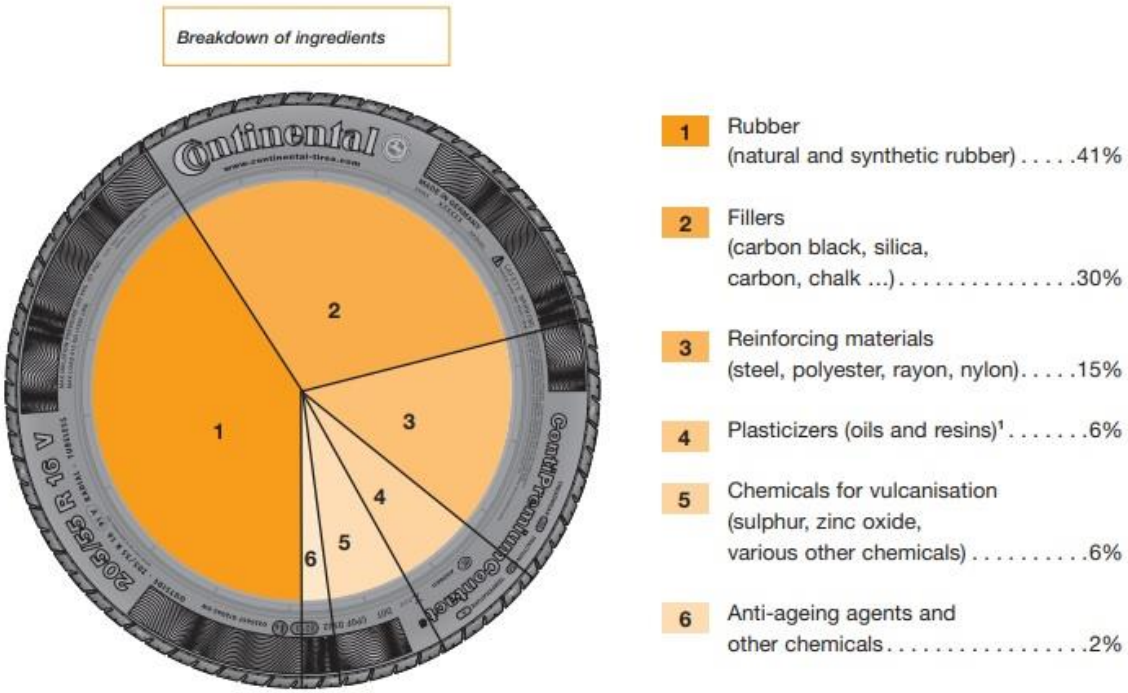

Figure 2.1: Ingredients of a passenger car tyre ContiPremiumContact 5, 205/55 R16 91V as a typical example [30]

Figure 2.1 shows the ingredients of a passenger car tyre with a typical weight of about 8.5 kg without the rim. On average, a modern car tyre contains up to 25 components and 12 different rubber compounds – natural and synthetic [31]. The textile industry and the steel

industry supply materials (basic materials such as rayon, nylon, polyester and aramid fibres or high–strength steel) for the manufacturing of tyres as the reinforcing materials [32].

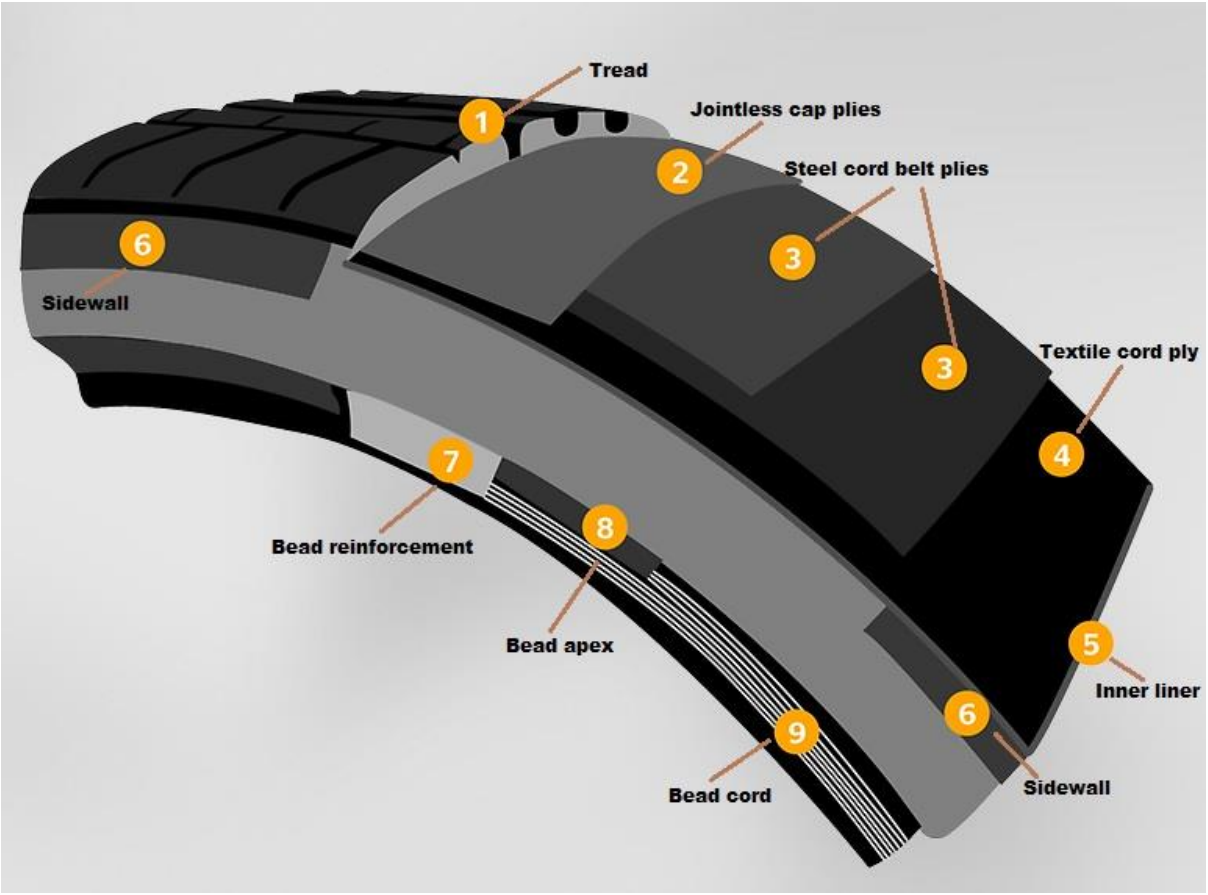

Figure 2.2: Schematic tyre section. Components of modern cars[33]

As shown in Figure 2.2, the parts of a modern car tyres can be grouped into two main structural elements: The tread and belt assembly, and the casing, each of them consisting of several layers. The tread made of synthetic and natural rubber is in contact with the road and ensures mileage, grip on the road, noise and water expulsion. The belt, which is a composite material consisting of rubber and steel cord, supplies the tyre with strength to ensure the structural stabilized and enhance performance, such as travel with high speeds, mileage and rolling resistance. The textile reinforcements can be found in different layers of tyre components: In the textile cord ply to control the internal pressure and maintain the tyre shape as well as in the bead reinforcement to enhance the directional stability [33].

Typical tyre cords are built up from yarns produced from filaments. The filaments are twisted “Z” into yarns and then back twisted “S” to form a cord. The unit “decitex” is used to describe the size of a cord, which is measured by its weight per unit length. Thus a 1440 x 2 nylon cord is formed from two 1440 decitex yarns twisted. The structure of the cords has influence on performance, e.g. more yarns in a cord result a higher strength [32].

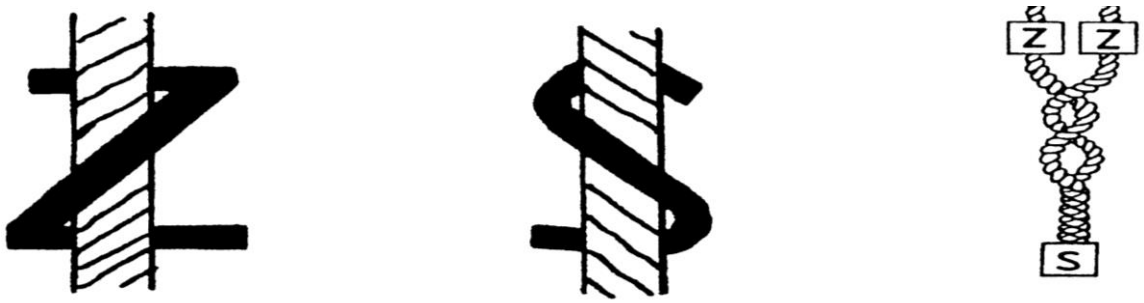

Figure 2.3: "Z" and "S" twisted filaments and the structure of cord [34]

The major usage of reinforcing cords is currently represented by five kinds of materials – steel, rayon, nylon, polyester and aramid [32]. In this study, rayon, nylon and polyester are used, and will be elaborated in this subchapter.

2.1.2 Rayon cord

Rayon is a generic form for an artificial textile material composed of reconstituted, regenerated and purified plant substance, viz. cellulose of cellulose compounds. The long chain polymer structure comes from nature and is only artificially modified, therefore it is called a semi-synthetic fibre [35].

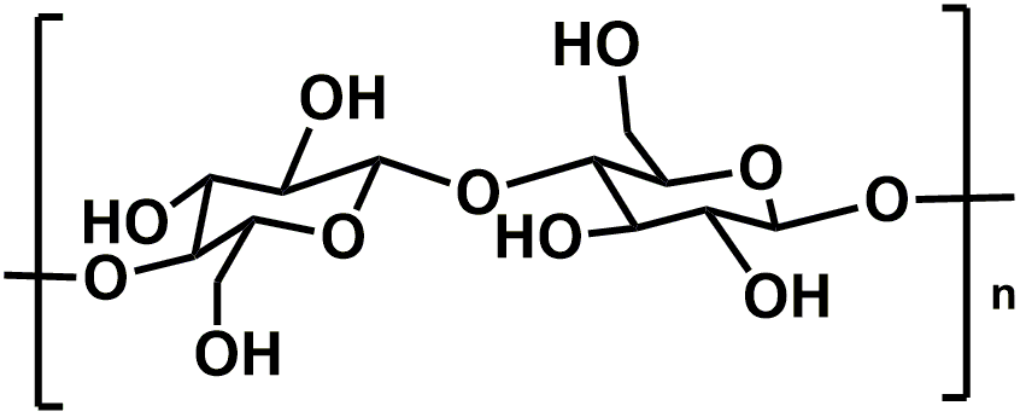

Figure 2.4: Chemical structure of cellulose fibre which is rayon made from

The first pneumatic tyre was developed by J. B. Dunlop with Irish flax as the reinforcing material in 1888. In the first 40 years, natural fibres, especially cotton, were the main reinforcing materials of the tyre. However, the cotton tyre cord failed to meet the requirements of growing demand of tyres. In 1923, the first man-made fibre tyre cord, rayon, was produced. Its demand started growing rapidly since the late 1930's [36].

Compared to cotton cords, the rayon cords have a higher strength to fracture. Together with other synthetic fibres, rayon is set as the substitute of cotton cords to produce a carcass ply. Since 2004, most pneumatic radial tyres with the aspect ratio of 0.65 to 0.82 use polyester cord as the carcass ply. This is because of the higher cost and the environmental concerns

during the production of rayon cord [32]. But on the other hand, rayon cord is preferred to be used for the high speed tyres with low aspect ratio [37, 38].

Rayon fibre is applied in passenger cars due to its advantage on low shrinkage, high modulus and good adhesion properties. However, the disadvantages such as lower strength and impact resistance make it lose the market share of truck tyres to nylon cords [32]. In addition, the rayon cord is hygroscopic with a low wet strength, and therefore, moisture might impact the tyre performance seriously. The moisture regain should be controlled to 2% or lower during the production of the tire [37].

2.1.3 Nylon cord

Nylon has become a generic term for aliphatic polyamides. In contrast to cotton and rayon, which are natural or semi-synthetic fibres, nylon is a completely synthetic fibre. The first example of polyamide was found in 1935 by Wallace Hume Carothers at DuPont's research facility as the first commercially synthetic thermoplastic polymer registered under the trademark Nylon® [39, 40]. For the purpose of simplicity, the term nylon is used in this work as a synonym for polyamide.

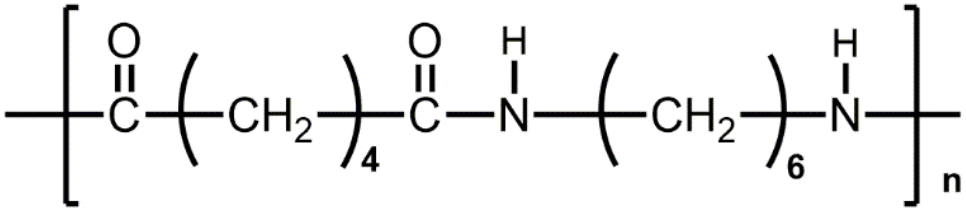

Figure 2.5: Chemical structure of polyamide 66 fibre

The rayon cord was utilised on truck tyres in the late 1940's. A new material with more strength was then required. Nylon cords were examined as the reinforcing material for truck tyres in the United States since 1947 and began to dominate the market after 1951 in Japan [36]. In a report in 2018, the nylon cord is expected to be the largest segment of overall tire cord fabrics market during the forecast period [41].

Two varieties of nylon materials are used in tyre industry as cord: Nylon 6 (made from opening up a monomer containing both amine and acid groups known as a lactam ring) and Nylon 66 (made from a condensation reaction between diamines and dibasic acids) [42]. Both materials have similar properties, the Nylon 66 has a weakness on the cost, but it shows higher resistance on moisture uptake and improved moisture tensile strength [32].

Due to the low modulus and the low glass transition temperature, and especially due to the poor ride quality, the nylon cord does not meet the requirement as the tyre belt of a passenger

car. But in the area of truck tyres, especially for medium and heavy-duty trucks, nylon cord is preferred because of its high strength, bruise and impact resistance and low heat generation. In these applications, nylon can be used in radial tyre carcass with belts made from steel or aramid [32].

2.1.4 Polyester cord

Polyester is a category of polymers which contain the ester functional group in the main chain. It refers commonly to polyethylene terephthalate (PET), which is produced from ethylene glycol and dimethyl terephthalate (DMT) or terephthalic acid. The first PET patent was registered in 1941 in England and makes up about 18% of world polymer production [43, 44]. PET is widely used in different areas: 60% of PET production is used for the synthetic fibres in different applications, which are the most used fibre in the world, 30% for the bottle production and 10% for other industrial use [44].

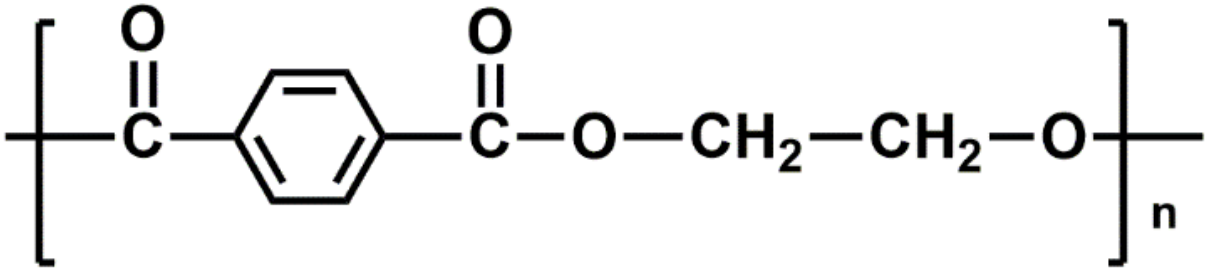

Figure 2.6: The chemical structure of polyester fibre

In the early 1960's, polyester cords were introduced by the tyre company Goodyear for reinforcing passenger car tyres [36]. The polyester cord has a higher strength than rayon cord and a better dimensional stability compared to nylon cord, therefore the polyester cord has become the dominant reinforcing textile for the radial carcasses of passenger car and light truck in North America and exhibit a steady growth worldwide in the last years [32].

The polyester cord is preferred as carcass material in radial tyres for passenger cars because of its balance of properties. But due to the hydrophobic nature of its surface, the ordinary RFL-type cord adhesives do not work well. In order to get a better adhesion with rubber materials, a specific dipping processes or a surface activation should be applied [45]. In addition, the polyester cord is not recommended for severe applications such as in high load trucks or in high-speed cars because of the rapid loss in properties under high temperatures above 120 °C [32, 46-48].

2.2 Hydrophilic behaviour of textile reinforced rubber materials

2.2.1 Basic definitions

2.2.1.1 Humidity and saturation

“Moisture is the water or other liquid diffused in a small quantity as vapour, within a solid or condensed on a surface.“ [49] Humidity is used to describe the concentration of moisture in the air.

In order to initially understand the moisture behaviour, a small, dry and closed box with a floor covered with pure water at a temperature T can be assumed. With time, the water will begin to evaporate so that the water molecules will enter the air, and therefore, a water vapour pressure is built. Due to the pressure of the water vapour, there will be a condensation rate for the water molecules from the vapour phase back to the liquid phase. This rate will be lower than the rate of evaporation in a certain time until they are equal, the state within this time is called unsaturated. If both the rate of condensation and evaporation are equal, the air in the box is saturated at the temperature T and the pressure at that time is called saturation vapour pressure, as shown in Figure 2.7 [50].

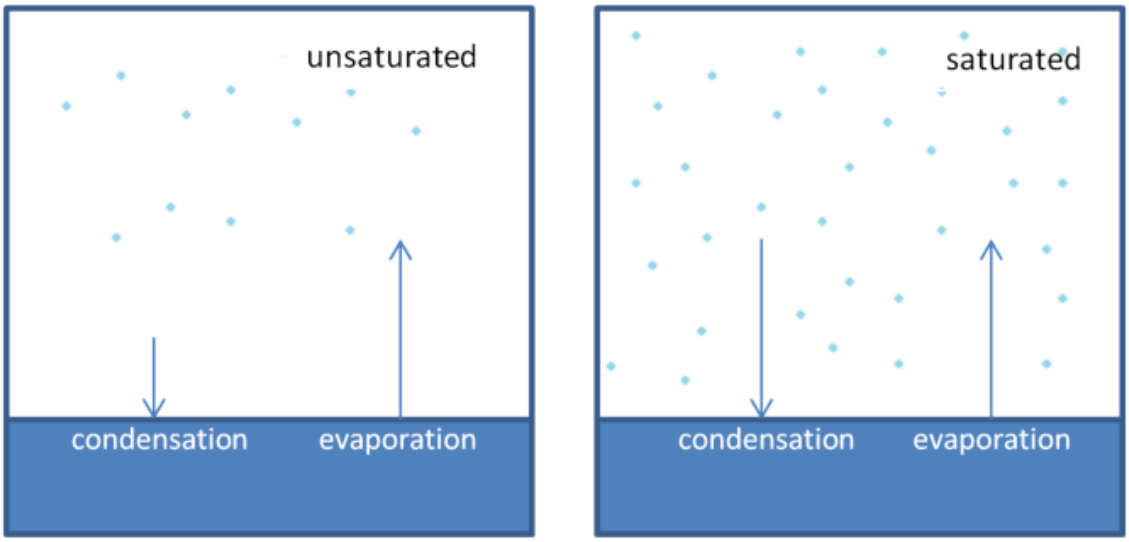

Figure 2.7: unsaturated- and saturated air[50]

Absolute Humidity

The absolute humidity describes the amount of water vapour presents in the air at a given temperature [51]. It may vary from 0 gram per cubic metre at 0 °C to 50 gram per cubic metre at 40 °C [52].

$AH = \frac{m_w}{V}$	*Where*	m_w*: mass of the water vapour* *V: volume of air and water vapour* *AH: absolute humidity in* g/m^3	*Equation 2.1*

The absolute humidity is calculated with *Equation 2.1*. The absolute humidity changes while the air volume changes. However, the volume is changing with temperature and pressure even without losing or gaining water vapour. To solve this problem, specific humidity is introduced which is ratio of water vapour mass and the mass of both dry air and water vapour. (*Equation 2.3*) In many different fields of science, such as the chemical industry, the absolute humidity refers sometimes also to mass of water per mass of dry air, which is called humidity mixing ratio and calculated with *Equation 2.2* [50]. It may avoid the problem above and suits therefore better by calculating heat and mass balance. Because m_w is less than 3 percent of m_a at normal pressure and a temperature at 30 °C. The humidity ratio and the specific humidity are practically equal [52, 53].

$r = \frac{m_w}{m}$	*Where*	m_w*: mass of the water vapour* m_a*: mass of dry air* *r: humidity ratio*	*Equation 2.2*
$SH = \frac{m_w}{m_a + m_w}$	*Where*	m_w*: mass of the water vapour* m_a*: mass of dry air* *SH: specific humidity in* g/kg	*Equation 2.3*

Relative Humidity

The relative humidity is the ratio of the absolute humidity divided by the amount of water vapour saturated at a given temperature [51]. The calculation of the relative humidity at the given temperature T is shown in *Equation 2.4*. The relative humidity is the ratio of the actual water vapour mass and the saturated water vapour mass [50].

$RH = 100 \left(\frac{m_w}{V} \Big/ \frac{m_s}{V} \right) = 100 \frac{m_w}{m_s}$	*Where*	m_s*: mass of the saturated water vapour* m_w*: mass of the water vapour* *V: volume of air and water vapour* *RH: relative humidity in %*	*Equation 2.4*

According to *Equation 2.2*, the humidity ratio under saturation can be calculated as shown in *Equation 2.5*. Both the water vapour and the dry air obey the ideal gas equation, thus the

saturation humidity ratio can be obtained as in *Equation 2.6 [50]* and *Equation 2.7*. The value of e_s depends only on temperature, thus the saturation humidity ratio is proportional to the temperature and inverse proportional to the total pressure [50].

If the expression of humidity mixing ratio is used, the relative humidity at a given temperature is the ratio which is calculated by dividing the actual humidity mixing ratio *r* through the saturation humidity mixing ratio r_s (*Equation 2.8*)[50].

$r_s = \frac{m_s}{m_a}$	*Where*	m_s*: mass of the water vapour under saturation* m_a*: mass of dry air* r_s*: saturation humidity ratio*	*Equation 2.5 [50]*
$r_s = \frac{\rho_s}{\rho_a} = \frac{\frac{e_s}{(R_v T)}}{\frac{(p - e_s)}{(R_a T)}}$	*Where*	ρ_s*: partial density of water vapour to saturate the air* ρ_a*: partial density of dry air* *p: total pressure* e_s*: saturation vapour pressure* R_v*: gas constant for 1 kg of water vapour* R_d*: gas constant for 1 kg of dry air*	*Equation 2.6 [50]*
$r_s \approx 0.622 \frac{e_s}{p}$	*Where*	*p: total pressure* e_s*: saturation vapour pressure*	*Equation 2.7* [50]
$RH = 100 \frac{r}{r_s} = 100 \frac{e}{e_s}$	*Where*	*r: humidity ration under temperature T* r_s*: saturation humidity ration under temperature T* *e: pressureof the water vapour* e_s*: saturation vapour pressure* *RH: relative humidity in %*	*Equation 2.8* [50]

According to *Equation 2.8*, the relative humidity is related to a given temperature T [50]. The relative humidity under different temperatures varies significantly. The relation between absolute humidity and relative humidity is illustrated in Figure 2.8. The mass of water vapour by 60% relative humidity and 40 ℃ is much more than the vapour mass at 100% and 20 ℃ [52].

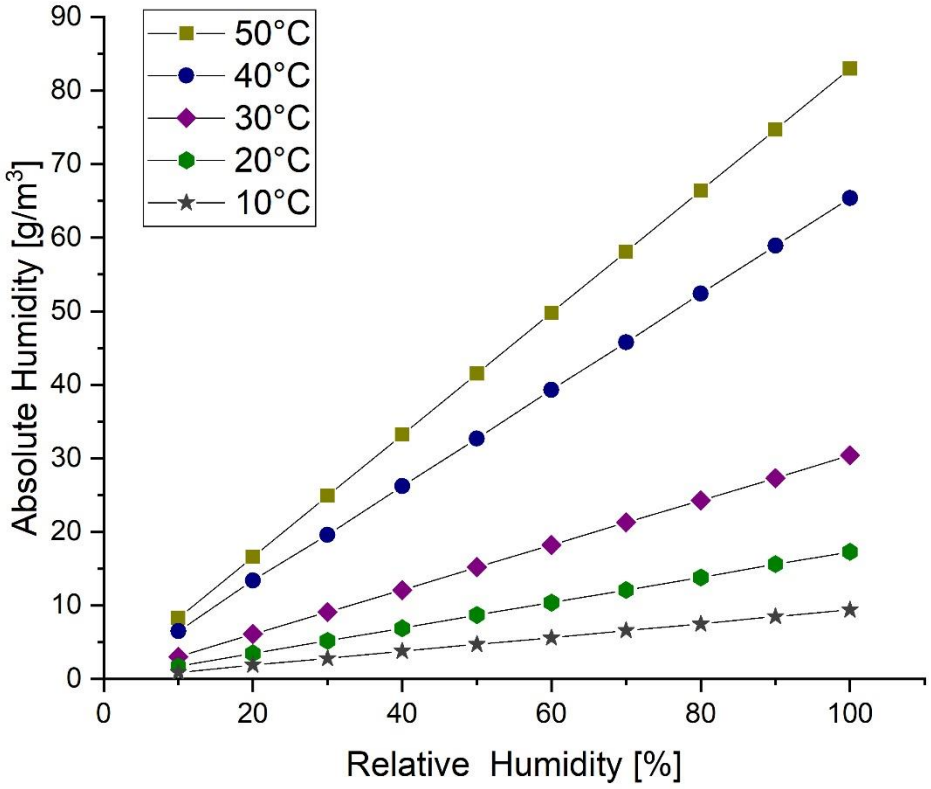

Figure 2.8: Relation between absolute humidity and relative humidity [52]

2.2.1.2 Sorption process

Traditionally, the theory of diffusion has been applied to help understanding the mechanism of moisture uptake behaviour in fibre and composite materials. The definition of sorption has been used to describe the physical and chemical processes by which one substance attached to another [54]. There are different articles under the expression sorption:

Adsorption

The word "adsorption" appeared in 1881 in the article from German physicist Heinrich Kayser [55]. The adsorbates, which are commonly molecular species, accumulates at the surface of adsorbent and forms there a film in the adsorption process [56]. The adsorption processes can be classified as physical sorption characterized by van der Waals forces and chemical sorption characterized by covalent binding. Electrostatic attraction may also be a characteristic of adsorption [57].

In the field of material science, the adsorption of water at a material surface has a great significance. The physically or chemically adsorbed water at the surface of a solid material

may have impact on the interaction with the adjacent medium or the chemical reaction pathways.

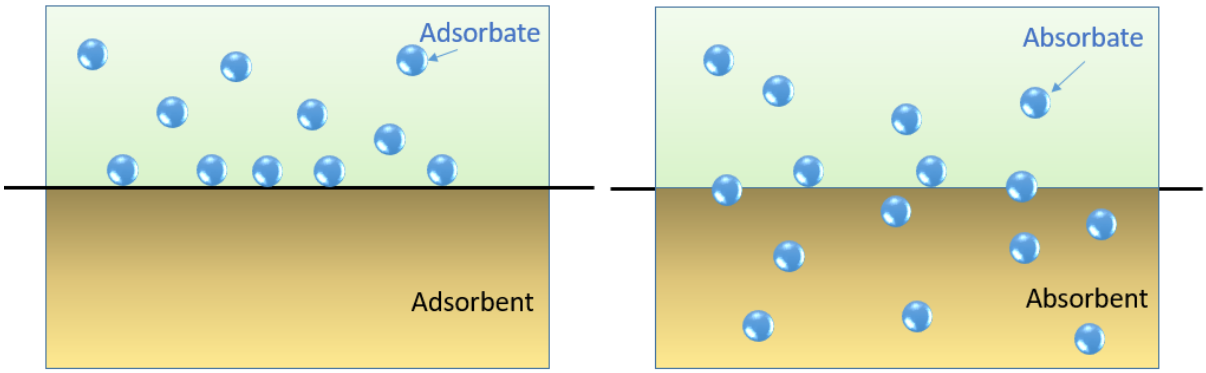

Figure 2.9: Mechanism of Adsorption and Absorption, illustrated based on [58]

Absorption

Absorption is the phenomenon, in which the absorbate, which is often atoms, molecules or ions, is retained by the absorbent, which is in liquid or solid state [59]. The absorption succeed often the adsorption process [58, 60]. As shown in Figure 2.9, the molecules in the absorption process are taken up into the absorbent volume, this process is different from adsorption which is a surface phenomenon [58].

The absorption can be also classified into physical and chemical processes. In a physical absorption e.g. water absorption in a hydrophilic solid substance there is no reaction but a polar interaction between water and the solid substance. By chemical absorption there is a chemical reaction between the absorbate and absorbent. The chemical absorption sometimes is combined with a physical absorption [61].

2.2.1.3 Diffusion

The word diffusion derived from the Latin word “diffusio”, which means “spread out” [62]. Diffusion is the movement of matter from one part of the system with higher concentration to another part with lower concentration. It is a result of random molecule motions to reduce the concentration gradient [63, 64].

The diffusion process is illustrated by an experiment in which a tall glass bottle filled with the solution of iodine in its lower part. If a certain amount of pure water comes from the top slowly, it can be observed that at first there is a boundary between the coloured part and the clear part. The clear upper part becomes coloured later with the colour of lower part turns lighter. In a final phase after sufficient time, the whole solution appears in a uniform colour. This process shows a motion of the iodine molecules from the lower to the upper part of the bottle, from the high concentration part to the lower concentration part, it is said the iodine

to have diffused from the solution into the water. In this experiment it can be observed that the molecules of iodine have a free motion in all the possible directions. However, there are more iodine molecules in the solution than in the water, until the homogeneous state is reached. Thus, the possibility that a molecule moves from the upper part is bigger than from the lower direction. This explains how the molecules move randomly but from higher concentration to the lower one. Once the diffusion is finished, the concentration gradient is also eliminated [63].

The first systematic experimental study of diffusion was done by Thomas Graham in the 1830s. He described in his publication in 1833 the phenomenon of gas diffusion. In 1855 Adolf Fick published papers about the law of diffusion, in which the famous Fick equations are described [65].

Fick's first law:

$J = -D\frac{dC}{dx}$	*Where*	*J: diffusion flux* *D: diffusion coefficient* *C: concentration* *x: position*	*Equation 2.9* [63, 64]

Fick's first law can be written in the form as shown in *Equation 2.9* in one dimension. According to the equation, the flux across a given unit area is proportional to the concentration gradient measured perpendicularly to the section. If the concentration gradient is set to 0, which means the system becomes homogeneous, the flux diffused through the section will be also 0. That fits the facts well [63, 64].

$\frac{\partial C}{\partial t} = D\frac{\partial^2 C}{\partial t}$	*Where*	*C: concentration* *D: diffusion coefficient* *t: time*	*Equation 2.10* [63, 64]

Fick's second law describes the change of concentration with the influence of the diffusion with respect to time, see *Equation 2.10*. Fick's second law can be derived from Fick's first law and the mass conservation if there is only a physical phenomenon in place [63, 64].

2.2.2 Hydrophilic behaviour of textile reinforcements

As it is mentioned in 2.1.2, **rayon** cords are widely used as a skeleton material to reinforce different rubber products. As shown in Figure 2.10, compared to the native cellulose (cellulose I), cellulose II, which is completely dissolved and subsequently re-crystallized from cellulose I, has thermodynamically the most stable structure [66-69]. Rayon fibres are produced from cellulose II by spinning the solutions into continuous fibres [25, 70-72]. As it is of biomass origin, rayon fibre is well known to be sensitive to moisture [73, 74]. The amount of moisture absorbed depends only slightly on temperature, but on the chemical

nature of the rayon fibre and its molecule structure, e.g. the amount of the hydroxyl groups of the cellulose and the degree of crystallinity [75].

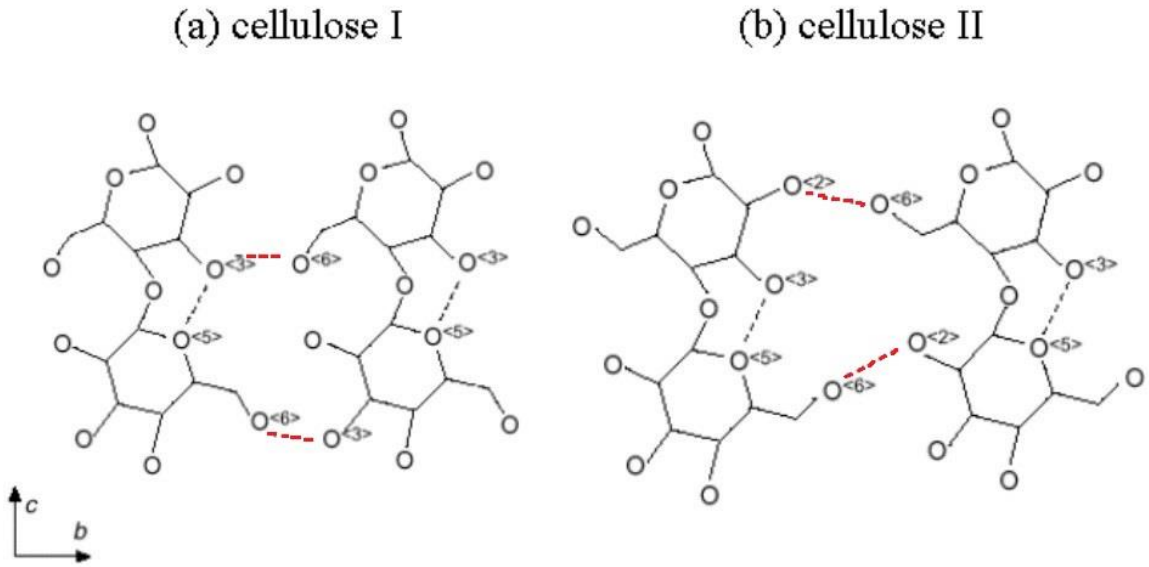

Figure 2.10: molecule structure of cellulose I and cellulose II[66]

Nylon (Polyamide) is one of the most important fibres on the world market of composite materials. However, the hygroscopic properties of this polymer, which means it absorbs moisture from the environment, restrict its applications [76]. Commercially available polyamide polymers can absorb up to 10% of water by dry weight depending on the relative humidity, temperature and the chemical structure of the polymer [77]. Figure 2.11 shows the molecule structure of nylon 66, which can form hydrogen bonds together with the water molecules using the polar amide groups [78, 79].

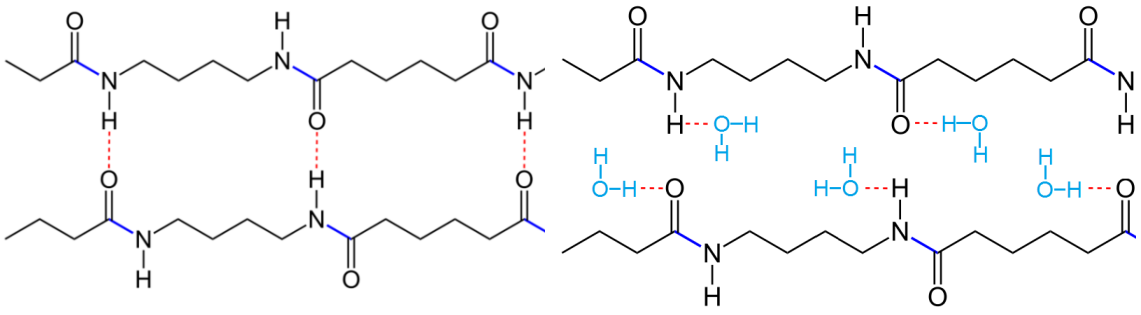

Figure 2.11: moisture absorption of nylon 66 fibre with hydrogen bonds

As in the case of rayon and nylon fibres, the main factors that influence the moisture uptake of polyester fibre such as PET fibre are the hydroxyl groups. However, the polyester fibre has a lower hygroscopic absorption as nylon and rayon. Therefore, the investigation on moisture uptake behaviour of tire cord in this work is not really relevant for PET fibre and so the research is focused on rayon and nylon cords.

Usually, the specimen is placed into a closed atmosphere at a certain temperature and relative humidity to absorb the moisture. Its content is determined periodically to clarify the relation between moisture absorption and storage time from the initial state to the saturation. The most common techniques using to determinate the moisture content within a given sample are based on the thermal analysis such as the Thermal Gravimetric Analysis (TGA), differential scanning calorimetry (DSC) and loss-on-drying (LOD). All these methods require drying the specimen to the initial state to calculate the moisture content. Such destructive methods have the disadvantage that the specimen might be destroyed and cannot be used for further tests anymore. Hence, it will not be used in the further analysis [76, 80].

K. Fischer introduced a chemical method now associated with his name: Karl-Fischer titration. In this measurement, water is removed from the specimen by heating it and passing dry nitrogen gas over it. The moisture is transferred into a methanol solution, which is titrated with the so-called Karl-Fischer reagent for the moisture determination. This method has also the same disadvantage as the thermal analysis, in addition, the use of toxic solvents on the specimen is also troublesome [81].

W. Camacho et al. introduced a method to measure the moisture content with Near-Infrared Spectroscopy (NIR), which is based on the measurement of light absorbed by the specimen. Together with light-fibre optics and Chemometrics, the NIR has become a simple but effective method. This non-destructive method allows the specimen to be measured in further experiments, e.g. mechanical tests, immediately after the determination of moisture content. But due to the optical limitation of the technique, NIR is not friendly enough for measuring specimens of dark colour [76, 82].

With an extension on the methodology, Camacho et al. developed partial least-square regression models to determine the moisture content directly from combined regions of the NIR spectra. But their experiment was limited only to PA66 [80].

One of the most important applications of fibres is for the apparel purpose. In this area, there are many publications since more than 80 years with the research target for textiles made with natural fibres to man-made fibres. E.g. P. Kenins performed measurements of fabric-to-skin friction with different kinds of fibres, like cotton and polyester. The results show that moisture has a large effect on friction, but this effect appears to be related to liquid water rather than to changes in humidity [83].

D. Negru et al. studied the moisture absorption and transfer through knitted fabrics made of natural and man-made fibres. Cotton, rayon and polyester were the investigation targets. According to the results, porous structure with more knits increases the moisture content no matter whether it is liquid or vapour form [84].

K. Kohata et al. performed research on the interaction between moisture and the cellulose based textiles with broad-line proton NMR spectroscopy. Result shows that the adsorbed water changes in its nature from strongly to weakly interacted water with the adsorbent, but no to the so-called free water even at saturation state [85].

2.2.3 Hydrophilic behaviour of textile reinforced rubber composites and the influence of moisture

Since the early stage of the 20th century, researchers have been busy with investigating the relation between fibres and moisture. Different fibres are utilised with the form of cords to reinforce rubber applications.

As the first synthetic fibre, rayon won also the focus from tire industry. R. C. Waller et al. found that oxygen and the absorbed moisture have large effects in accelerating the degradation of rayon tire-cord at high temperatures. The rayon cord ages more rapidly than nylon cord in evacuated cubes but much slower than it if unlimited air is provided [86].

In 1940s, J. H. Dillon et al. tested different tire cords such as rayon and nylon under elevated humidity (1.6 -65%) and temperature (20-165 ℃). The cords were then measured with a tensile test machine and a creep apparatus. The results showed that the tenacity of viscose rayon cords decreases with increasing temperature at constant regain in the range of 0-5%. The creep curve of rayon cords is nearly linear in the range of creep times from 0.002 to 20 hours. The creep curves of nylon show a tendency to increase in slope at times beyond 1 hour. [87] .

In the publication from E. Honold et al. the elastic moduli of rayon and nylon cords are measured, decreased elastic moduli with increased humidity (from 40% to 90%) are reported. In the opinion of the authors, any investigation of tire cords aimed at the improvement of failure resistance of tires should include the tests at a critical condition such as 90 ℃ and 90% R.H. [88].

P.R. Willet et al. measured the viscoelastic properties of tire cords made of rayon, nylon and polyester under different environment conditions. The results show that the moisture affects the cords in different ways, with greatest effect being at lower temperatures. A higher moisture content results in higher loss modulus E" for rayon, and lower for nylon and polyester under certain conditions [89].

S. Ramezani studied the moisture absorption of nylon 6 and nylon 66. The cords were stored at 65% R.H. and 20 ℃ for 24 hours. The moisture regain was measured by heating the specimen to 105°C. The mechanical properties were measured with a tensile machine. With the so-called H-adhesion test and Fourier Transform Infrared Spectroscopy (FTIR), the

influence of moisture on adhesion was measured. The result shows a slight reduction in tensile strength, a considerable drop of adhesion, and an increase in elongation-at-break [90].

W. E. Claxton et al. performed tests with a dynamic flatspot machine on tyres with nylon cords. The specimens were stored under different environment conditions before testing. The result shows that the cords are affected by the moisture, but the flat-spot indices FSI obtained are well below the objectionable level even under high relative humidity test conditions [91].

E. R. Gardner investigated the effect of moisture on textile-rubber composites. Tyres with cords made of nylon, rayon and polyester were investigated. The result shows that the control of moisture content by using a desiccant would contribute to the manufacture of an inexpensive tyre with good resistance to separation under severe conditions of operation [92].

Most of the contributions above are older than 40 years. In these years, the tyre cord production has made huge improvements. The tyre cord and the adhesion techniques have been also developed further. The textile reinforcements investigated do not suit the current requirements anymore.

Z. Li et al. has evaluated the effects of heat and moisture on the characteristics and tensile strength of resorcinol-formaldehyde-latex (RFL) coated rayon cords and the adhesion to natural rubber (NR) /styrene-butadiene rubber (SBR). The results show that the moisture absorption affects the characteristics and the mechanical properties of rayon cords significantly. But the chemical state of the RFL layer and the static adhesion of the cord/rubber matrix were not obviously affected [93]. The specimens were stored in a desiccator and periodically taken out to determine the moisture content with a normal balance which leads to insufficient accuracy due to the fast sorption/desorption processes.

2.3 Mathematical modelling of the moisture uptake behaviour of textile reinforced rubber

ISO 62 [94] and ASTM D570 [95] are standard methods for measuring the water absorption by immersion. The absorption of liquids is determined by gravimetric methods, and the mass increases of the order of the original mass of the specimen. This approach can be extended to study the diffusion of moisture in textile reinforcements. The methods described in Chapter 3.2.1 can be used [63, 96].

$M(t) = 100 \times \frac{M_t - M_0}{M_0}$	*Where*	*M (t): moisture content in percent* M_t*: mass of moist material* M_0*: mass of dry material*	*Equation 2.11*

The most common methods to model the moisture absorption behaviour are based on the Fick law. The moisture mass M absorbed in the specimen in percent at the time *t* is calculated from the mass M_t and the initial mass M_0 as shown in *Equation 2.11*[97].

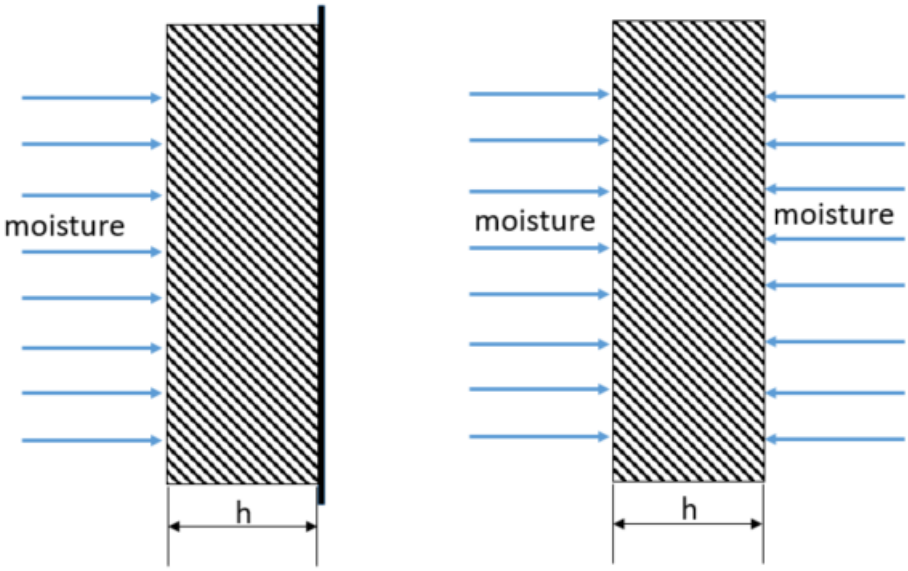

Figure 2.12: one dimensional diffusion [97]

It was found that the moisture content of the specimen can be calculated in Equation 2.12, if the following requirements are satisfied: 1) the diffusion is one dimensional (Figure 2.12), 2) the temperature and moisture content distribution inside the specimen are initially uniform and c) the temperature and moisture of the environment are constant [97].

$M = G(M_s - M_i) + M_i$	*Where*	*M_s: moisture content under saturation state* *M: moisture content* *M_i: initial moisture content*	*Equation 2.12*

The G is the time dependent parameter calculated with *Equation 2.13*:

$G = 1 - \frac{8}{\pi^2}\sum_{n=0}^{\infty}\frac{1}{(2n+1)^2}exp\left[\frac{-D(2n+1)^2\pi^2 t}{4h^2}\right]$	*Where*	*D: diffusion constant* *h: thickness of specimen* *G: time independent parameter*	*Equation 2.13 [97-99]*

In *Equation 2.12*, if the initial moisture content is 0 which means the specimen is dried, the parameter G is:

$G = \frac{M - M_i}{M_s - M_i} = \frac{M}{M_s}$	*Where*	*M_s: moisture content under saturation state* *M: moisture content* *M_i: initial moisture content*	*Equation 2.14*

More than 40 years ago H. Carter et al. introduced a model based on the theory of adsorption on surfaces with the name Langmuir law or two-phase model of Carter and Kibler, and applied the method on modelling the moisture absorption in composite resins. The moisture absorption can be explained quantitatively by assuming that the absorption consists of both mobile and bound phases. Molecules of mobile phase diffuse with a diffusion coefficient D and become bound with a probability of γ per unit time. The molecules of bound phase are emitted and become mobile with a probability of β per unit time [100].(*Equation 2.15*)

$\begin{cases} \frac{\partial n}{\partial t} = D\left(\frac{\partial^2 n}{\partial r^2} + \frac{1}{r}\frac{\partial n}{\partial r}\right) + \frac{\partial N}{\partial t} \\ \frac{\partial N}{\partial t} = \gamma n - \beta N \end{cases}$ $\gamma n\infty = \beta N\infty$	*Where*	*D: diffusion coefficient* *n: number of mobile molecules per unit volume* *N: number of bound molecules per unit volume* *γ: probability per unit time that a mobile molecule becomes bound* *β: probability per unit time that a bound molecule becomes mobile* *r. diameter*	*Equation 2.15 [100]*

W.K. Loh et al. developed a dual- stage uptake model which consists of two Fickian diffusion kinetics occurring in parallel. Each diffusion kinetic has a separate diffusion coefficient and saturation levels. The sum of the saturation levels gives the total moisture absorption of the specimen in the steady state under the given conditions. (*Equation 2.16*)

$M = M_{s1}\left\{1 - \frac{8}{\pi^2}\sum_{n=0}^{\infty}\frac{1}{(2n+1)^2} exp\left[\frac{-D_1(2n+1)^2\pi^2 t}{4h^2}\right]\right\} + M_{s2}\left\{1 - \frac{8}{\pi^2}\sum_{n=0}^{\infty}\frac{1}{(2n+1)^2} exp\left[\frac{-D_2(2n+1)^2\pi^2 t}{4h^2}\right]\right\}$ $M_{s1} + M_{s2} = M_s$	*Where*	D_1*: diffusion coefficient 1* D_2*: diffusion coefficient 2* *h: thickness of specimen* M_{s1}*: moisture content of stage 1 under saturation state* M_{s2}*: moisture content of stage 2 under saturation state*	Equation 2.16

A. Célino et al. have applied the models of Langmiur law, the Dual- stage Fick's law and the classical Fick's law on natural fibres. Different natural fibres are stored under certain environment condition or immersed into water. The models have been used to fit the result from the immersion measurements. The model of Dual-stage Fick's law gives similar shape as the classical Fickian model. The Langmiur model performs a better result on the prediction because the theory of Langmiur actually describes the immersion in liquid water quite well, whereas the Fick's law suit better when the fibres are exposed into a vapour conditioning [101].

A. Espert et al. investigated the water absorption in natural cellulose fibres in polymer composites. The process of water absorption was found to follow the kinetics and mechanisms described by Fick's law. The diffusion coefficient was depended mainly on the temperature by means of Arrhenius law as shown in Equation 2.17 [102].

$D = D_0 exp\left(-\frac{E_a}{RT}\right)$	*Where*	D*: diffusion coefficient* D_0*: permeability index* E_a*: activation energy* R*: universal gas constant* T*: temperature*	Equation 2.17 [102]

3 Materials and methodology development

In this chapter, the materials and the methodologies applied for the experiments in this work are introduced. The methodologies are divided into two parts: The characterization of moisture uptake behaviour and the characterization of the influence of moisture on textile cords.

Specifically, the classical method of characterization of moisture content and a modern test method which has some advantages are compared. The sample preparation approach of the moisture characterisation is also adjusted to suit the requirement of measuring the textile cords, the rubber matrix and the rubberized textile cords which have different characteristics and geometries.

For mechanical analysis, the standard testing methods were adjusted slightly by adding the moisture absorption process before the tests are performed according to the standard. Different instruments with climate function are chosen to complete this research task, so that the result of the moisture content characterisation can be used to determine the relationship between moisture content and the mechanical properties.

Before mechanical tests are performed to determine the influence of moisture on cord-to-rubber adhesion, some non-destructive methods are introduced to determine possible internal failures.

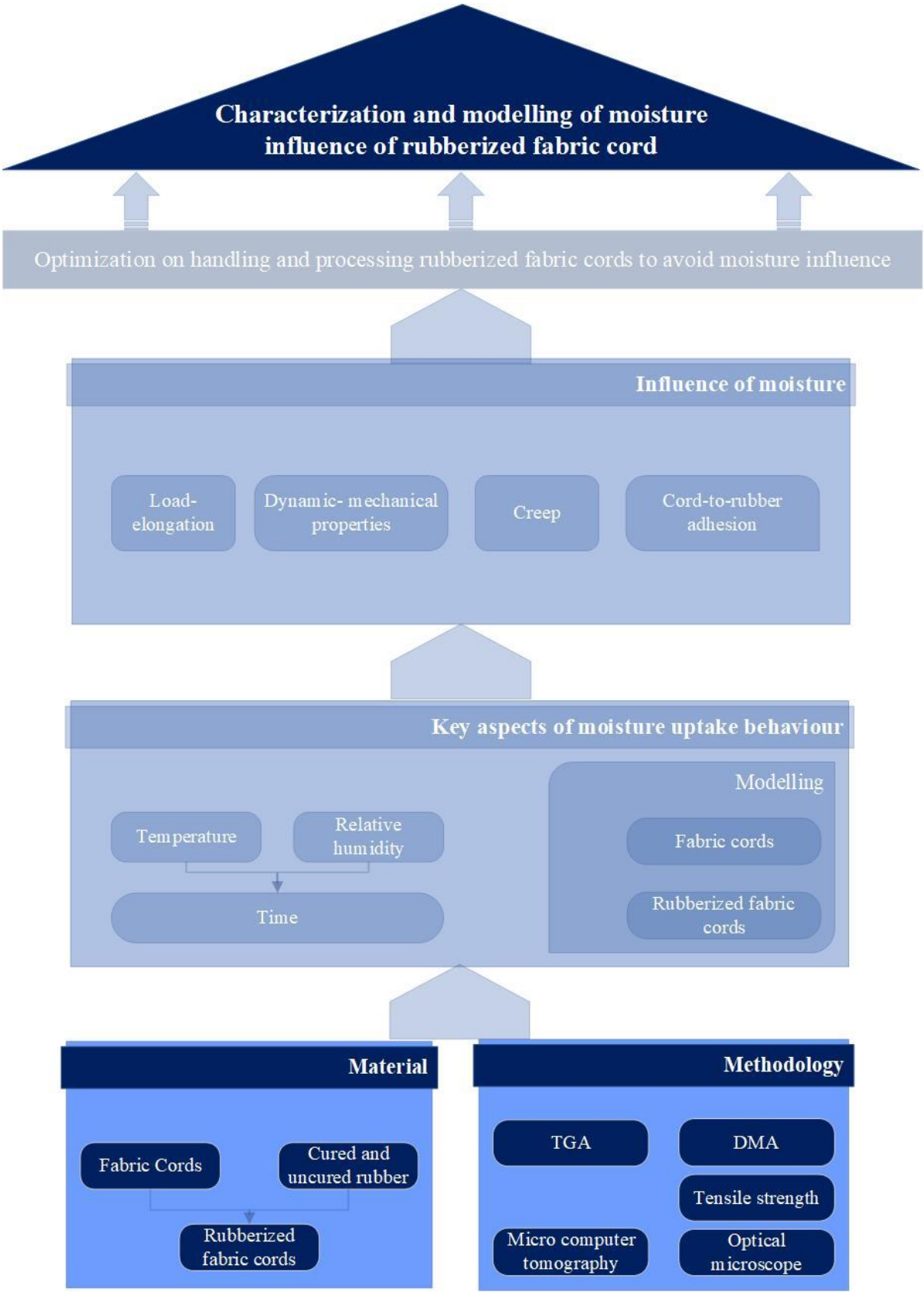
Characterization and modelling of moisture influence of rubberized fabric cord
Optimization on handling and processing rubberized fabric cords to avoid moisture influence
Influence of moisture
Load-elongation
Dynamic- mechanical properties
Creep
Cord-to-rubber adhesion
Key aspects of moisture uptake behaviour
Temperature
Relative humidity
Time
Modelling
Fabric cords
Rubberized fabric cords
Material
Fabric Cords
Cured and uncured rubber
Rubberized fabric cords
Methodology
TGA
DMA
Tensile strength
Micro computer tomography
Optical microscope

3.1 Materials

3.1.1 Textile cords

Three types of textile cords are investigated: nylon, rayon and polyester. Due to the properties of the different cords, nylon and rayon are considered as the main research objectives. All these cords are commercially available and were kindly supplied by Continental Reifen Deutschland GmbH.

3.1.1.1 Nylon 6.6

Two types of Nylon 6.6 cords (polyamide 6.6) with different warp constructions are considered and investigated in this thesis comparatively. An overview of their properties is provided in Table 3.1.

Table 3.1: Properties of investigated nylon cords

Properties	*Nylon Thick*	*Nylon Thin*
Warp Material	*Nylon 6.6*	*Nylon 6.6*
Warp Yarn Supplier	*Shenma*	*Polyamide High Performance*
Warp Construction	*1400 dtex x2*	*940 dtex x 2*
Weft material	*Cotton*	*Cotton*
Edge Type	*Inlaid Edge*	*Inlaid Edge*
Weave Type	*L1/1*	*L1/1*
Square Meter Weight	*0,319 kg/m2*	*0,162 kg/m2*

As the main material, nylon cord from Shenma Industrial Co., Ltd, Henan, China with a construction of 1400dtex x 2 (“nylon thick”) is used here to investigate the moisture uptake behaviour and the influence of the absorbed moisture on different mechanical properties. As reference, nylon cord from Polyamide High Performance GmbH, Wuppertal, Germany, (“nylon thin”) with a construction of 940 dtex x 2 is used to observe the influence of the construction on moisture uptake behaviour.

3.1.1.2 Rayon

To investigate the moisture uptake behaviour, four types of rayon cords are used: Two sorts of commercial rayon cords with different constructions (1840 dtex x 2 and 1440 dtex x2) and each type with or without RFL dip. The use of cords with different constructions may help understanding both the moisture uptake behaviour itself and the influence of the cord construction on this behaviour. By measurements on cords without RFL dip, the influence of dip on the moisture uptake behaviour can also be observed.

3.1.1.3 Polyester

Polyester cord is approximated as non-moisture-sensitive material according to its micro structure. To confirm the approximation and for comprehensiveness of the research, commercial polyester cords (630 dtex x2) are investigated.

3.1.2 Rubber Compound

Table 3.2: Recipe of skim compound systems without fibres[phr]

Compound / *Ingredient*	*50 N660*	*50 N660 OH*	*20 N660*	*50 N339*	*50 N339 OH*	*20 N339*	*0 CB*
TSR 83/20 Start /Delta/ class2	*70*	*70*	*70*	*70*	*70*	*70*	*70*
SSBR2150/S / TC/DRY/ ML62/A	*30*	*30*	*30*	*30*	*30*	*30*	*30*
N 339	*-*	*-*	*-*	*50*	*50*	*20*	*-*
N 660	*50*	*50*	*20*	*-*	*-*	*-*	*-*
Treated distillate arom extr.	*5*	*5*	*5*	*5*	*5*	*5*	*5*
Zinc Oxide gran	*4*	*4*	*4*	*4*	*4*	*4*	*4*
Stearic acid	*2*	*2*	*2*	*2*	*2*	*2*	*2*
TMQ	*1.8*	*1.8*	*1.8*	*1,8*	*1,8*	*1,8*	*1.8*
Resocinol TECHN	*3*	*-*	*3*	*3*	*-*	*3*	*3*
HMMM Resin 65%	*2*	*-*	*2*	*2*	*-*	*2*	*2*
MBTS	*0,8*	*0,8*	*0,8*	*0.8*	*0.8*	*0.8*	*0,8*
SOLUBLE Sulfur OT 1	*2.5*	*2.5*	*2.5*	*2.5*	*2.5*	*2.5*	*2.5*

In order to understand the moisture uptake behaviour of calendered cord system, eight different skim compound recipes were developed. The natural rubber as technical specified rubber (TSR) and solution styrene-butadiene rubber (SSBR) were used in these recipes. All other ingredients such as activator, softener, anti-aging agents, accelerator and sulphur were identical, but filler type, filler content and resin content were varied. Further information is provided in Table 3.2.

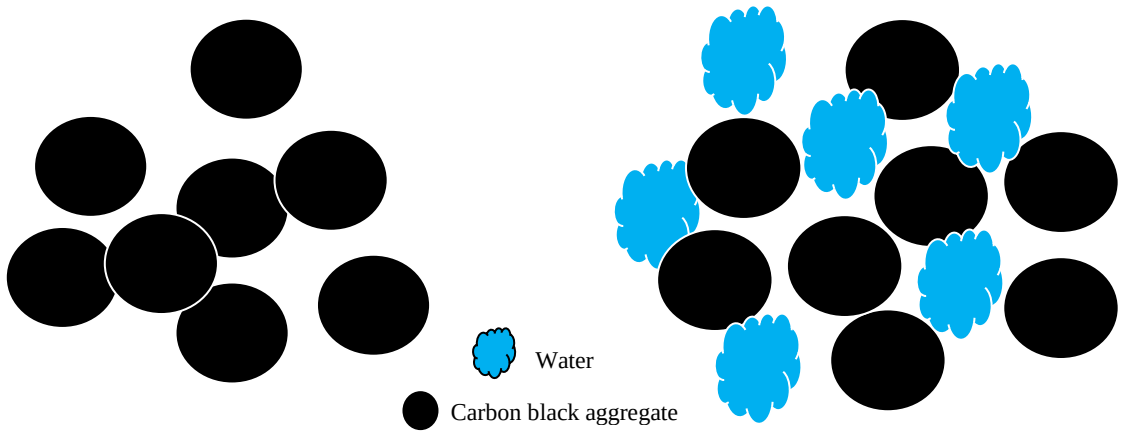

Figure 3.1: Carbon black network with water

Because of its large content within the system, the surface area of carbon black may dominate the moisture uptake behaviour of the rubber compound as shown in Figure 3.1. Table 3.3 shows the properties of the two types of carbon black in the skim compounds. The surface ratio between N339 and N660 is about 2.6, which means that at the same content, N339 has 2.6 time more contact surface with the moisture than N660.

Table 3.3: Properties of carbon black in the skim compound system

	N339	*N660*
BET surface area (NSA)	*91 m^2/g*	*35 m^2/g*
External surface area (STSA)	*88 m^2/g*	*34 m^2/g*

The resin content within the skim compound is not as large as the filler content. But due to its properties, resin may absorb moisture from the environment. The resin has been therefore removed from some of the skim compounds, in order to identify its influence on moisture absorption comparatively.

All the rubber compounds were mixed and then vulcanized at Continental according to the in-house standard. The rubber sheets were stored at low temperature (4°C) in order to prevent them from aging and any other pre-conditioning.

3.1.3 Rubber composites

Calendered materials from Continental Reifen GmbH, Hannover, Germany are utilised to study the moisture uptake behaviour of reinforced rubber and the influence of absorbed moisture on the mechanical properties.

The samples for the pull-out test and the peel test which aim to determine the influence of moisture on cord-to-rubber adhesion are prepared in the laboratory using the approaches described in section 3.2.2.2.3 and 3.2.2.2.4. The nylon cords from Shenma Industrial Co., Ltd, Henan, China with a construction of 1400 dtex x 2 and commercial rubber matrix are used on the sample.

3.2 Methodology development

3.2.1 Methodology for characterization of the moisture uptake behaviour

The moisture uptake behaviour is measured classically by using a climate chamber and a balance. The samples are put into the climate chamber to take up moisture under certain air condition for a certain time. Periodically, the samples are to be taken out of the chamber and weighed on a balance. With the aid of the weight, a curve can be built to show the mass changes versus time.

However, it is hard to get a flawless time plan to make sure that the samples are weighed in a precise time [103]. The mass change of the moisture uptake shows a nonlinear behaviour. That means that there is a short time window in which the sample should be measured more frequently, which can be seldom achieved manually, especially for the fibres which absorb the moisture very fast because of their large surface. Besides, the weighing process itself is also hard to be accomplished because of the low speed of the hand operation. The sample mass already changes very fast after it is taken out of the climate chamber. Therefore, it is hardly a stable, accurate value to be read.

Considering the weakness of the classical method, the moisture uptake behaviour of textile fibres, the rubbers and the rubber composite materials are measured in this work by simultaneous thermal analysis using a TGA/DSC device from Mettler Toledo, Columbus, USA, combined with humidity generator from proUmid GmbH, Ulm, Germany, (Humidity 0%- 90%, Temperature 20 °C- 60 °C), the so-called Sorption TGA.

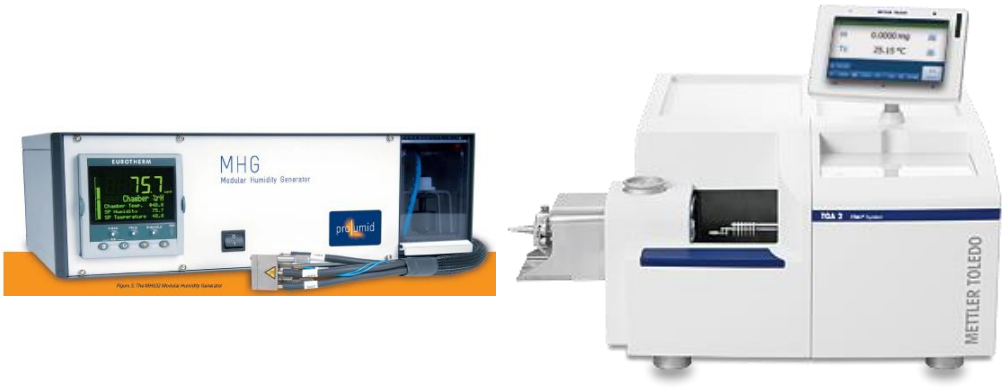

Figure 3.2: Sorption TGA, combination of a TGA/DSC 2 from Mettler-Toledo with the MHG from proUmid [104, 105]

In the simultaneous thermal analysis, the ultra-micro balance of the thermo-gravimetric analysis and the heat flow sensor of the differential scanning calorimetry are combined to detect the thermal events and the mass changes synchronously. With the help of heat flow

curve, which is an addition to the classical TGA measurement, the moisture uptake behaviour can be determined more precisely[105].

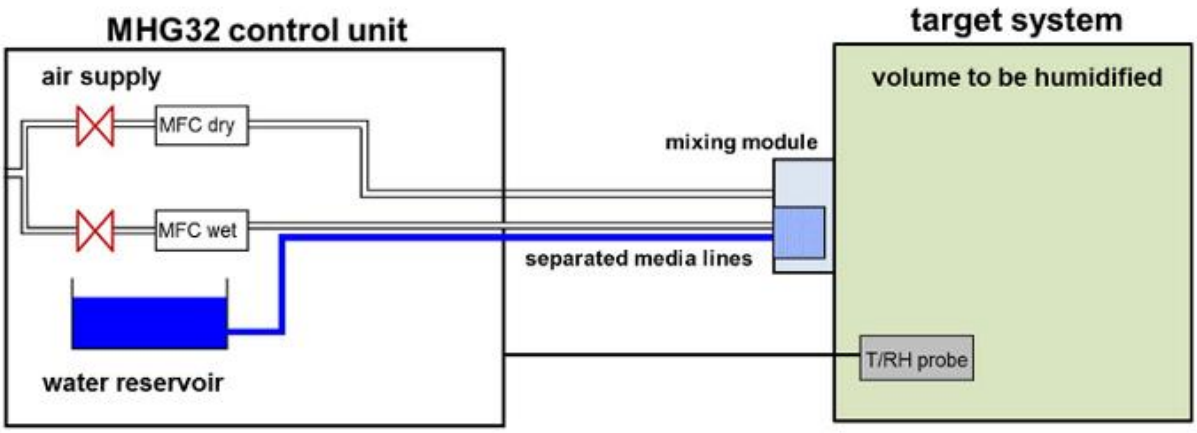

Figure 3.3: Schematic diagram of a MHG32 humidity generator from proUmid[104]

In order to simulate a storage condition with a specific temperature and air humidity, the humidity generator is connected to the TGA/DSC device. The generator consists of a central control unit, an external mixing module and a humidity sensor in the chamber. The control unit can monitor and regulate the flow rates of dry and wet gas. The nitrogen is used as flow gas to bring the moisture as wet flow into the mixing module and will be mixed there with the dry flow. The generated humid air is then supplied into the chamber directly. Compared to the standard instrument, in which the humid air with a certain target value is produced and then transferred in order to fill the chamber with a static speed, the dynamical regulation of the wet flow as applied here is much faster and more precise[104, 105].

3.2.1.1 Methodology for characterising fibre textiles

The fibre textiles are stored in the factory with a protection foil outside until they are supplied to the calender. Therefore, the influence of convection effects can be practically neglected. To check the influence of convection, a pre-test has been performed with the Sorption TGA. Before the measurement starts, the textile fibres were placed into a crucible with a volume of 150 µml to get the same form as the samples which are measured with the crucible. After that, the autoloader of the instrument is disabled and the samples of fibre textile without crucible are put on the balance manually.

In Figure 3.4, a sample without crucible has a higher moisture uptake speed than the one with crucible during the middle phase of the process due to the convection effect. This convection effect comes from the supply air which brings the moisture the into the test chamber. At the beginning phase there is no obvious different between the two curves. The

influence of the convection effect on saturation moisture content is also not so obvious as on the absorption speed in the middle stage of the sorption process.

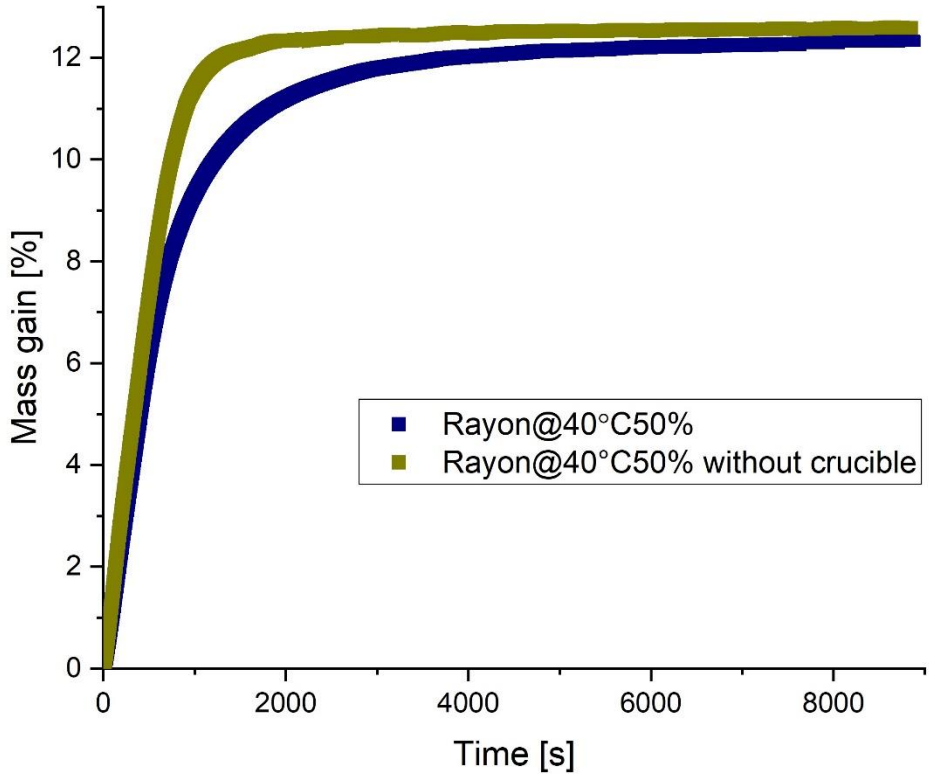

Figure 3.4: Pre-test to identify the influence of the convection effect

To avoid this convection effect, which may accelerate the moisture uptake, the crucible is used for all Sorption TGA measurements. The textile sample is cut down from the fabric cord and spiralled placed into the crucible, so most surface of the fibre is open to the air. Each sample has been cut into a same length of 100mm. The twist structure and the protection of the dip was inevitably broken by cutting the sample, which lead to an acceleration of moisture uptake at that cut position. This acceleration is minimized by using a long sample, which minimizes the proportion of the surface of the ends.

Besides, the Sorption TGA provides the possibility to dry the sample within the chamber at high temperature. Usually, rayon cords are dried in an oven at 105 ℃ for 60 minutes according to standard procedures. However, due to the humidity sensor of MHG which is placed in the chamber to monitor the humidifying, it is suggested to use a temperature below 60 ℃. Polyamide 66 cords and polyester cords are also dried in the Sorption TGA chamber directly at a temperature of 60 ℃ and 0% R.H. Due to the restriction of humidity from the

humidity generator, a humidity range between 20% and 90% within a range of temperature between 20 °C and 40 °C are chosen as measurement condition.

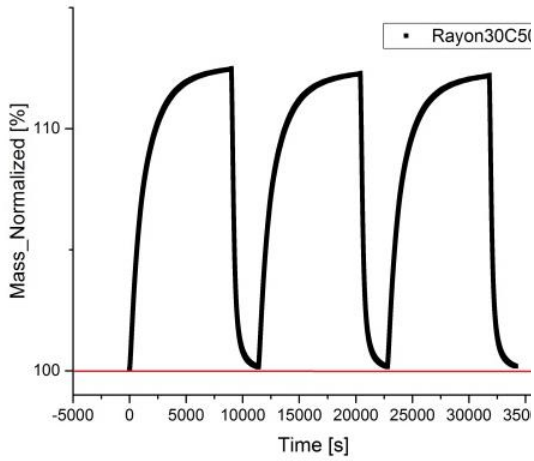

Figure 3.5: Wet- and dry process repeats by TGA/DSC

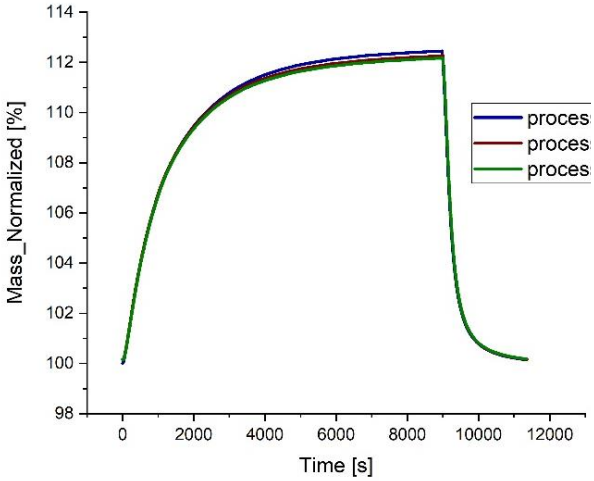

Figure 3.6: Overlapping of multiple wet- and dry processes

In order to guarantee the reproducibility of the measurement, multiple dry-wet processes are performed to ensure that there are only physical phenomena during the moisture uptake processes. Figure 3.5 shows the normalized mass change of rayon cord versus time under triple repeated wet (30 °C, 50% R.H.) dry (60 °C, 0% R.H.) process. The mass remains nearly the same after each wet-dry process as shown with help of the auxiliary line marked in red colour. In Figure 3.6, the mass change curves from all the three processes are shown overlapped, where the curve tendency is nearly the same. This indicates that only physical phenomena occur within the sample, without any chemical changes and material damages during the multiple wet-dry processes, and that the moisture uptake process is reversible after the drying process.

3.2.1.2 Methodology for characterizing rubbers

The analytical objects are both unvulcanised and vulcanized rubber compounds. The sample is cylindrically punched out with a thickness of 1 mm and a diameter of 6 mm. The sample is vertically placed into the crucible on its round edge as shown in Figure 3.7. This ensure as much contact surface with the moisture as possible.

To avoid premature vulcanization of rubber compounds, high temperatures are avoided during the drying process. The temperature of 23°C and dry flow gas are used to help with the drying, the wet phase is also extended from several hours to one week according to the pre-tests.

Figure 3.7: Sample of rubber for Sorption TGA measurement

3.2.1.3 Methodology for charactering rubber composite materials

The sample is cut from a calendered sheet of rubber-textile composite material with a length of 50mm, which fits the volume of the crucible. In order to ensure the reproducibility, each sample has the same number of openings because of the weft cords (Figure 3.8). The weft openings are blocked with glue before the measurement to prevent the moisture diffused from the openings, as shown in Figure 3.9. Besides, in order to obtain the diffusion velocity of the humidity through rubber, measurements with the sample, on which all the openings (weft and both ends) are blocked, are also applied.

Figure 3.8: Opening because of the weft cords

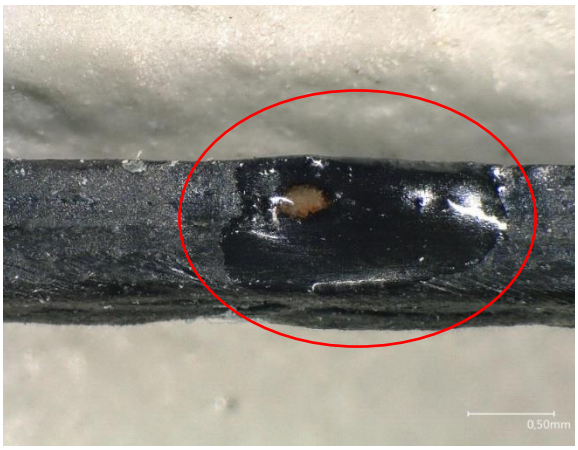

Figure 3.9: Weft opening treatment with glue

To reach the saturation point, the duration of the measurements is extended to one week. Same climate conditions as the measurements on textile cords and rubbers are applied.

3.2.2 Methodology for characterization of the influence of moisture

3.2.2.1 Mechanical properties

For the mechanical properties, load-elongation testing, dynamic mechanical analysis (frequency sweep) and creep testing are considered

3.2.2.1.1 Cross section of the sample

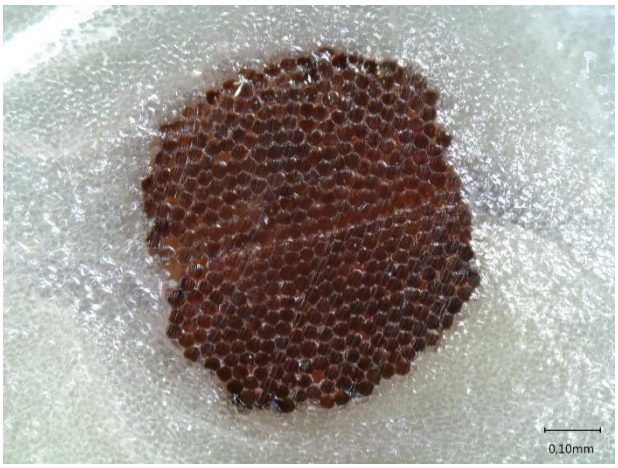

Figure 3.10: Cross section of PA6.6 cord

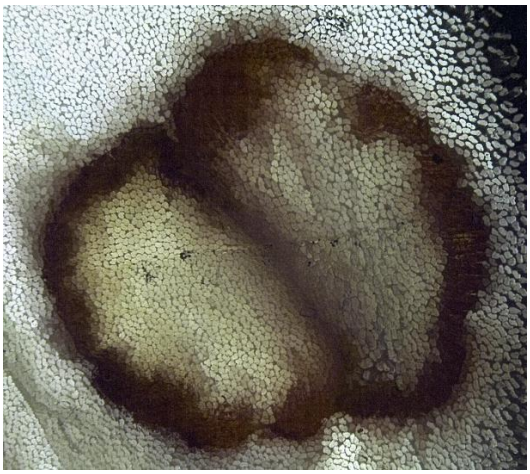

Figure 3.11: Cross section of rayon cord

The cross section of the sample is necessary for calculating the load. Figure 3.10 shows the cross section of a PA6.6 cord, which is cured in resin. The cured sample is then observed under the optical microscope. In Figure 3.11, the cross section of a rayon cord is shown. The rayon cord with dip coating is pushed through a metal holder together with the surrounding cotton fibres. Under the optical microscope, the coating boundary can be detected.

As shown in Figure 3.10 and Figure 3.11, the diameter of the cord can be determined by calculating the summation of each filament, the diameter of a single filament can be determined with help of software. However, it is hard to precisely detect the thickness of the dip coat, because of its non-homogeneous distribution.

Considering the geometry from Figure 3.10 and Figure 3.11, the cross section of textile cord can be regarded as round. With the density from the manufacturer, the diameter can be calculated with Eq. 3.1.

$d = 2\sqrt{\frac{m}{\pi \rho l}}$	*where*	*m: mass of the sample* *ρ: density of the cord* *l: length of the sample*	*Eq. 3.1*

3.2.2.1.2 Load-elongation testing

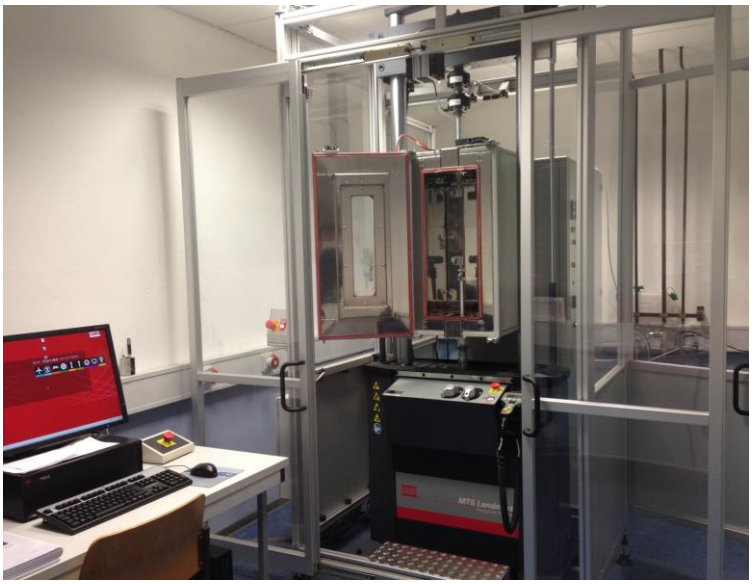

Figure 3.12: Load frame with environmental chamber of MTS Systems from MTS Systems Corporation, Minnesota, USA

Figure 3.13: Pneumatic tension clamps

According to the standard of ASTM D885, DIN53815 and DIN51220, the load-elongation test is applied on a tensile tester. In order to observe the influence of moisture, a servo-hydraulic load frame with environmental chamber from MTS Systems Corporation, Minnesota, USA (Figure 3.12) is chosen. To meet the requirement of the standards, changes to such as new sensor are applied to the machine [106]. For fabric cords the pneumatic tension clamp is used according to the standard [107-109]. (Figure 3.13)

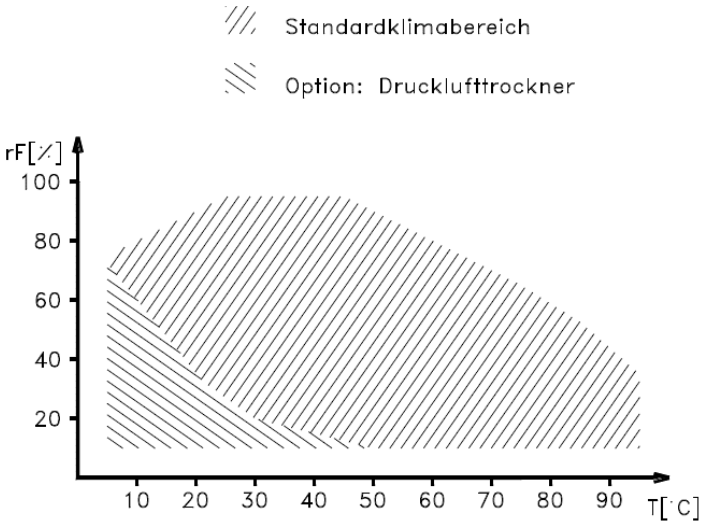

Figure 3.14: climate range of the environmental chamber of MTS tester[106]

Figure 3.15: sample storage with desiccator filled with silica gel

One of the most important reason to choose the load frame from MTS is the climate chamber. With the help from it, the storage of samples under certain air condition is realized. But due to the big volume of the chamber, the velocity of conditioning is not satisfactory. Therefore,

the dry process before the moisture load is separated from the testing procedure. As shown in Figure 3.15, the desiccator filled with desiccant (silica gel) is used to storage the sample after drying process using the oven. Classically by using the desiccator, only a few silica gels are used under the sample to dry the inner air. After pre-tests under these conditions, it has been confirmed that the speed of recovery to the low humidity level after the opening of the desiccator is very low and can be neglected,

Table 3.4: Storage time to get target moisture content for rayon cord at 40 °C 30% [s]

moisture adsorbed%	*1%*	*2%*	*3%*	*4%*	*5%*	*6%*
1840x2 Raw	*65*	*140*	*230*	*343*	*495*	*727*
1840x2 Dipped	*101*	*232*	*388*	*590*	*880*	*1400*
1220x2 Raw	*42*	*93*	*153*	*229*	*329*	*481*
1220x2 Dipped	*73*	*161*	*269*	*413*	*624*	*1035*

According to the standard procedure, the samples are removed from the drying desiccator immediately before mounting in the tensile tester. The tensile test starts within 10 seconds after the sample is taken out of the desiccator including the whole clamping process for the dry sample. For the samples with humidity, the dry samples from the desiccator are also used to ensure the reproducibility of the experiment. The results from the Sorption TGA measurements are used to define the environment setting within the chamber. Table 3.4 shows the example of rayon cord. The dry sample is stored in the chamber under the setting until the target moisture content is reached. After that, the load-elongation test is started immediately with a clamping length of 250mm under an extension speed of 300mm/min.

3.2.2.1.3 Dynamic mechanical analysis

The aim of the dynamic mechanical analysis (DMA) is to study the influence of moisture on dynamic mechanical properties. The measurements are performed on a DMA Q800 device with DMA-RH accessory from TA Instrument, New Castle, USA. The sample is fixed inside the DMA with a tension clamp.

Figure 3.16: The TA Instruments Q800 Dynamic Mechanical Analyser and DMA-RH Accessory[110]

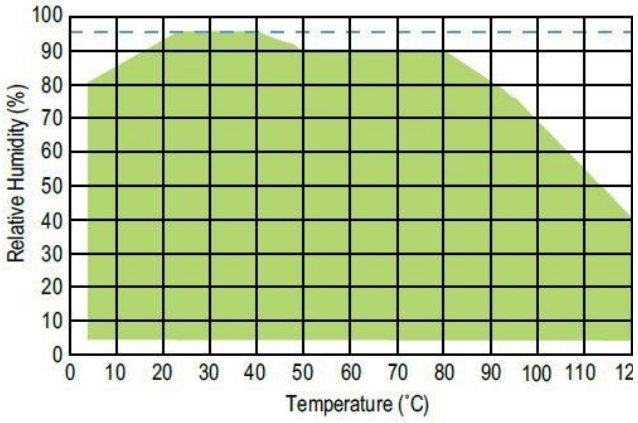

Figure 3.17: Environment range of the DMA-RH Accessory[110]

As shown in Figure 3.16, the DMA-RH Accessory (2) is a precision environmental system, which has an accurate control of temperature and relative humidity for DMA measurements. Once the measurement starts, the defined value is transferred from the DMA to the accessory. The gas is pre-heated there and mixed with a prescribed ratio. The humid air is then delivered to the DMA chamber (1) through the heated vapour-transfer line (3) to achieve the target humidity. The vapour-transfer line is maintained at a temperature above the dew point of the humidified gas to prevent the occurrence of condensation[110].

However, compared to the MHG on the Sorption TGA, the DMA-RH Accessory has limitations on the rate of heating (1 °C/min) and humidifying (2%/min), since it uses always the pre-calculated ratio of dry- and humid gas to fill the chamber, with no consideration on the present state. On the other side, the MHG can monitor the humidity and regulate the flow ratio online, it uses higher humid rates to approach the target and then lower the rate to get to the set value precisely.

Due to the limitations of the DMA-RH Accessory, a similar method as by load-elongation testing is not suitable, because the regulation takes usually more time than the storage itself. Nevertheless, the data from Sorption TGA measurements can still be used to help with defining the testing procedure. In Figure 3.18, the saturation points shown versus temperature and relative humidity. Since the saturation point is the maximum value of mass increment due to the moisture uptake, the mass of the sample will be stable after the saturation is reached. Storing the sample under the saturation conditions may help with overcoming the long regulation time of the DMA-RH Accessory.

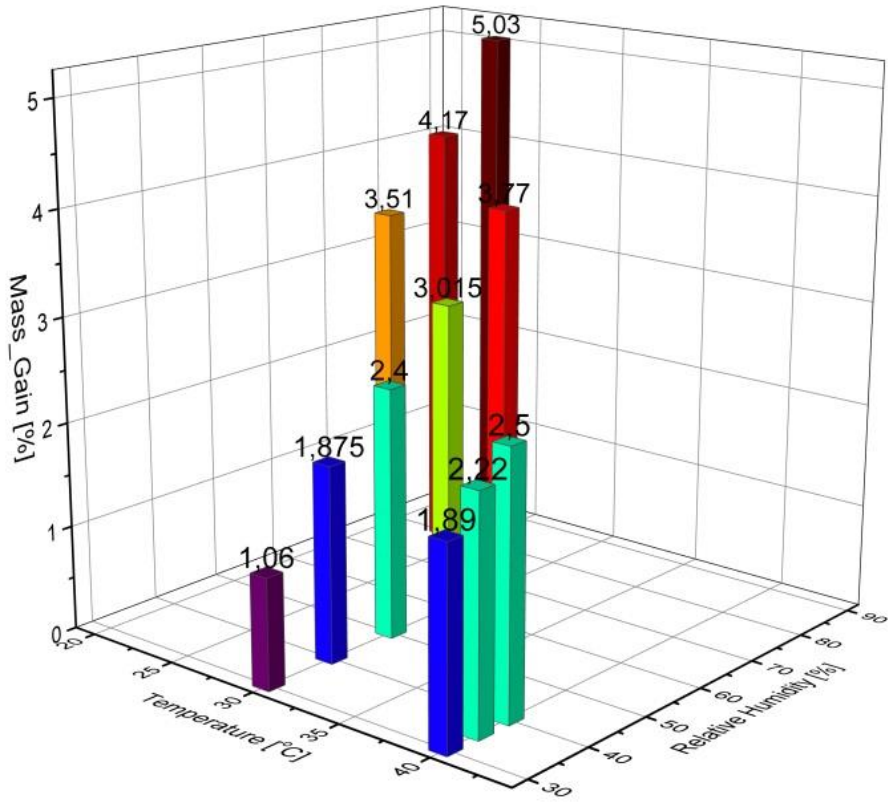

Figure 3.18: Relation between saturation point (%), temperature (°C) and relative humidity (%) for PA6.6 cord

The DMA Multi-Frequency module is chosen. The sample will be dried and then stored in the desiccator to keep from humidifying, and then it is taken out and clamped at once. The DMA-RH Accessory starts to fill the chamber with dry gas immediately once the chamber is closed so that the relative humidity drops down to 0%. The procedure is defined with an isothermal time to ensure the saturation. After the saturation is reached, the frequency sweeps from 10^0 Hz to 10^2 Hz are performed.

3.2.2.1.4 Creep test

The creep test is also performed on the DMA Q800 device with DMA-RH accessory from TA Instrument (Tension clamp). Same as by the frequency sweep, the DMA-RH Accessory is also applied. The data from the Sorption TGA measurement as in Figure 3.18 are also used to help with setting up the measurement.

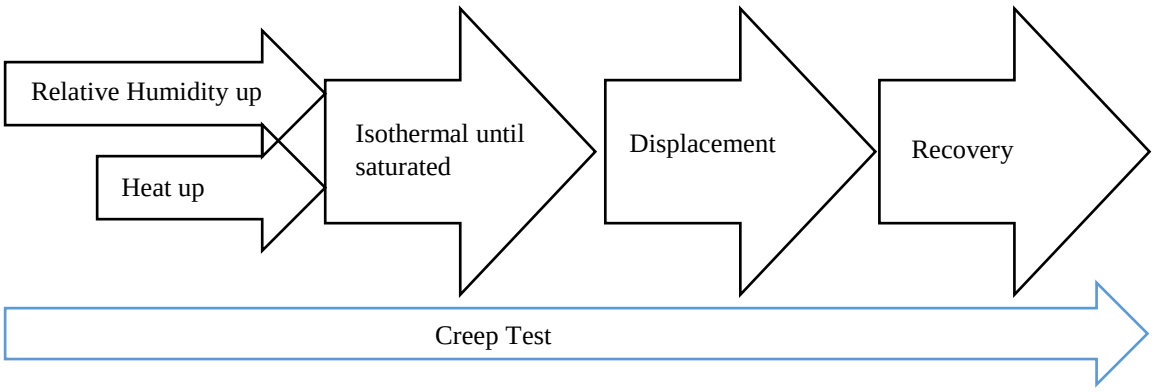

Figure 3.19: Test procedure of creep test

The test procedure of the creep test is shown in Figure 3.19. The DMA-RH Accessory uses pre-heated gas with humidity to fill up the chamber, which means that the humidity and the temperature are settled at same time. The isothermal step starts only if both temperature and humidity have reached the prescribed value. The length of the isothermal step is defined according to the Sorption TGA data, so that the saturation is achieved after this step and the moisture content in the sample stays stable during the creep test.

The creep test is composed of two parts: Firstly, a load of 60 MPa is applied for a specific time (80-120 min), so that the creep behaviour of the sample is observed. In the second part, the load will be removed to investigate the recovery.

3.2.2.2 Influence of moisture on rubber-cord adhesion

The adhesion is one of the most important factors for the fibre reinforced rubbers. Classically, the pull-out test is applied to test the adhesion between rubber and metal cord, the peel test for the rubber-textile interaction.

3.2.2.2.1 Dip coat

To observe the dip coat during the moisture uptake measurement, images with different magnifications are taken periodically by the optical microscope (OM) VHX6000 from KEYENCE, Osaka, Japan. The depth composition function contributes with full focus on the images, also on the uneven surfaces[111].

Figure 3.20: Optical microscope VHX6000 from KEYENCE [111]

Figure 3.21: Textile cord fixed on the glass slide

The dry sample of textile cord is fixed on a glass slide with methyl acrylate glue and is marked on a certain position. Then images will be taken with the OM on that position. The sample is then placed into the climate chamber to get the moisture for a certain time. Images are periodically taken with the OM on the same marked position to check if there are any changes on the dip coat outside the textile cord as shown in Table 3.5.

Table 3.5: Test setup of optical microscope

Textile cord	*PA6.6 and rayon*
Image magnifications	*300x and 1000x*
Storage time	*0, 1h, 2h, 4h, 24h and 72h*

3.2.2.2.2 X-Ray micro computed tomography

Before the destructive tests, such as the pull-out test or the peel test, a non-destructive test like X-Ray inspection is applied. The high-resolution computed tomography with X-Ray is a valuable tool for failure analysis. With the 3D function, the failure caused from the moisture can be found precisely.

The X-Ray micro-computed tomography (micro CT) is performed on the CT-Compact from ProCon X-Ray GmbH, Sarstedt, Germany (Figure 3.22). As shown in Figure 3.23, the X-Ray beam comes from the source horizontally. In the middle, there is a rotating holder on which the sample is placed. On the other side, the panel detector collects the X-Ray information.

Figure 3.22: CT-Compact from ProCon X-Ray GmbH[112]

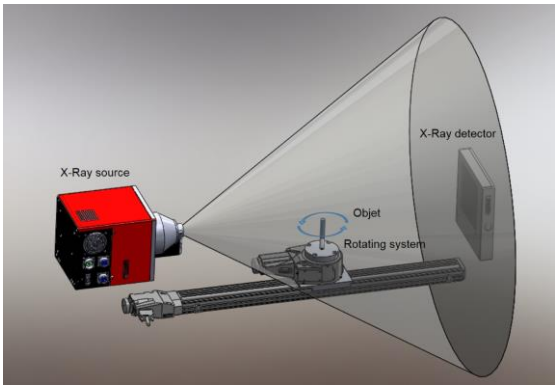

Figure 3.23: X-Ray micro computed Tomography[113]

Two different sample preparation methods for the micro CT test are used. Firstly, the cords are dried under standard condition, put into the climate chamber, and stored there for certain time under the conditions according to the data from Sorption TGA to get the moisture level desired. The result of the storage is verified by the moisture analyser from Mettler Toledo. As a second step, the cords are taken out of the climate chamber and immediately placed into the mould as shown in Figure 3.24. The sample is vulcanized together with the rubber compound. The benefit of this method consists in the shorter storage time to get the target humidity in the sample, because of the faster moisture uptake of the fabric cords. However, even at higher speed there is an unavoidable limitation: the textile cord loses moisture also with a higher speed of handling after it is taken out of the chamber and especially during the vulcanization under high temperature and pressure.

Figure 3.24: Curing Mould for pull out test

Figure 3.25: Pull out test with universal tester from ZWICK[114]

Considering the limitation of the method with the fabric cords, a second method with the calendered materials is applied. The sample is cut down from a large sheet of calendered material and placed into the climate chamber to get the moisture level. The storage condition is also defined from the data of Sorption TGA measurements. Due to the property of calendered material, the storage time is extended from several hours to 14 days (example for 40 °C and 90% R.H.). After the storage, the sample is taken out of the climate chamber

and immediately vulcanized under prescribed conditions. In order to prevent the loss of moisture, the size of the sample is prepared as large as possible (about DIN A4 size) and the sample for the micro CT is cut down from the middle of the sheet.

3.2.2.2.3 Pull-Out Test

The pull-out test is one of the classical methods to test the adhesion, especially for testing the adhesion between rubber and steel cord. In the pull-out test, the pull-out force of the reinforcement material (cord) out of the vulcanized rubber block is determined as the static adhesion. In order to suit the requirement of the test, adjustment on the mould is done. Due to the strength of the fabric cords, the adhesion surface (length) of rubber-cord is decrease to 0.5 mm to prevent the tension fracture (see Figure 3.26 and Figure 3.27).

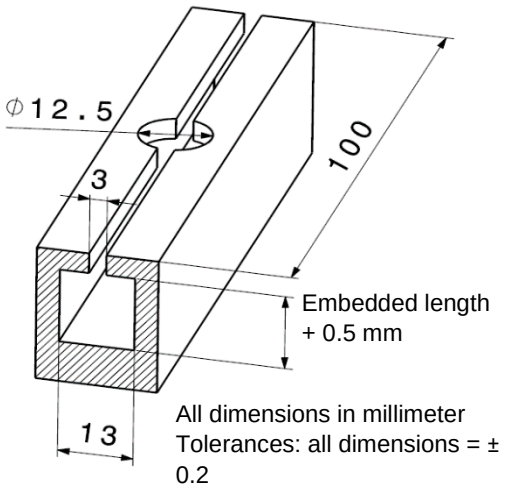

Figure 3.26: Specimen holder for pull-out test

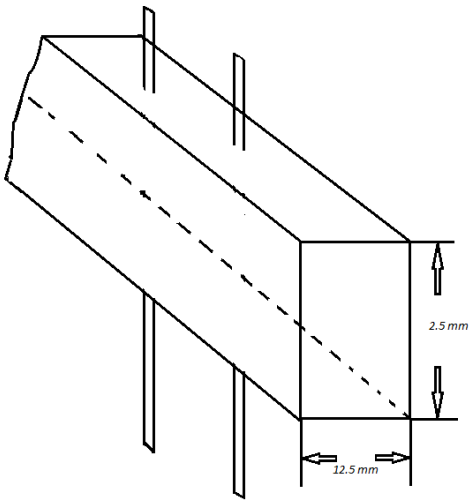

Figure 3.27: Sample of pull-out test

The fabric cords are dried in the desiccator filled with desiccant for at least three weeks. The cords are treated immediately after taken out of the desiccator to assemble the dry sample. Another sheet of cords is kept in the clime chamber to get moisture levels between 40 °C and 90% R.H. for 24 hours, so that they are saturated. The „wet" samples are assembled with the humid cords. Both sorts of samples are vulcanized immediately after assembly.
The vulcanization conditions are:

Time: 10minutes ± 10 seconds,

Temperature: 170 °C ± 2 °C.

The measurement is performed on a Tensile Tester Z010 from ZWICK, Ulm, Germany, equipped with pneumatic jaw clamps and with a pull-out speed of 125 mm/min ±5 mm/min. The test is done according to ASTM D2229 and ASTM D1871[115, 116].

3.2.2.2.4 Determination of strip adhesion (Peel Test)

The adhesion between rubber and its reinforcement is normally determined by performing a peel test in which the separating forces as well as the coverage are evaluated. The sample is assembled according to Figure 3.28 in five layers: Two outer layers of calendared reinforcing fabric cords, two inner layers which composed of test compounds and test fabric cords and in the middle the separate foil. The completed sample is shown in Figure 3.29.

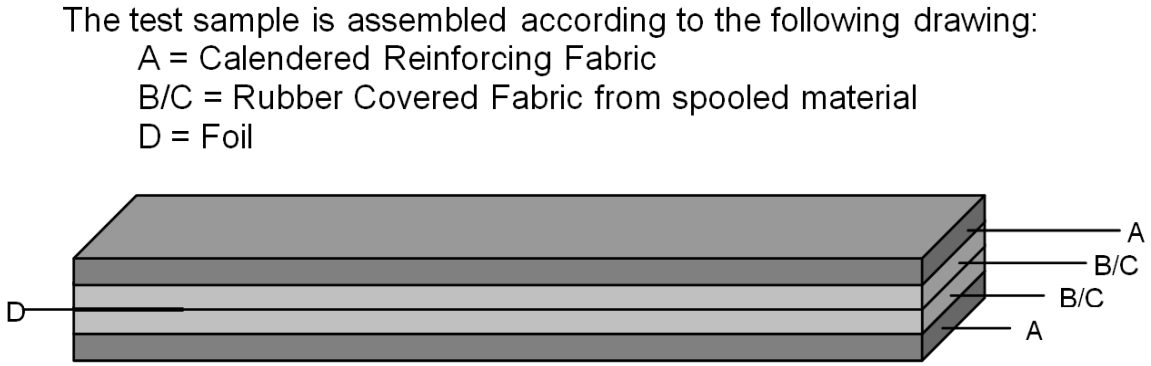

Figure 3.28: Sample structure of peel test

Similar as in the pull-out test, the calendered materials are dried in the desiccator to build the dry sample. For the sample with humidity, the calendered materials are kept in the climate chamber at 40 °C and 90% R.H for two weeks. Both samples are assembled and vulcanized without delay.

The sample is vulcanized according to the condition in 3.2.2.2.3 in the mould shown in Figure 3.30. After curing, the samples are parallelly cut to the cords to a width of 25 mm ± 0.5 mm.

Figure 3.29: Sample of peel test

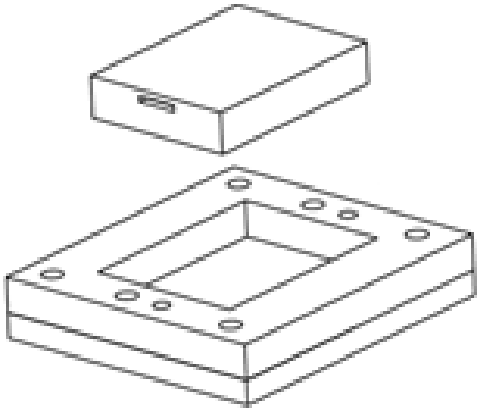

Figure 3.30: Curing mould for peel test

The peel test is performed with a Tensile Tester Z010 from ZWICK with pneumatic jaw clamps. The traverse speed of the tensile tester is 100 mm/min with a separation length of 40 mm (see Figure 3.31). During the test, the separating force is recorded, the median value of all the increasing adhesion force peaks is calculated for each measurement. The static adhesion is the average of the median value from all the three tests. The measurement is set up according to ASTM D885MA, DIN 53530, Din ISO6133 and ISO 36[107, 117-119].

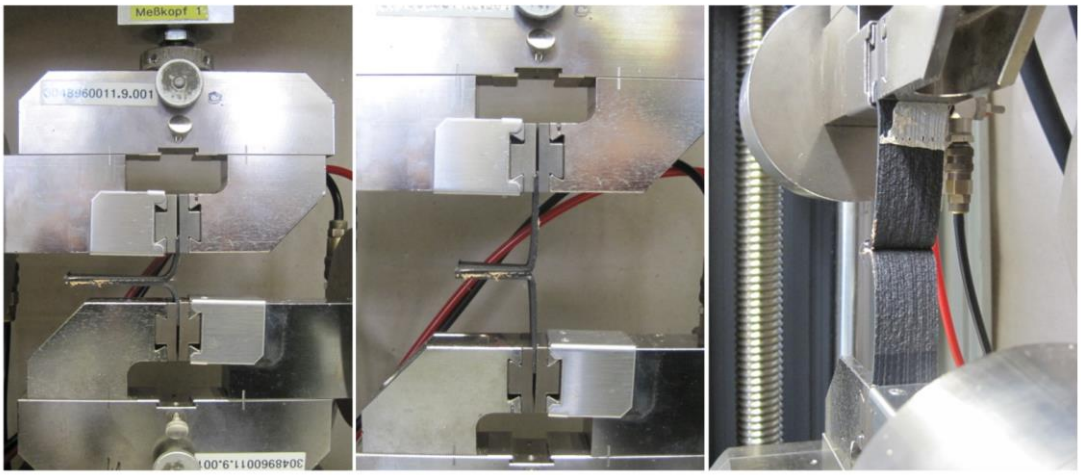

Figure 3.31: Peel Test with ZWICK Z010

3.2.3 Summary

In this section, the test methods to characterise the moisture uptake behaviour and the influence of absorbed moisture on mechanical properties are introduced. According to the results of pre-tests and considering the features of the research objectives, adjustments on the methods are performed in order to meet the requirements. The methods development consists in three parts: a) the classical methods are extended with humidity function; b) the test procedures are adjusted considering the moisture absorption process; c) a special sample preparation is performed to suit the requirement of the research.

More test accuracy compared to the classical methods can be achieved with the enhanced methods. This accuracy has a significant importance for the scientific research. The reproducibility of the measurements and inferences can be guaranteed by considering the extra requirements associated with moisture and adapting the method to suit them.

4 Characterisation of moisture uptake behaviour

In this chapter, the results of moisture absorption experiments on reinforcing materials, rubbers and reinforced rubbers are illustrated and discussed.

The moisture uptake behaviour of three kinds of textile tyre cords are studied. Experiments are performed under different environment conditions according to the working conditions of the instrument. One of the most important objectives of this research is to determine the relation between environment conditions and the absorbed moisture amount. With the Sorption TGA supported by the humidity generator, the moisture absorption process can be monitored without the impact factor of the classical method such as the accuracy problem of manual weighting and the fluctuation of the condition caused from opening the climate chamber. The relation between moisture content, storage time, temperature and relative humidity illustrated in this chapter can be used as basics for mathematical modelling and further investigation on mechanical properties.

For the rubber matrix and the rubberized textile cords, the experimental time are prolonged to obtain the view of the complete moisture absorption process. Since rubber is a complex system, it is reasonable to study the influence of different ingredients on moisture absorption behaviour. For the rubberized textile cords, the influence of opened ends on the moisture absorption is noteworthy. The experiments are performed therefore with closed and open ends to identify the influence of the ends.

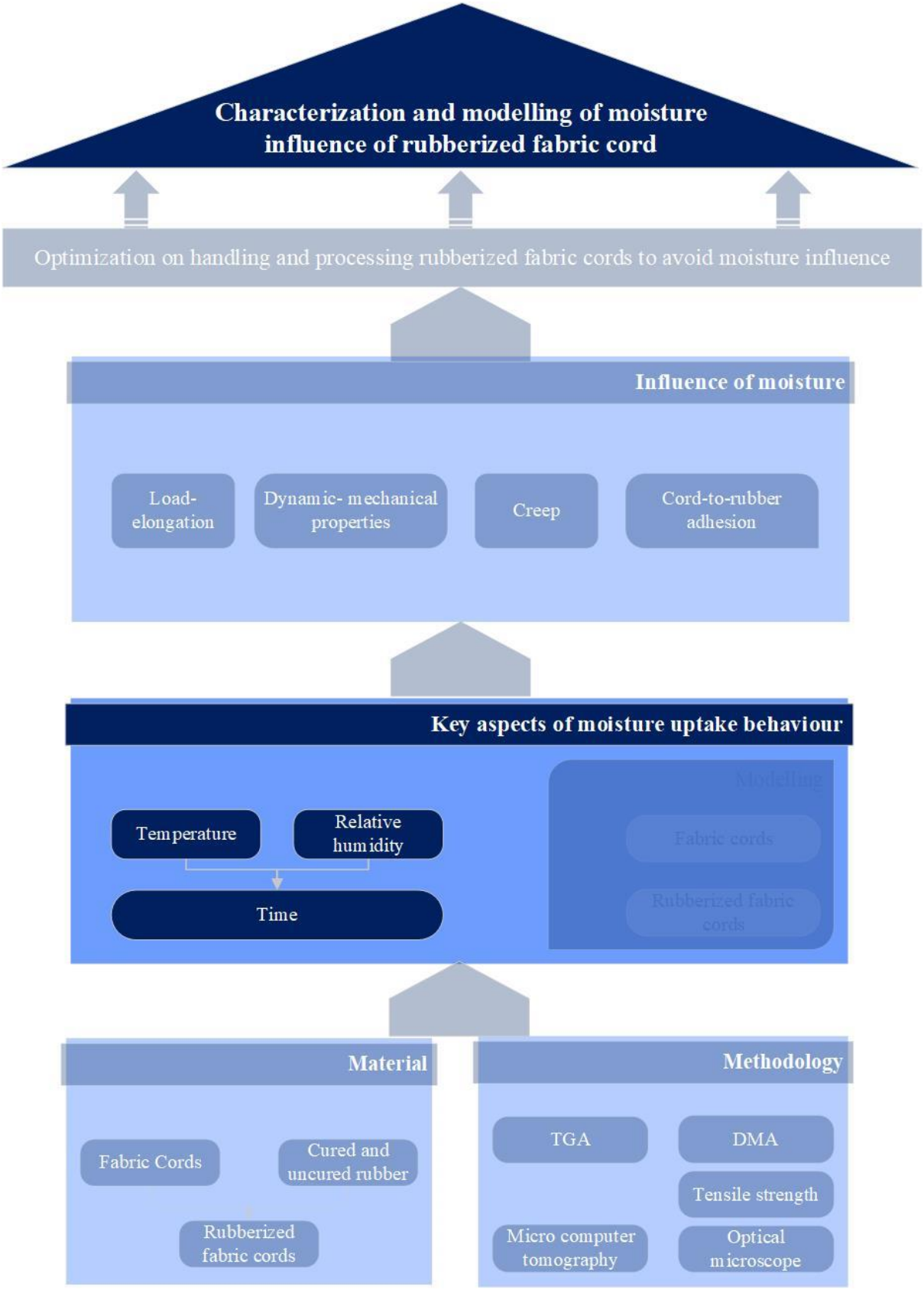
Characterization and modelling of moisture influence of rubberized fabric cord
Optimization on handling and processing rubberized fabric cords to avoid moisture influence
Influence of moisture
Load-elongation
Dynamic- mechanical properties
Creep
Cord-to-rubber adhesion
Key aspects of moisture uptake behaviour
Temperature
Relative humidity
Time
Modelling
Fabric cords
Rubberized fabric cords
Material
Fabric Cords
Cured and uncured rubber
Rubberized fabric cords
Methodology
TGA
DMA
Tensile strength
Micro computer tomography
Optical microscope

4.1 Textile Cords

4.1.1 Rayon cords

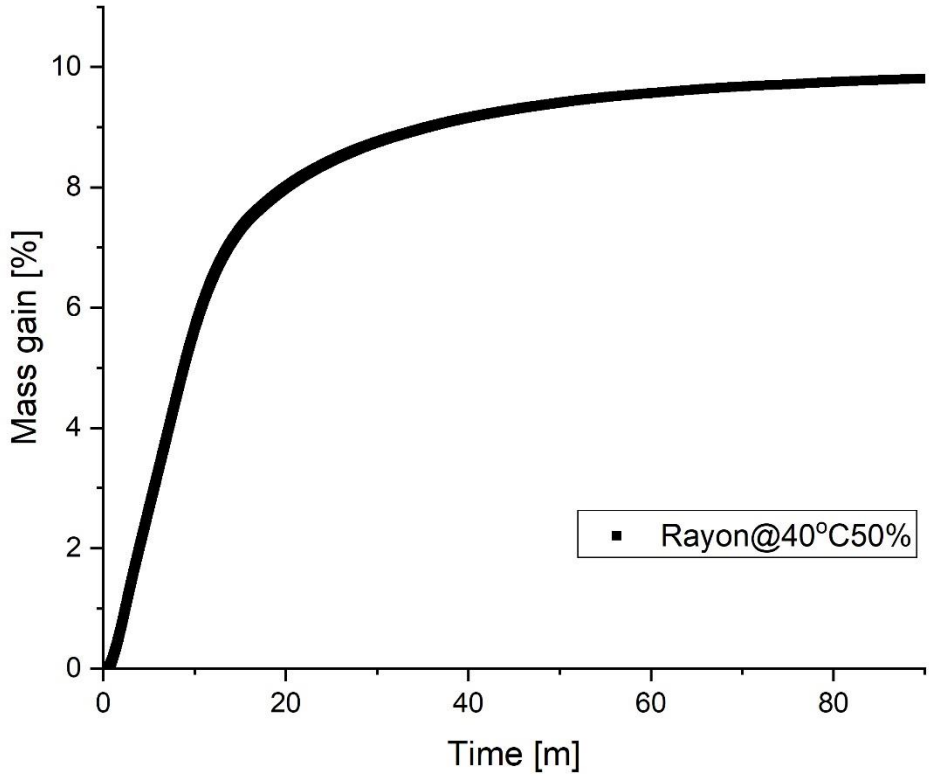

Figure 4.1: Sorption TGA curve from moisture content determination of rayon cord at 50% R.H. and 40 ℃

According to the methods mentioned in section 3, the moisture content in the rayon cords are determined with the thermal gravimetric analysis with help of a humid generator. The RFL treated rayon cord was dried firstly in the oven at 150 ℃ for 60 minutes. The Sorption TGA measurement which is set to 40 ℃ and 50% R.H. starts after the sample is placed into the Sorption TGA chamber. The mass of the specimen is recorded every second and forms a curve which illustrates the mass changing tendency from dry specimen to the saturation.

The real time mass of the specimen is calculated with *Equation 2.11* to get the mass gain resulted from moisture absorption in percent. The absorbed moisture content against time is plotted in Figure 4.1. It is observed that the specimen absorbs moisture rapidly from the environment during the first stage in which the curve has nearly a linear slope. The velocity of absorption decreases after the first stage until reaching the saturation point after a longer period. No more moisture is absorbed after the specimen is saturated and the mass remains the same all the time.

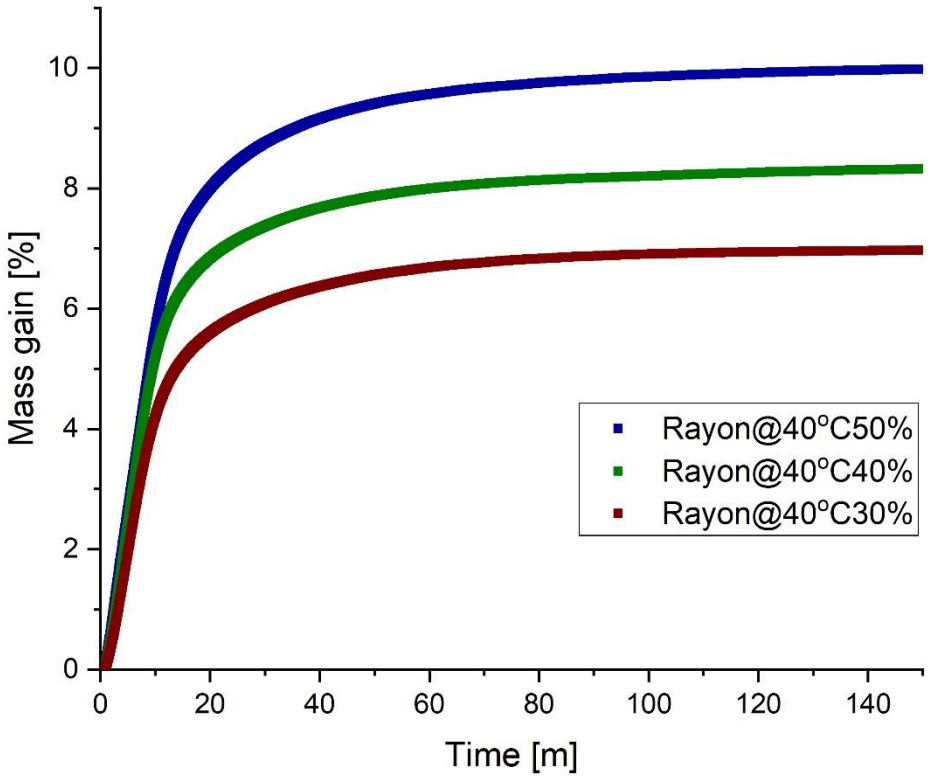

Figure 4.2: Moisture content determination of rayon cord at 30%, 40% and 50% R.H. and 40 °C

Figure 4.2 illustrates the absorbed moisture content in percent at 40 °C but 30%, 40% and 50% relative humidity. In the first stage, all the three curves have nearly the same slope until the end of the linear stage. In this stage, most of the moisture absorption is contributed by the surface of sample. Since all the samples have nearly the same geometry, the moisture absorbed in this stage vary therefore no much. After the curve at 30% relative humidity firstly leaves the linear stage with its slope starts to decrease, the second and the third curves remain the stage and hold the same slope until each of them reaches the stage ends respectively. All the three curves grow with a decreasing velocity until the plateau, which means a slope of value 0.

The slope of the curves indicates the velocity of the mass changes. The higher and linear slope in the first stage represent an obvious higher speed of mass increasing which is resulted from the moisture absorption. The saturate state is reached respectively from different curves in which the mass of the specimen stays steady.

Since the three experiments vary only on relative humidity, the different relative humidity under the same temperature means different moisture content in the air. According to section 2.2.1.1, the amount of moisture which can be absorbed depends on the absolute moisture

content in the air. The more moisture the air contains, the higher the saturation point lies. It explains the plateau of the curve at 50% lies above the other two curves.

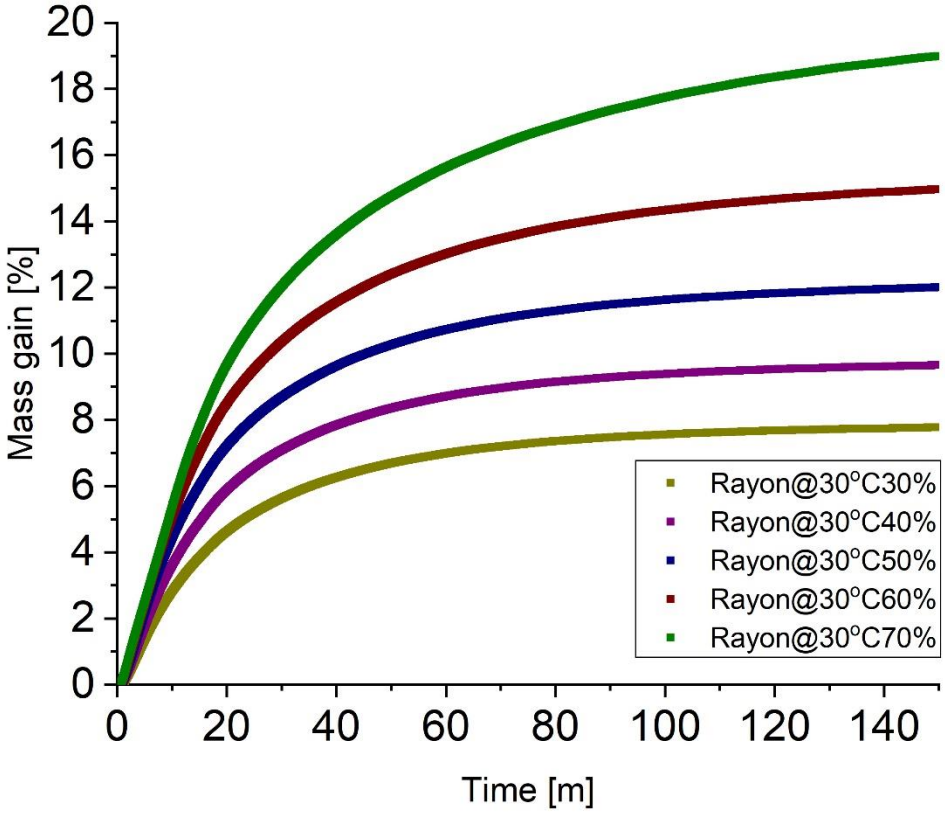

Figure 4.3: Moisture content determination of rayon cord at 30%, 40%, 50%, 60% and 70% R.H. and 30 ℃

The results of experiments with rayon cord specimens at 30 ℃ and 30%-70% relative humidity is illustrated in Figure 4.3. The curves have similar tendency as the curves from the experiments at 40 ℃. The specimen under lower relative humidity finishes the first stage earlier than the one under higher relative humidity. After the specimen enters the second stage, the velocity of absorption starts to decrease, the slope of the curve is also decreased so that is lower than other curves with higher relative humidity.

Since the moisture content in the air depends on the relative humidity at the same temperature, the specimen at 70% can absorb obviously more moisture than the other from the environment. In comparison to the results at 40 ℃ in which the specimens have been also stored 150 minutes under environment condition, the curves at 30 ℃ failed to reach the saturation, especially the curve at 60% and 70% relative humidity. The specimens under these conditions need more time to get saturated because of the diffusion characteristics according to Fick's law.

In Figure 4.4, the result of the Sorption TGA measurements at 20 °C and various relative humidity are plotted. The curves show a similar behaviour as in Figure 4.2 and Figure 4.3. The specimen under higher humidity can absorb significantly more moisture, but due to the time limit, the saturation cannot be reached. The tendency of mass increasing at the end of the experiment is also distinctly different from the curves at 30 °C and 40 °C, and not only the ones with high relative humidity. Thus, the specimens at 20 °C need more time to get the steady plateau which means the saturation point.

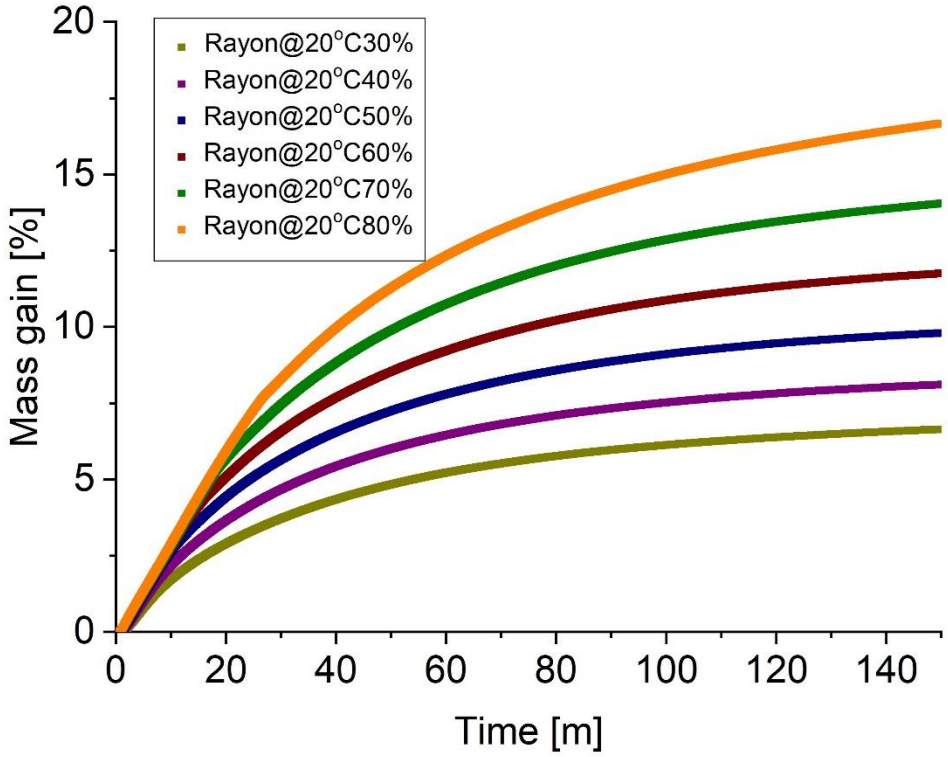

Figure 4.4: Moisture content determination of rayon cord at 30% - 80% R.H. and 20 °C

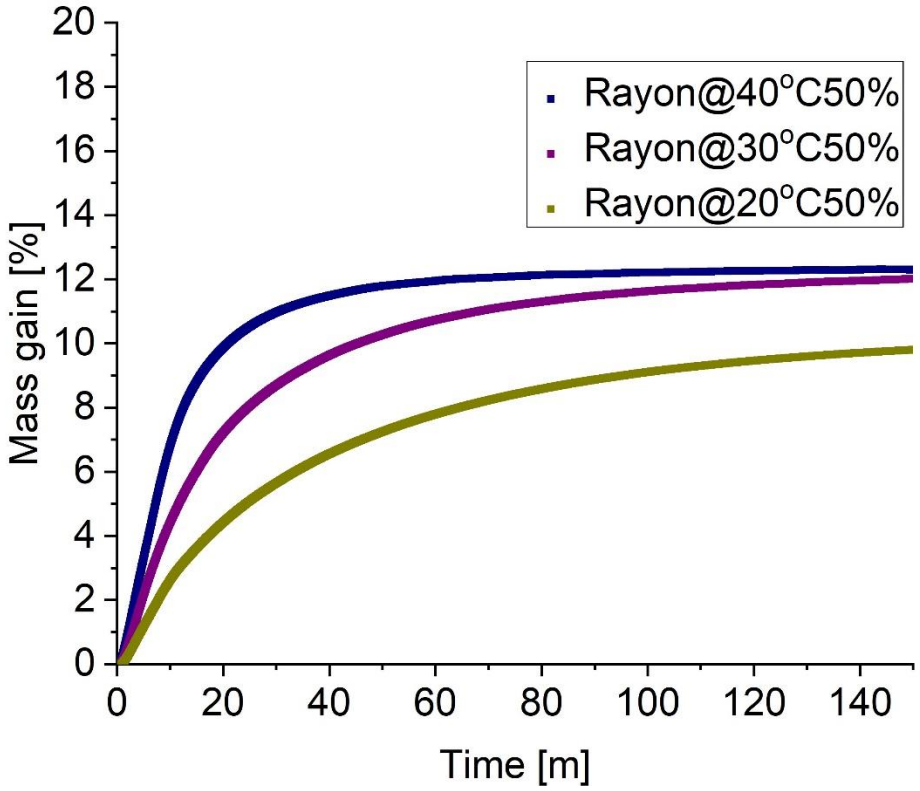

Figure 4.5: Results of Sorption TGA measurements at 50% relative humidity, 20 °C, 30 °C and 40 °C

The influence of temperature on moisture uptake behaviour at 50% relative humidity and various temperatures from 20 °C to 40 °C is shown in Figure 4.5. All the three curves tend to reach the similar saturation point which is marked with the plateau. In Figure 4.5, the curve which describes the moisture uptake behaviour of rayon cord at 50% relative humidity and 40 °C has reached the steady stage after about 60 minutes. It takes about 140 minutes for the specimen at 30 °C. The specimen at 20 °C fails to reach the plateau within the experiment time of 150 minutes.

At the end of the measurement, both specimens at 30 °C and 40 °C stop to absorb moisture from the environment and remain in a steady state. The specimen at 20 °C is still increasing its mass with a decreasing velocity, but shows the tendency to reach the plateau in a coming time.

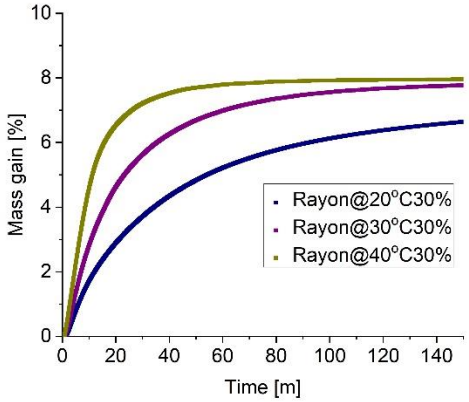

Figure 4.6: Results of Sorption TGA measurements at 30% relative humidity, 20 °C, 30 °C and 40 °C

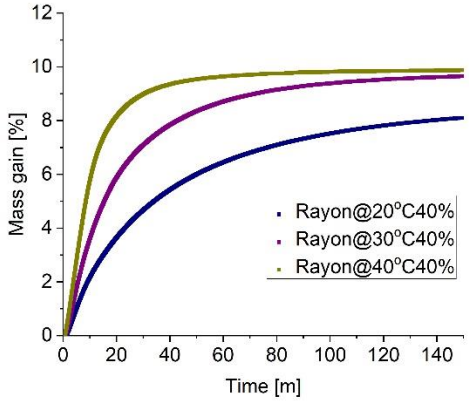

Figure 4.7: Results of Sorption TGA measurements at 40% relative humidity, 20 °C, 30 °C and 40 °C

Similar tendency can be found in all the results from Sorption TGA measurements under different environment conditions as illustrated in Figure 4.6 and Figure 4.7. L. Coutinho extends the experiment with environment condition at lower humidity area (10% and 20%) with higher temperature (50 °C and 60 °C) and gets a similar result in her master thesis [120], as shown in Table 4.1.

Since the three experiments differ on temperature, the results conform to the work from Cotterill [75], in which the influence of temperature on the amount of absorbed moisture at saturation is reported as minimal.

Table 4.1: Environment condition of Sorption TGA measurements on rayon cords

Temperature	20 °C	30 °C	40 °C	50 °C	60 °C
Relative Humidity	10%, 20%, 30%, 40%, 50%, 60%, 70%, 80%, 90%	10%, 20%, 30%, 40%, 50%, 60%, 70%,	10%, 20%, 30%, 40%, 50%,	10%, 20%	10%, 20%

The Sorption TGA experiments are performed mainly in the range between 20 °C and 40 °C. The reason is to investigate the moisture uptake behaviour in the storage during the processing of tyre products. Due to the limitation of the instrument and to avoid the condensation of moisture in the Sorption TGA chamber and in the humidity generator, the setup of relative humidity range is based on the instruction from the instrument producer. According to the pre- test, the moisture absorption is a physical process, which means it is possible to predict the behaviour using mathematical methods.

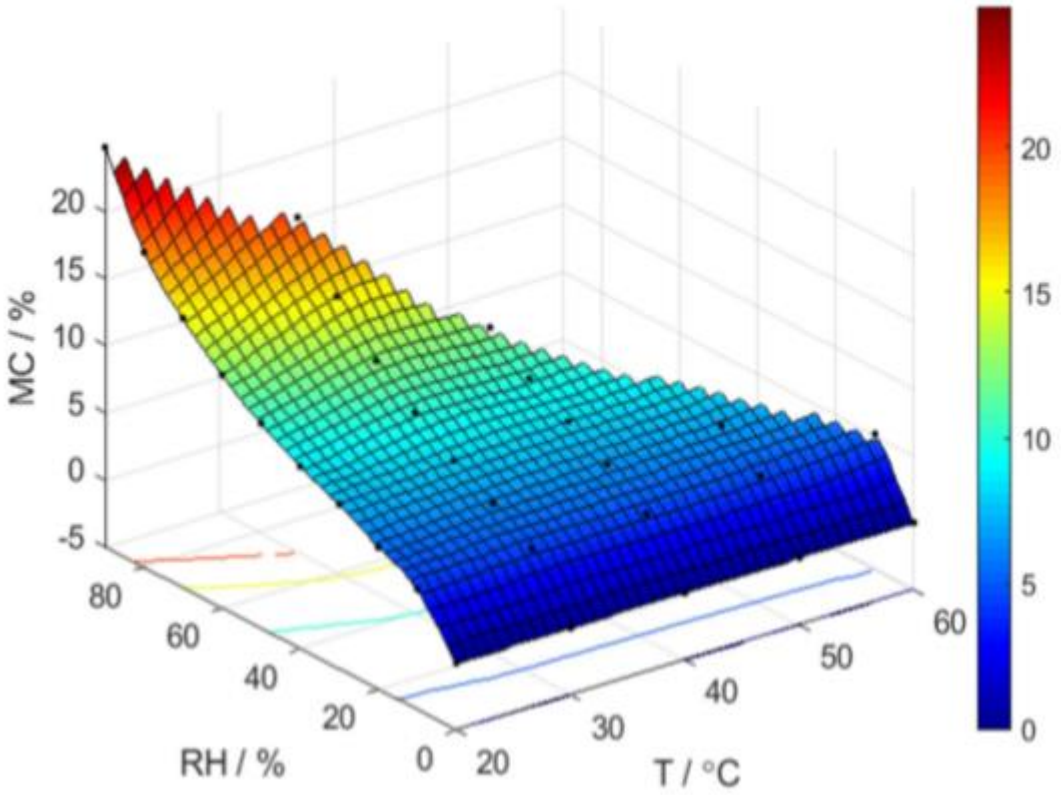

Figure 4.8: Three-dimensional representation of the moisture content behaviour for rayon[120]

The relation between temperature, relative humidity and the moisture content at equilibrium can be found in Figure 4.8. The three-dimensional (3D) plot which relates the saturation moisture content of rayon (z-axis) at given conditions of temperature (x-axis) and relative humidity (y-axis) is based on the results of this thesis with the extension data from L. Coutinho. Using the fitting tool from MATLAB, it is easy to perceive how the atmospheric conditions have a significant impact on the saturation moisture content of rayon cords.[120]

4.1.2 Nylon cords

The moisture contents in the nylon cords after the storage at 30% -40% relative humidity and 40 °C are illustrated in Figure 4.9. Compare to the results of rayon cords in last section, nylon cords have a similar behaviour of moisture uptake. Due to the limit of instrument under high temperature, the measurements are performed at 30% -40% relative humidity to avoid the condensation.

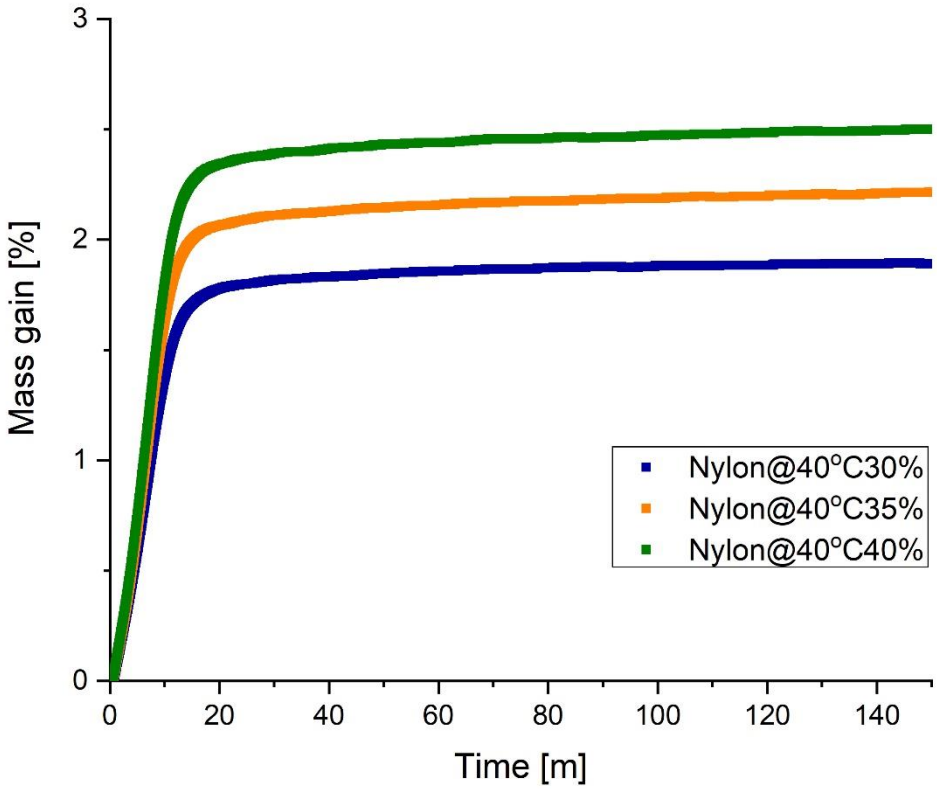

Figure 4.9: Moisture content determination of nylon cords at 30%, 35% and 40% R.H. and 40 °C

As shown in Figure 4.9, the mass of the nylon cords increases with a nearly linear speed in the first stage of the absorption. The curve under lower relative humidity leaves the linear stage earlier than the one under higher humidity. The mass of all the specimens keeps on increasing with a decreased velocity in the second stage until the steady state is reached. Unlike the behaviour of rayon cords, nylon cords stay shorter in the second stage. It takes less time for the nylon cord to reach the saturation than for the rayon cords. Besides, the nylon cords stay a bit longer in the linear stage than the rayon cords at this temperature, which can be identified from the linear slope of the curves.

All experiments at 40 °C last 150 minutes. Rayon cords absorb significant more moisture (about 9.9% at 40 °C and 50%) from the environment than the nylon cord, which absorbs at 40 °C and 50% relative humidity only about 2.5% moisture of its own mass.

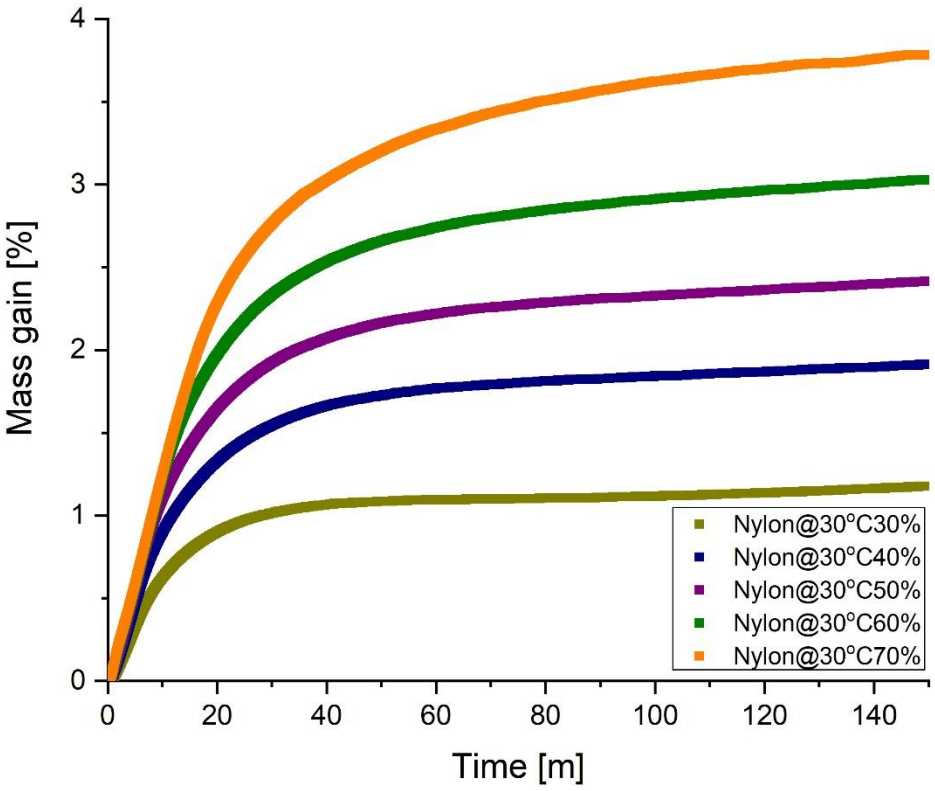

Figure 4.10: Moisture content determination of nylon cords at 30%, 40%, 50%, 60% and 70% R.H. and 30 ℃

Figure 4.10 shows the similar tendency of the moisture uptake behaviour at 30 ℃ for the nylon cords compared to the results at 40 ℃. Similar to the rayon cords, the curve measured under higher relative humidity needs more time to exit from the linear stage in which it absorbs the moisture with a higher velocity. The nylon cords also fail to reach the saturation at 30 ℃ within the 150 minutes experiment. The result is more significant on the specimens under higher relative humidity than the lower ones.

Like at 40 ℃, nylon cords absorb less moisture than rayon cords in the experiment. The tendency shows also a lower saturation point of nylon cord than the one of rayon.

Due to the enhanced performance of the instrument in the experiment, the nylon cords are measured at 20 ℃ and 30% -90% relative humidity. As it is illustrated in Figure 4.11, the specimen absorbs more moisture under higher relative humidity. The distribution of moisture content in the second stage of absorption is growing with the relative humidity. It can be observed that the difference between 30% and 40% is doubled while comparing the moisture content at 80% and 90%.

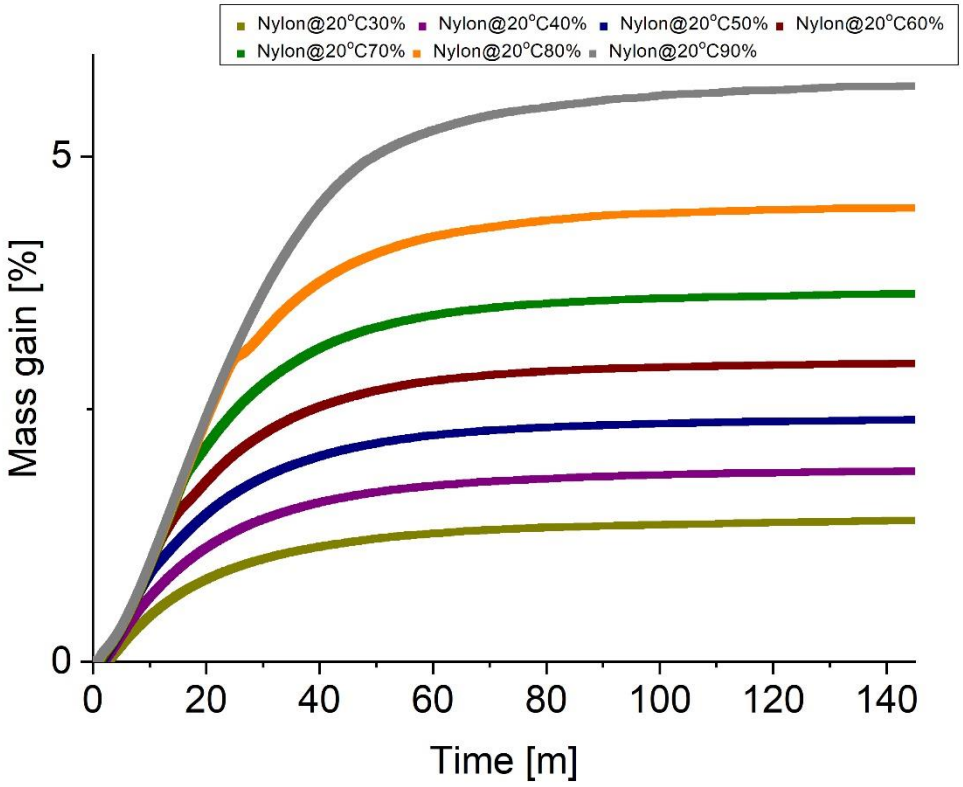

Figure 4.11: Moisture content determination of nylon cord at 30% - 90% R.H. and 20 °C

The rayon cord absorbs at 20 °C and 80%relative humidity by the end of the measurement about 16.7% moisture of its own mass. The value for nylon cord is only about 6.1% under the same conditions.

The influence of temperature on moisture absorption under the same relative humidity is depicted in Figure 4.12. The specimen at 40 °C absorbs moisture with the highest velocity of the three specimens. It reaches the plateau after about 30 minutes. The specimens at 30 °C and 20 °C fail to reach the plateau in the experiment time, but both tends to reach the plateau in a later time with the same sequence of temperature.

In analogy to rayon cords, the moisture uptake behaviour of nylon cords under the same relative humidity is influenced by temperature. The specimen absorbs moisture with higher velocity under higher temperature so that it can reach the saturation point earlier under the higher temperature. The influence of temperature on the moisture content at the saturation point is minor, which conforms the result from Cotterill [75] and the systematic behaviour described by Fick's law.

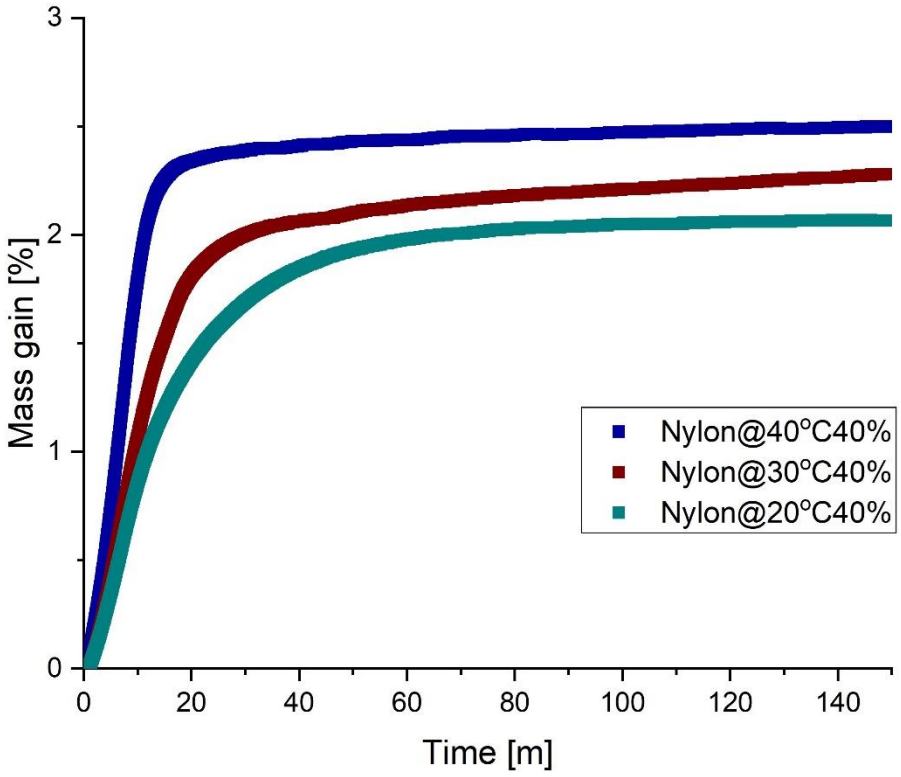

Figure 4.12: Results of Sorption TGA measurements on nylon cords at 50% relative humidity, 20 ℃, 30 ℃ and 40 ℃

Similar tendency can be found in all the results from Sorption TGA measurements under different environment conditions as shown in Table 4.2. J. Oliveira extends the experiment with environment condition at lower humidity area (10%, 15% and 20%) with higher temperature (50 ℃) and gets a similar result in his master thesis [121].

Table 4.2: Environment condition of Sorption TGA measurements on nylon cords

Temperature	***20 ℃***	***30 ℃***	***40 ℃***	***50 ℃***
Relative Humidity	*10%, 15%, 20%, 30%, 40%, 50%, 60%, 70%, 80%, 90%*	*10%, 15%, 20%, 30%, 40%, 50%, 60%, 70%,*	*10%, 15%, 20%, 30%, 40%, 50%,*	*10%, 15% 20%*

Table 4.3: Moisture content at saturation for nylon cords

	20 °C	***30 °C***	***40 °C***	***50 °C***
10%	*0.62*	*0.71*	*0.88*	*0.85*
15%	*0.83*	*1.00*	*1.23*	*1.20*
20%	*1.01*	*1.29*	*1.56*	*1.55*
30%	*1.59*	*1.89*	*1.90*	
40%	*2.12*	*2.22*	*2.57*	
50%	*2.67*	*2.78*	*2.85*	
60%	*3.35*	*3.38*		
70%	*3.51*	*3.94*		
80%	*4.31*			
90%	*5.21*			

The moisture content at saturation can be found in Table 4.3 which is built based on the Sorption TGA results of this study and the extended experiments from J. Oliveira. It is expected to have the similar moisture content at same relative humidity. But due to the thermal expansion there is a slight swelling of the cords under higher temperature so that more moisture can be accumulated in the free space. The moisture content at higher temperature is therefore slightly higher than at lower temperature.

As it had already been carried out by L. Coutinho for rayon cords, a three-dimensional figure is illustrated in Figure 4.13. The relation between the temperature (x-axis), the relative humidity (y-axis) and the moisture content at saturation (z-axis) can be easily found there. The referred diagram was also plotted in MATLAB using the data from Table 4.3 [121].

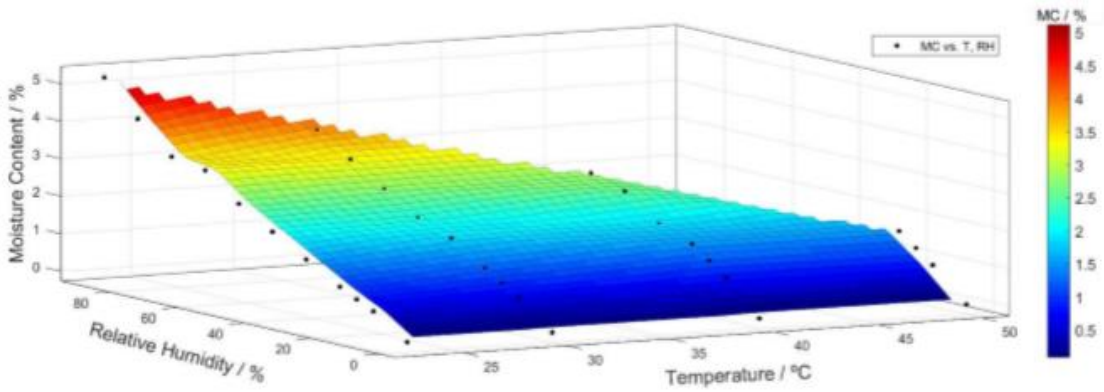

Figure 4.13: Three-dimensional (3D) representation of the moisture content behaviour for nylon[121]

4.1.3 Polyester cords

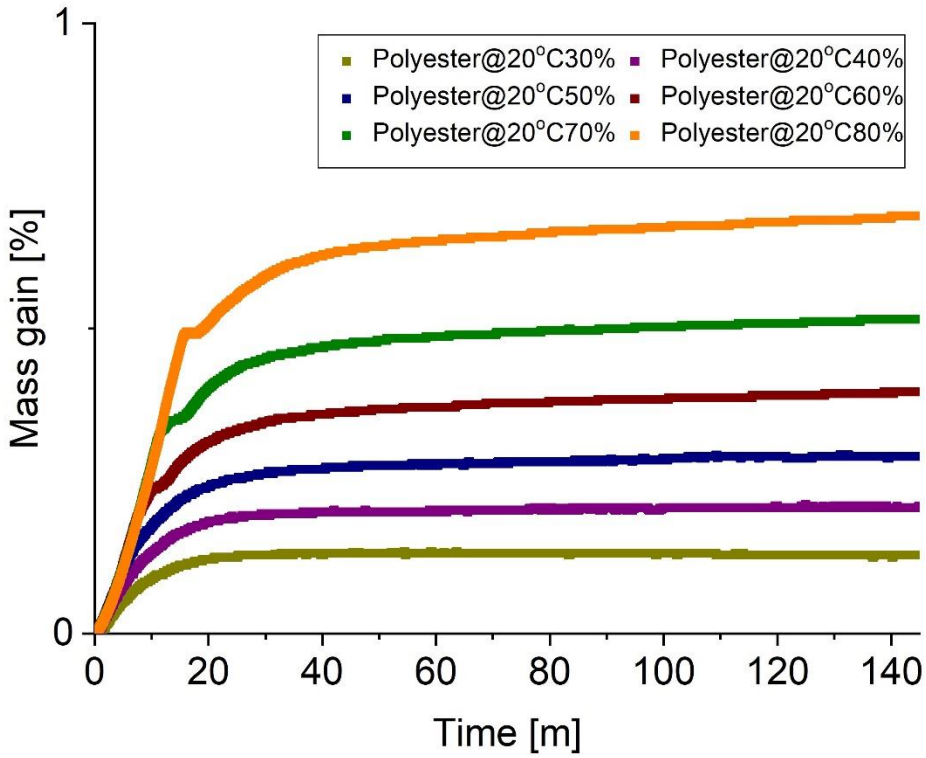

Figure 4.14: Moisture content determination of polyester cords at 30% -80% R.H. and 20 ℃

It was mentioned in section 4.1.1 and section 4.1.2 that the specimen absorbs more moisture under higher humidity. As discussed in section 2.2.2, polyester cords are not as hygroscopic as rayon and nylon cords. Thus, experiments are done only at 20 ℃ under different relative humidity from 30% to 80%.

The results of the experiments are illustrated in Figure 4.14. The curves of mass gain have similar tendency as with rayon and nylon cords because of the moisture absorption, in which the mass changes firstly faster in the linear stage and then slows down to zero velocity. The relative humidity has significant influence on the moisture content at the saturation point, the higher the relative humidity the higher the saturation point. At 20 ℃, the polyester cords absorb not more than 0.5% moisture of its own mass under a relative humidity below 70%. From the curve distribution, the moisture content of the polyester cords will go not over 1% under all humidity conditions.

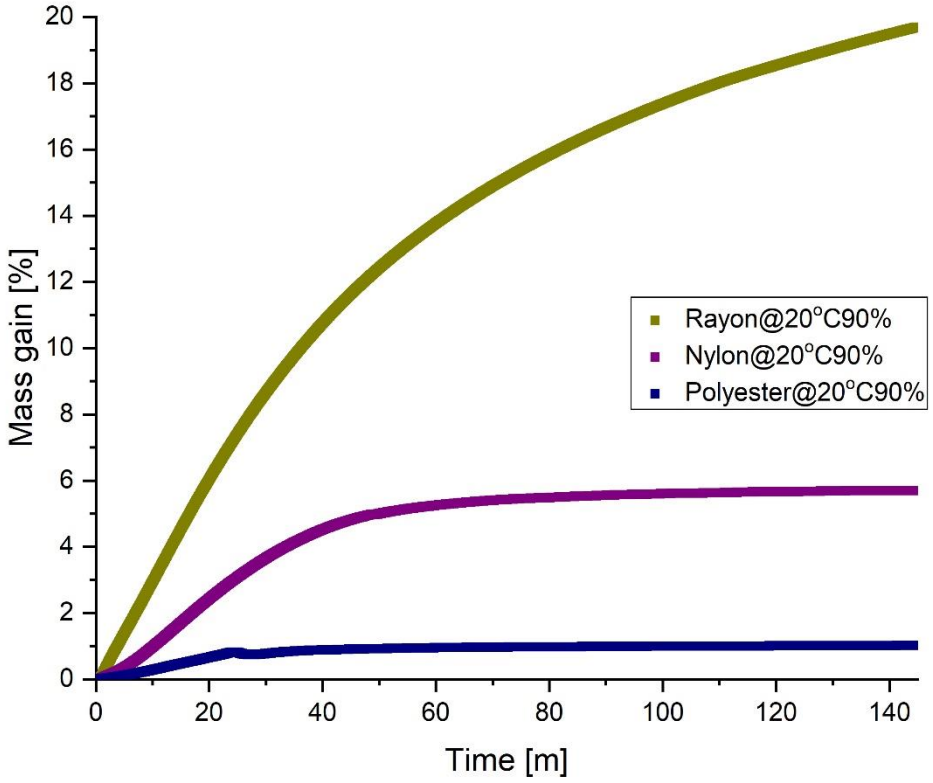

Figure 4.15: Comparison of the moisture uptake behaviours from rayon, nylon and polyester cords at 90% R.H. and 20 ℃

In Figure 4.15, the results of moisture uptake behaviour from all the three kinds of cords are compared. Within the experiment time, polyester cord reaches the saturation state successfully, as the other two kinds of cords are still absorbing moisture from the environment. At 90% relative humidity, the rayon cord absorbs more than 19.7% moisture on its own mass, the value for nylon is about 5.7%, and for polyester only 1.01%. With these values, the statement can be made that the moisture in polyester does not have so much influence as rayon and nylon cords.

4.2 Rubber compounds

4.2.1 Moisture uptake behaviour of rubber

The rubbers are processed according to the recipes in Table 3.2. To investigate the moisture uptake behaviour of the rubbers, further Sorption TGA measurements are done according to the test methods described in section 3.2.1.2. For the purpose of simplicity, the term compound is used in this work as a synonym for uncured compound.

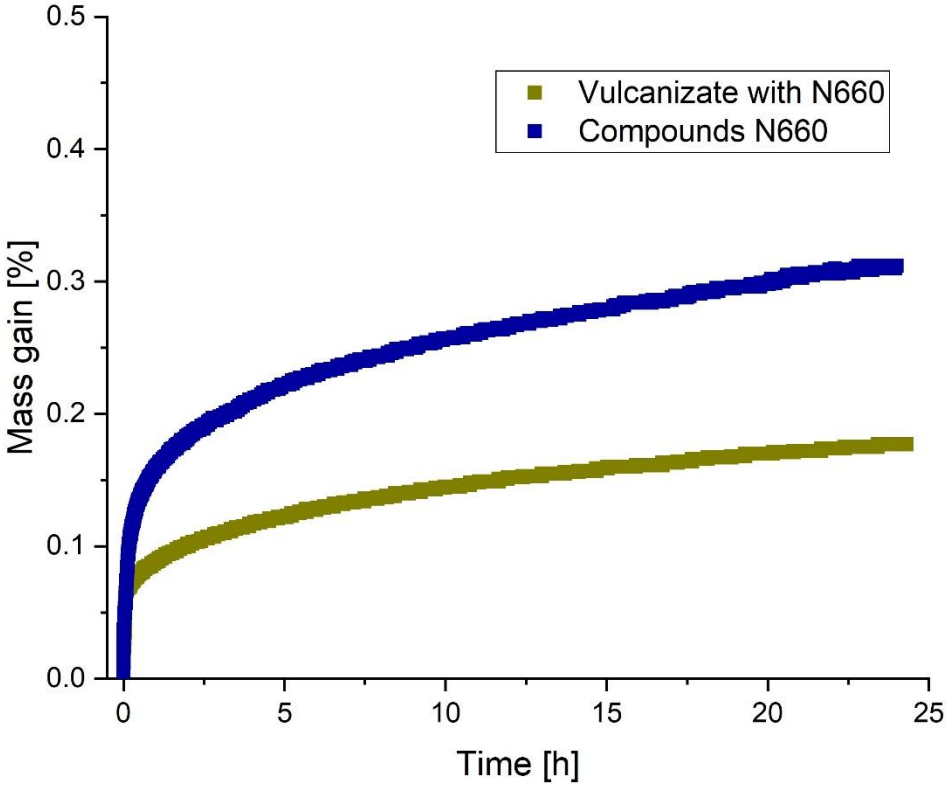

Figure 4.16: Sorption TGA curve from moisture content determination of rubber compound and vulcanizate at 40% R.H. and 40 °C

The result of Sorption TGA measurement on an uncured rubber compound and its vulcanizate which is processed according the recipe 50N660 in Table 3.2 is shown Figure 4.16. The specimens of both uncured rubber compounds and the cured rubber compound have only a negligible amount of increased mass after the storage of 24 hours under the experimental condition. Since the curves have similar shape as the curves of the textile cords, the phenomena of moisture absorption can be determined.

The process of the absorption can also be divided into the previously mentioned two stages, the linear stage with a high velocity and the second stage with a decreasing velocity. Both

curves grow with a linear slope in the first stage for less than 10 minutes, much shorter compared to the textile cords. The second stage begins immediately and lasts until the end of the experiment for about 24 hours. Both specimens fail to reach the equilibrium within the experiment time.

The specimen of uncured rubber absorbs obviously more moisture form the environment than the vulcanizate under the same conditions. One of the reasons is the elimination of the free space in the compound material under the heat and pressure during vulcanization. On the other side, the loss of hydrophilic groups from some ingredients, such as the resorcinol because of the crosslinking, has also an influence on the absorbed moisture content.

4.2.2 Moisture uptake behaviour of different ingredients

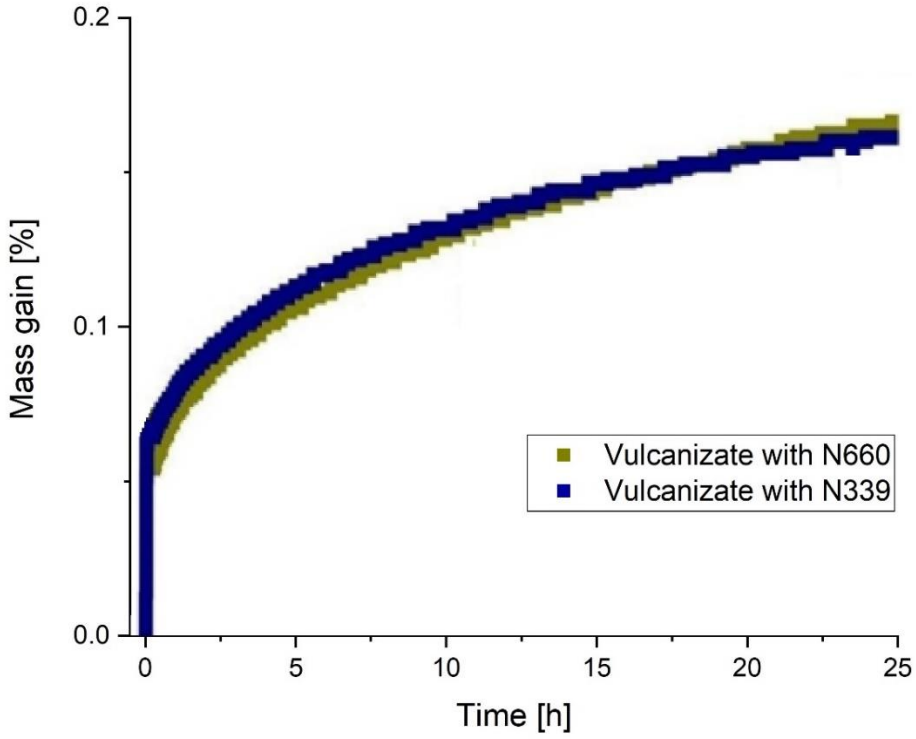

Figure 4.17: Influence of carbon black type on moisture uptake behaviour of rubber

The influence of filler type on moisture absorption is illustrated in Figure 4.17. The recipes of both specimens vary only on the carbon black type. Both curves have almost the same shape and tendency, even the scale range of Sorption TGA is set to a very low value to be able to determine the mass changes. This indicate that the carbon black type has nearly no influence on the moisture absorption behaviour on rubbers.

In Figure 4.18, the results of Sorption TGA measurements on specimens with different carbon black content are shown. All the three specimens behave similarly under the same environment conditions. The specimen without filler absorbs the most moisture at any time. It has an obviously longer, linear stage at the beginning. The specimen with 20 phr carbon black leaves the linear stage after the specimen filled with the most carbon black (50 phr) and jumps into the second stage with a decreasing velocity. The specimen with no filler almost reaches the equilibrium with in the 24 hours experiment time, while the other specimens still have a significant mass gain at the end of the experiment.

The amount of the ingredients to be added in a rubber system are expressed in parts per hundred rubber (phr). The phr describes the quantities of an ingredient per 100 units of base polymer, which means for a certain amount of rubber, if the filler has a smaller amount in phr, the mass all other ingredients will be increased. In the recipes with lower carbon black amount, the absolute amount of other hydrophilic ingredients, such as resorcinol and HMMM resin, is therefore larger than in the specimen with a higher carbon black content. Thus, the specimen with less carbon black content absorbs more moisture from the environment.

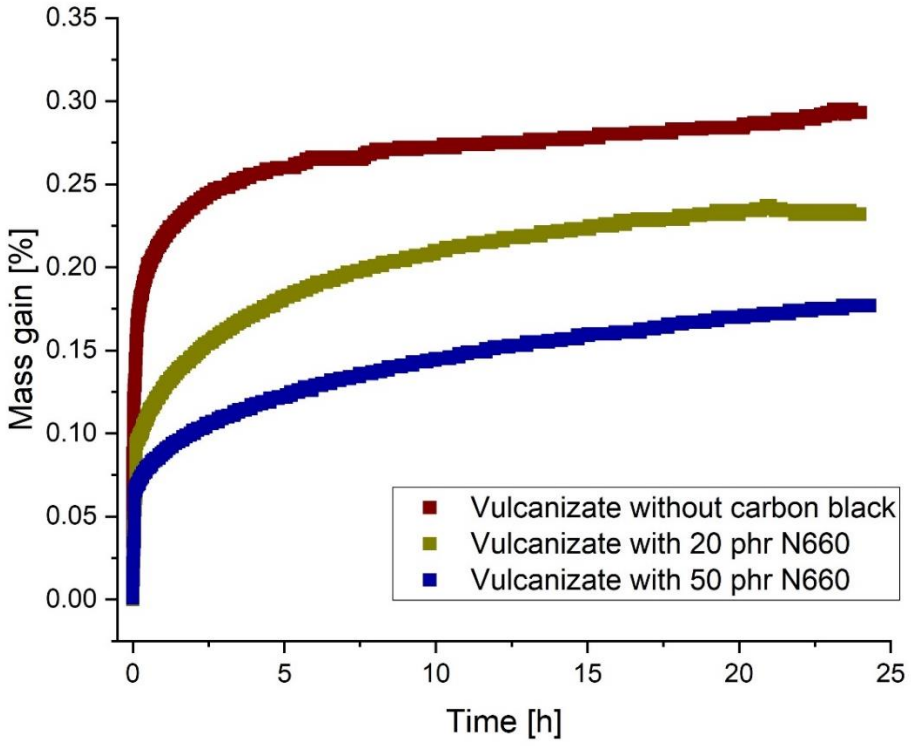

Figure 4.18: Influence of carbon black amount on moisture uptake behaviour of rubber

The influence of resorcinol and HMMM resin, which are known as important ingredients to improve the adhesion of organic and inorganic reinforcing materials to natural/synthetic rubber compositions, are investigated and shown in Figure 4.19. The compound with resorcinol and resin absorbs more moisture as it stays in the linear stage longer than the

specimen without resorcinol and resin. Both specimens fail to reach the saturation at the end of the experiment.

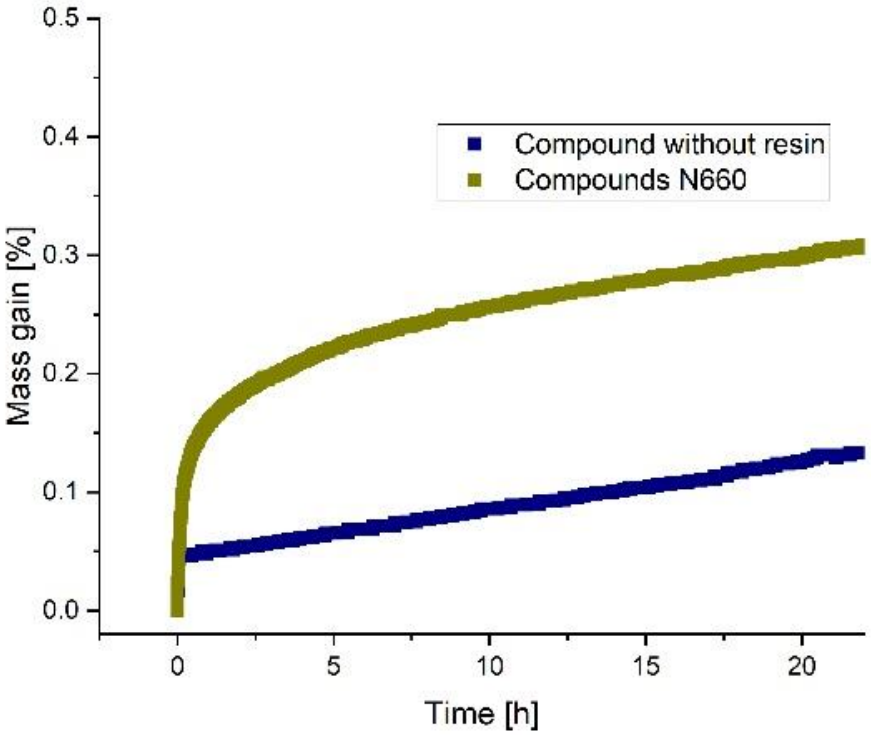

Figure 4.19: Sorption TGA measurement to determine the influence of resin on moisture uptake behaviour of rubber compounds

4.3 Rubber composite material

In order to investigate the moisture uptake behaviour of rubber composite material, the calendered material composed of rubber and polyamide reinforcements is used. Since it is difficult to process the calendaring of rubber and textile material in laboratory, the material has been supplied by Continental Reifen GmbH, Hannover, Germany. As it is mentioned in 3.2.1.3, the measurement is performed using the same Sorption TGA instrument supported by the humidity generator under the same environment conditions as applied on the textiles and rubbers.

From the results of the Sorption TGA measurements on textile and rubbers, the saturation point of rubber is hard to be reached within a short time. However, rubber is the main material which has contact with the atmosphere, as the most of surface from textile reinforcement is covered by rubber through the calender process. To get a comprehensive result, the experiment time is set up to 5 days.

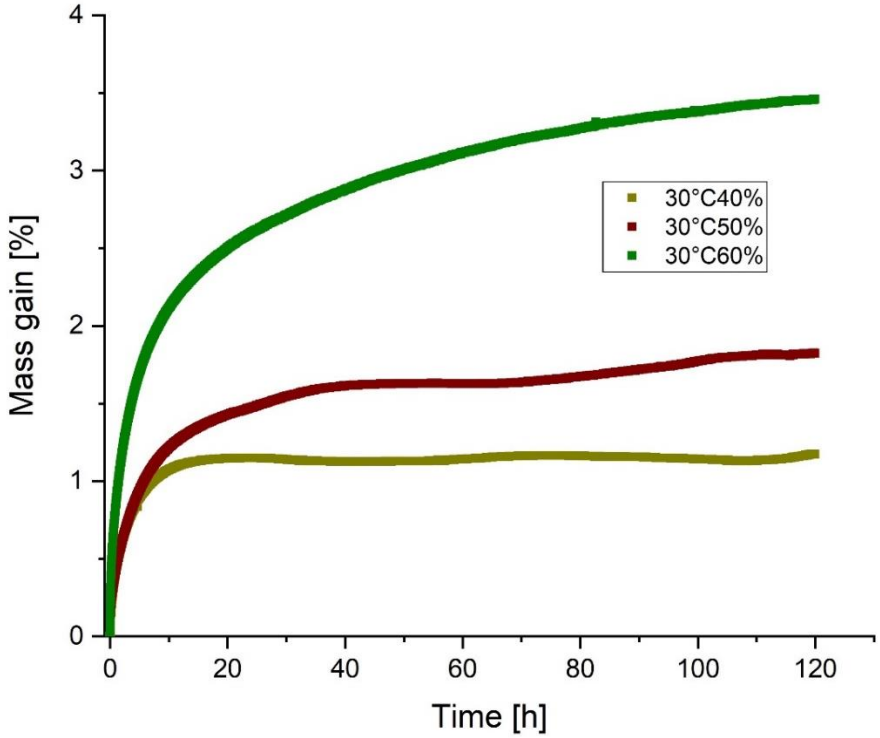

Figure 4.20: Moisture content determination of rubber composite with same nylon amount at 40%, 50% and 60% R.H. and 30 °C

Figure 4.20 shows the result of Sorption TGA experiment for 5 days to determine the moisture content within a sample cut down from the calendered material according the method described in 3.2.1.3. The curves have similar shape as the result of Sorption TGA measurements on textiles and rubbers. It takes about 10 hours for the sample to exit from

the linear stage. The sample under 40% relative humidity reaches its semi-equilibrium, which has a plateau like shape after about 20 hours. It takes more than 30 hours for the sample at 50% to reach the same state. Both of the samples have shown potential of further moisture uptake. The other sample which is measured at 60% relative humidity is not able to reach its saturation point with the experiment time of 120 hours.

Some of the curves of the experiments with time longer than 24 hours have some unexpected fluctuation. That are due to the performance of the instrument especially the humidity generator with a limited water tank. Fortunately, they do not have so much impact on the curve tendency because of their narrow range.

From the result of section 4.2, the moisture amount of rubbers under different environment conditions can be determined. In order to ensure that the moisture absorbed by the rubber has only a small influence on the moisture uptake behaviour of the entire composite, the Sorption TGA measurement is performed at 30 °C and 60% which are the conditions with the highest absolute moisture content in the air.

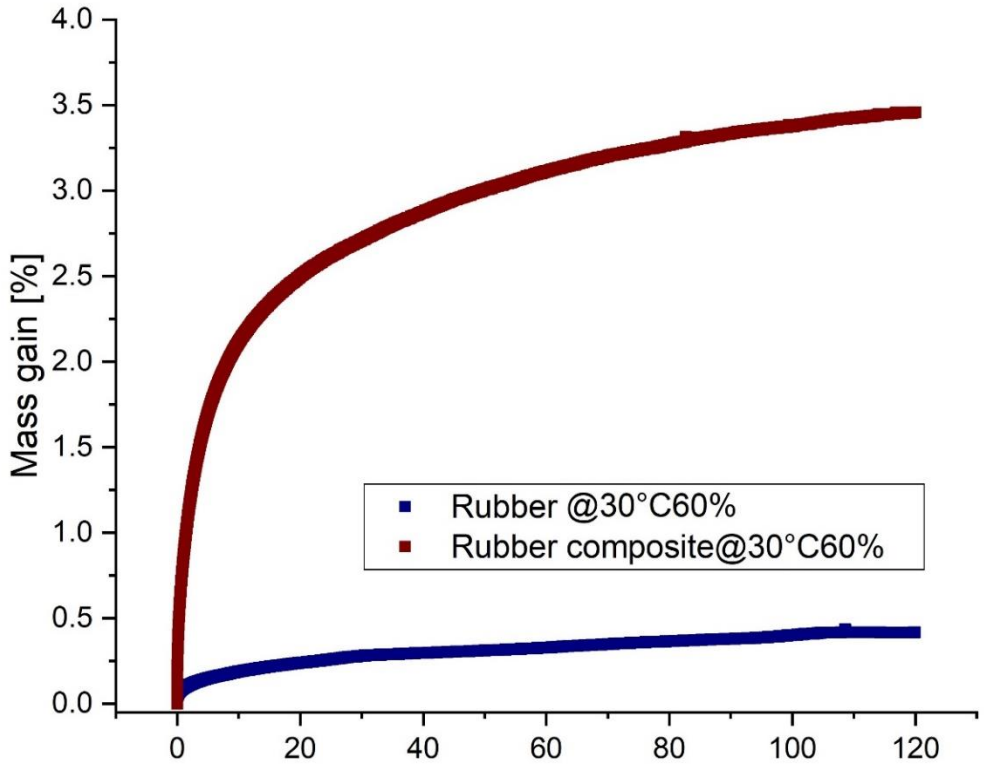

Figure 4.21: Moisture content determination of rubber used in the composite material at 60% R.H. and 30 °C, compared with the rubber composite under same condition

The result of the experiment is shown in Figure 4.21. The rubber used in the composite absorbs about 0.41% moisture of its own mass. It is only a bit more than 10% of the total

moisture absorbed by the composite sample from the environment. Thus, similar result can be found as mentioned in section 4.2.

To determine the influence of the open ends on the moisture uptake behaviour, which cannot be avoided during processing of the calendered materials, samples are prepared and measured as described in section 3.2.1.3. The results of the measurements with the sample whose both ends are closed are illustrated in Figure 4.22.

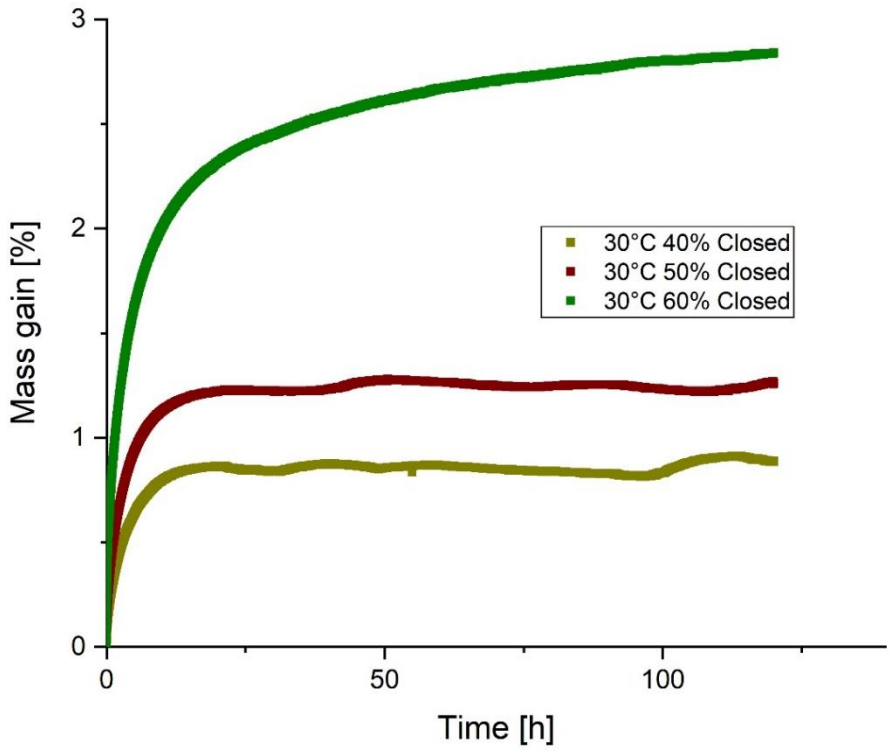

Figure 4.22: Moisture content determination of rubber composite with both ends closed at 40%, 50% and 60% R.H. and 30 °C

As demonstrated in Figure 4.22, the curves have similar velocity in the linear stage but a different in-stage time. The sample under lower humidity exits the first stage of the curve earlier than the one under higher humidity, and the mass keeps on increasing with a decreased speed in the second stage until the plateau which indicates the semi-equilibrium is reached. Unlike the sample with open ends, the closed ends have an influence on the velocity, especially in the second stage. The sample in Figure 4.22 at 50% humidity shows the semi-saturation state is reached after a time of 20 hours, nearly the same as the sample at 40%, and then increasing with only tinny amount on its mass. The sample at 60% also fails to get any plateau within the experiment time.

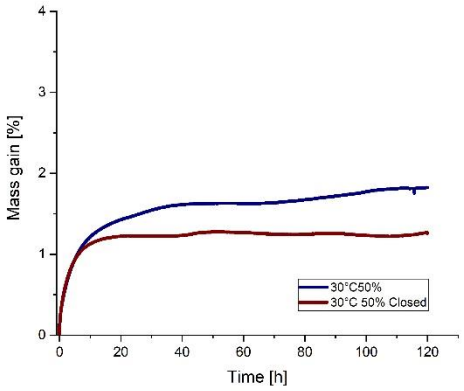

Figure 4.23: Results of Sorption TGA measurements at 50% relative humidity, 30 °C on rubber composite with open and closed ends

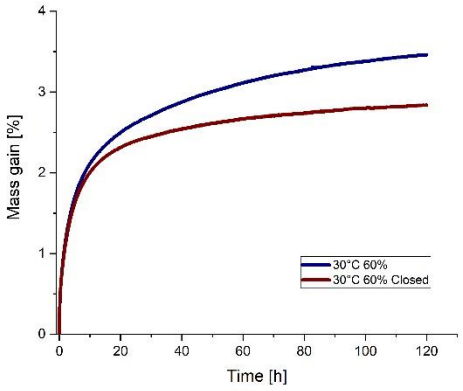

Figure 4.24: Results of Sorption TGA measurements at 60% relative humidity, 30 °C on rubber composite with open and closed ends

To get a comprehensible comparison of the moisture uptake behaviour of samples with open and closed ends, curves are shown in Figure 4.23 and Figure 4.24. There is an obvious difference of absorbed moisture amount between the sample with open and closed ends. Through the opened ends, the moisture can be absorbed more easily as it diffuses through the rubber. This tendency seems to become larger with increasing time.

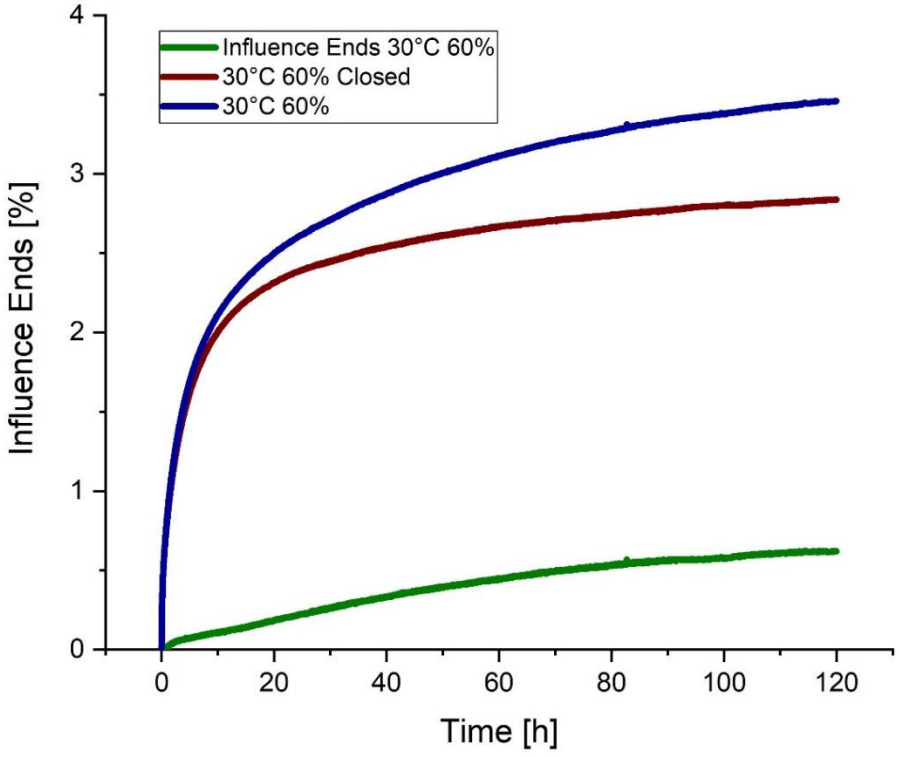

Figure 4.25: Influence of the ends compared to the moisture uptake of the sample

The influence of the ends at 30 °C and 60% relative humidity is calculated with Equation 4.1 and illustrated in Figure 4.25. The influence of the ends is not obvious at the beginning of the experiment but increases with the time. The absolute amount of moisture which is

absorbed through the ends is not more than 20% compare to the total absorbed moisture amount. But, it slowly dominates the mass gain after a long time of storage. The moisture uptake can be limited, if the humidity of the room, where the rubber composite material with opened ends are stored, can be controlled.

$M(t)_{ends} = M(t)_{opened} - M(t)_{closed}$	*Where*	$M(t)_{ends}$*: mass of moisture absorbed through the ends at time t* $M(t)_{opened}$*: mass of moisture absorbed from the sample with opened ends at time t* $M(t)_{closed}$*: mass of moisture absorbed from the sample with closed ends at time t*	*Equation 4.1*

4.4 Summary

In this chapter, the moisture uptake behaviour of different components from rubber composite materials used in the tyre industry were investigated. The main contribution of this chapter for further studies can be summarised as follows:

1. Based on the results from Sorption TGA measurements under different environment conditions on textile reinforcements made from rayon, nylon and polyester, the key aspect which influences the moisture uptake behaviour of textile cords are investigated systematically. Different textile cords perform similarly with regard to moisture uptake. According to Fick's law, all the cords absorb with a high, linear velocity after they entered the humid condition. After a certain time, which is related to the temperature under same humidity and to the humidity under same temperature, the samples start with the second stage absorbing moisture with a decreasing velocity until they reach the saturation point.

   The moisture amount absorbed by the textile from the environment is related to the relative humidity under the specific temperature. Higher relative humidity ensures higher moisture content in the sample at the equilibrium state. The velocity of moisture absorption under same relative humidity is decided mainly by the temperature. The sample under higher temperature reaches the equilibrium state earlier than the sample under lower temperature. Because of the chemical structure of cellulose, the rayon cords can absorb about 20% moisture of its own mass at 90% and 20 °C, which is far more than the other two kinds of cords investigated. The nylon cords absorb a bit more than 5% under similar conditions due to the hydroxyl groups of polyamides. The moisture content in the polyester cords has an upper limit of only 1% in the equilibrium state, which is recognised to be not so moisture sensitive as rayon and nylon.

2. In the investigation on moisture uptake behaviour of rubber, which is the matrix in the rubber composite material, the Sorption TGA measurements with similar settings, but longer experiment time were performed. Rubber performs similar as the textiles in the experiments. The results show also similar trends and distribution under different environment conditions.

   The influence of other ingredients in the rubber compounds was also clarified in the further experiments. Different recipes were used to process the rubber compounds and vulcanizates in order to suit this requirement. Results show that the type of carbon black has nearly no influence on the moisture absorption. The amount of carbon black has an influence of the moisture absorption because with lower filler

content, the relative mass of other hydrophilic ingredients in the rubber system will be higher so that the total absorbed moisture amount is also higher than the rubber with high filler content. Resorcinol and HMMM resin which are used to enhance the adhesion between rubber matrix and textile cords can absorb moisture with their hydroxyl groups. Their influence is relatively small compared to the textile because of their limited amount in the rubber compounds.

Rubber can absorb moisture from the environment but only in very low dimension compared to the textiles. But the influence of some hydrophilic ingredients should not be ignored.

3. The rubber composite materials, which are calendered materials consisting of a rubber matrix and textile reinforcements, were tested with Sorption TGA. The performance of the calendered material is similar to the single components. The rubber matrix has a „negative" influence on moisture absorption, it slows down the whole process compared to the pure textile cords. Most of the samples fail to reach their equilibrium within the 5 days experiment, which indicates the influence of rubber matrix on the moisture uptake behaviour. The open ends of the textile materials have also an influence on the moisture uptake according to the result of the experiments. About 20% of the moisture is absorbed through the open ends.

4. The results of the Sorption TGA measurements can be utilized as base for further experiments to investigate the influence of the absorbed moisture on different properties of the materials. In addition, the data can also be used to model the moisture uptake behaviour mathematically.

5 Mathematical modelling

With mathematical models the moisture uptake behaviour of certain materials can be predicted with less experiments performed. It is therefore important for the tyre industry to build a mathematical model based on the databank of different materials. The moisture content in the materials can be estimated with knowledge of the storage condition, storage time and the model. The tyre producer can regulate the storage condition to reduce the moisture influence on the performance of the end product.

In this chapter, the mathematical modelling is performed based on the experimental data to predict the moisture uptake behaviour of textile cords and the textile reinforced rubber materials. All the experimental data used for model fitting and their verification are obtained from the Sorption TGA measurement described in section 3.2.1 and chapter 4.

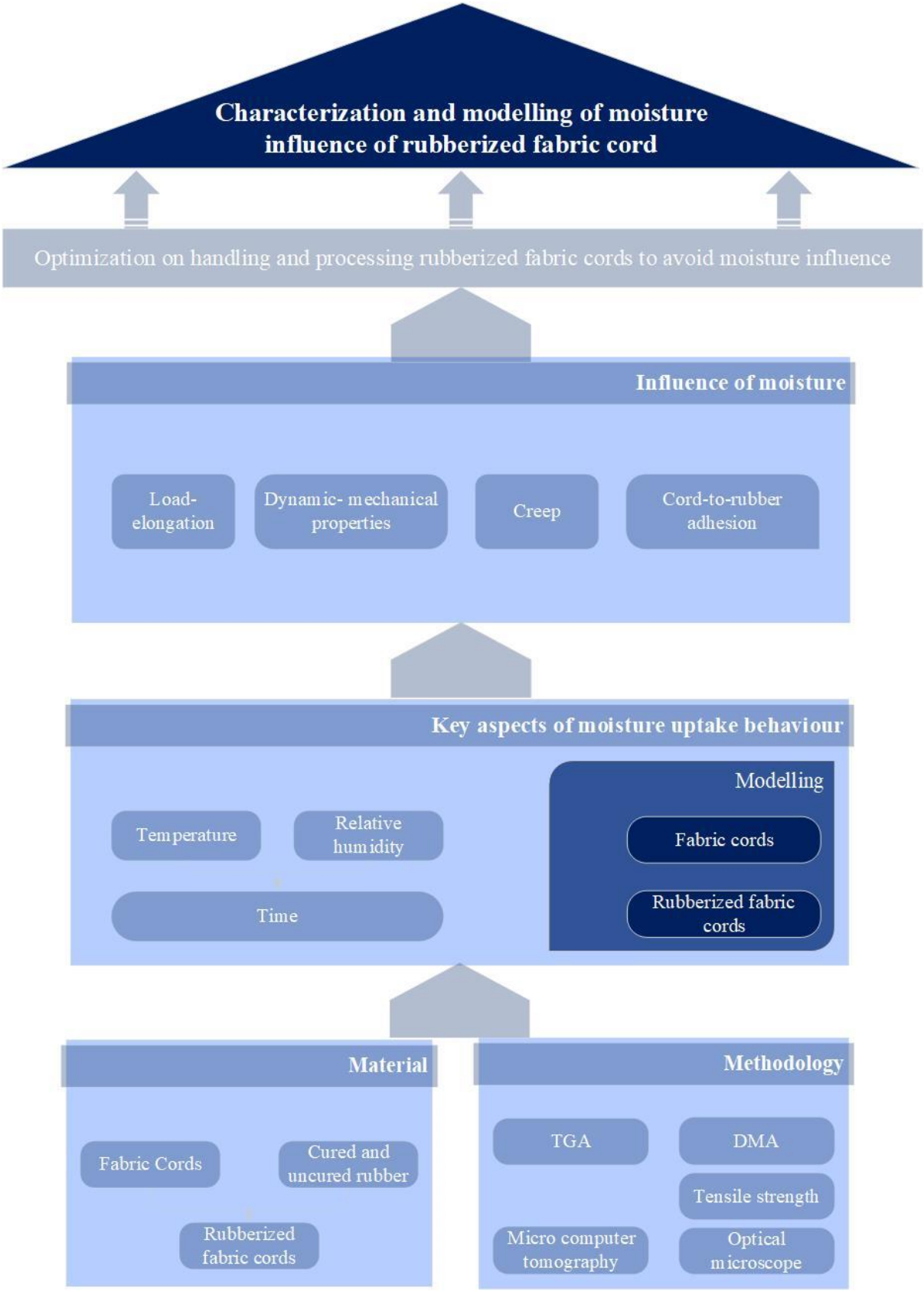
Characterization and modelling of moisture influence of rubberized fabric cord
Optimization on handling and processing rubberized fabric cords to avoid moisture influence
Influence of moisture
Load-elongation
Dynamic- mechanical properties
Creep
Cord-to-rubber adhesion
Key aspects of moisture uptake behaviour
Temperature
Relative humidity
Time
Modelling
Fabric cords
Rubberized fabric cords
Material
Fabric Cords
Cured and uncured rubber
Rubberized fabric cords
Methodology
TGA
DMA
Tensile strength
Micro computer tomography
Optical microscope

5.1 Mathematical modelling on moisture uptake behaviour of textile fibres

To predict the moisture uptake behaviour of the textile fibres, the mathematical model based on Fick's law is chosen according the investigation of A. Célino et al. [101]. As described in section 2.2.1.3, Fick's first law can be written in the form as shown in *Equation 2.9*, if it is used to solve a one-dimensional problem.

Since the cross section of the textile cords can be regarded as round form as described in section 3.2.2.1.1, the cord has been assumed as cylindrical in shape with a radius *r* which is much smaller compared to its length for the purpose of modelling. In this case, the diffusion behaviour can be considered as radial, and therefore, it can be treated as a one dimensional problem. [101]

Through consideration of the one-dimensional case, *Equation 2.13* can be expanded in terms of mass gain as a function of time to [97-99]:

$C(t) = C_s\left\{1 - \frac{8}{\pi} exp\left[\frac{-\pi^2 Dt}{l^2}\right]\right\}$	*Where*	C_s*: moisture content at saturation* $C(t)$*: moisture content at time t* *l: diameter of the sample* *D: Diffusion coefficient*	*Equation 5.1 [97-99]*

According to C. Shen and G. Springer, *Equation 5.1* can be approximated and used for practical purpose as [97-99]:

$C(t) = C_s\left\{1 - exp\left[-7.3\frac{Dt}{l^2}\right]\right\}^{3/4}$	*Where*	C_s*: moisture content at saturation* $C(t)$*: moisture content at time t* *l: diameter of the sample* *D: Diffusion coefficient*	*Equation 5.2*

5.1.1.1 Modelling on rayon cords

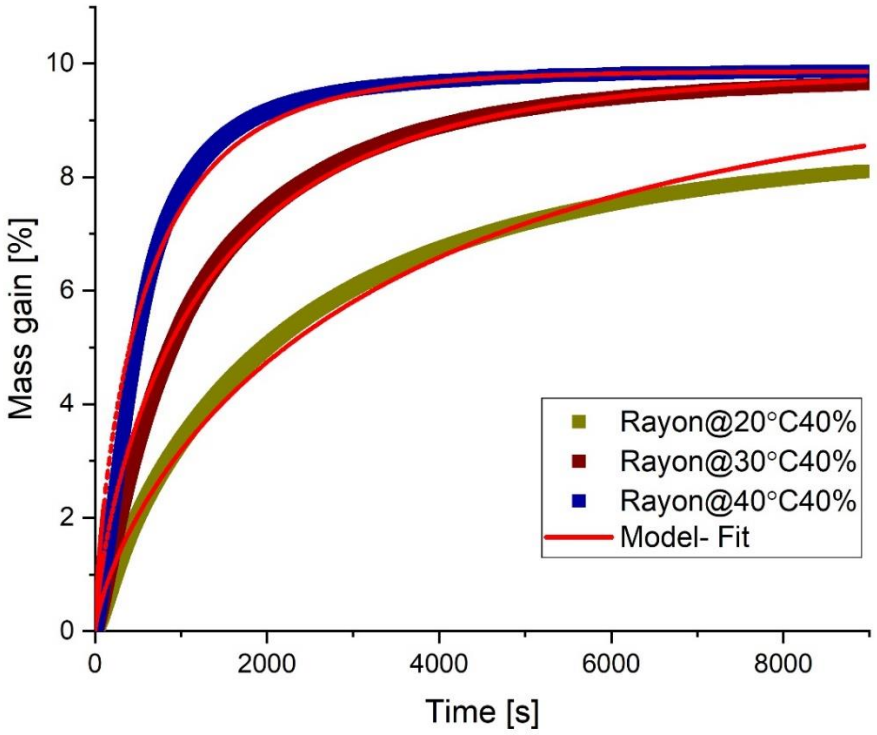

Figure 5.1: Model fitting on the result of measurements at 20 ℃-40 ℃ and 40% relative humidity

In order to determine the diffusion coefficients, the method of model fitting is used. The results of model-fitting are shown in Figure 5.1, Figure 5.2 and Figure 5.3. As illustrated, the model is applied to fit all the curves at different environment conditions. The data produced from the model are in good agreement to the experimental data, especially under higher temperature. Under 20 ℃, the model underestimated the moisture absorbed because the motion of the water molecule. The Brownian motion of the water molecular is proportional to the temperature. This random motion is lower at 20 ℃ than it at 40 ℃, it takes therefore longer for the sample to absorb the moisture at lower temperature.

In analogy to the results from Sorption TGA measurements, all the fit curves are heading to the same saturation point with different curve slopes which are related to the diffusion coefficient *D* at different environment conditions. The diffusion coefficient at different conditions can be found in Table 5.1. The distribution of the value can be rated as very good, and according to the standard deviation, indicates that the influence of relative humidity on the diffusions coefficient is only minor which also coincides with the results in chapter 4.

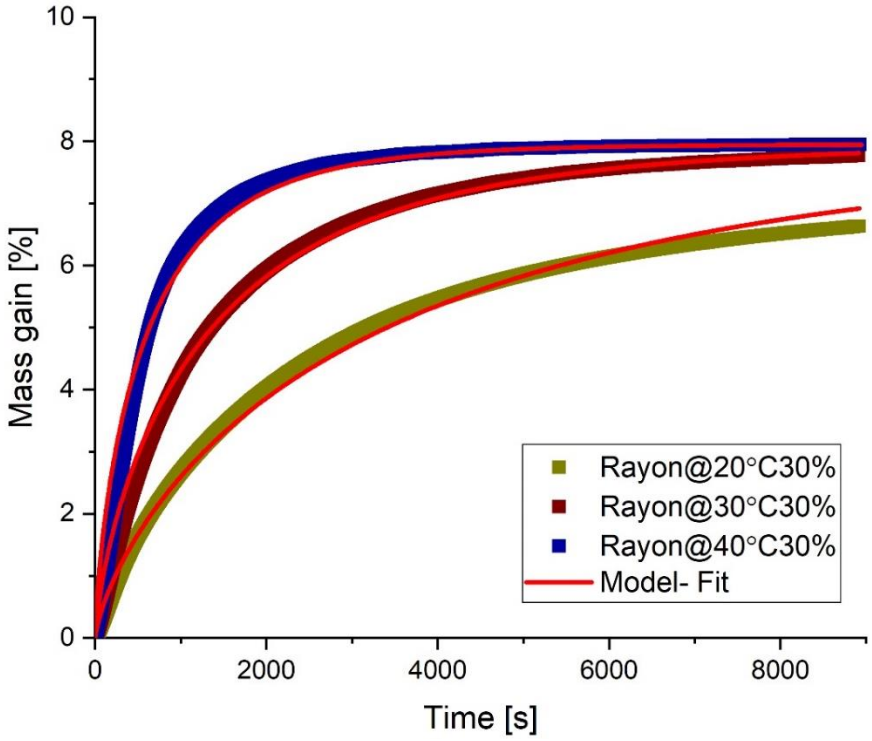

Figure 5.2: Model fitting on the result of Sorption TGA measurements at 20 °C-40 °C and 30% relative humidity

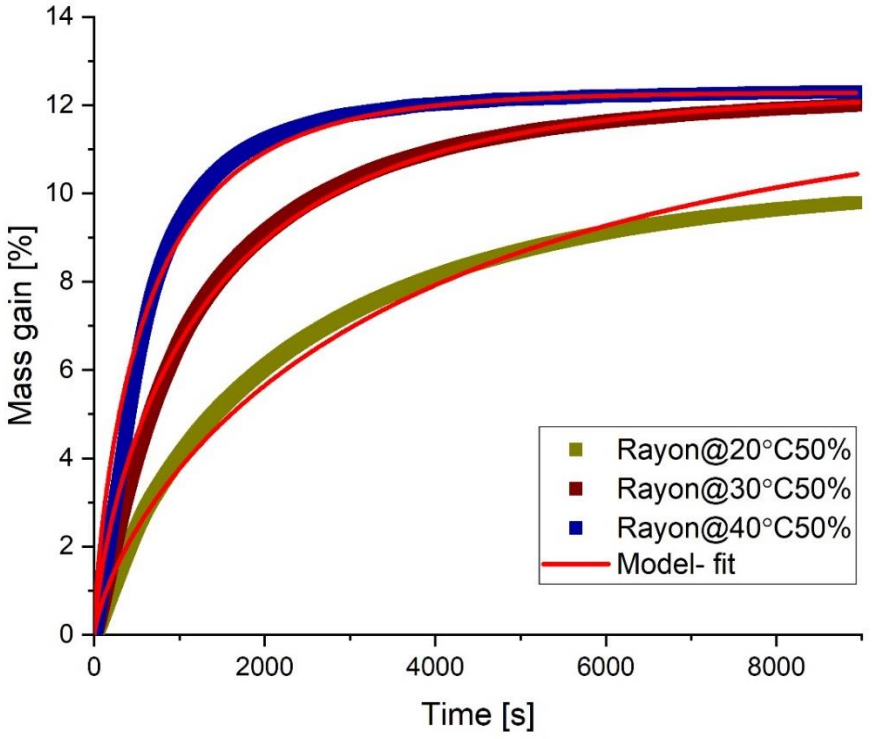

Figure 5.3: Model fitting on the result of Sorption TGA measurements at 20 °C-40 °C and 50% relative humidity

Table 5.1: Diffusion coefficients *D* determined from Sorption TGA results using model-fitting methods

R.H. / *Temperature*	*30%*	*40%*	*50%*	*Mean Value*	*Standard Deviation*
20 ℃	*5.69144E-6*	*5.57499E-6*	*5.12818E-6*	*5.46487E-6*	*±2.97338E-7*
30 ℃	*1.41533E-5*	*1.4519E-5*	*1.38849E-5*	*1.41857E-5*	*±3.18277E-7*
40 ℃	*3.05686E-5*	*3.07731E-5*	*2.80621E-5*	*2.98013E-5*	*±1.50965E-6*

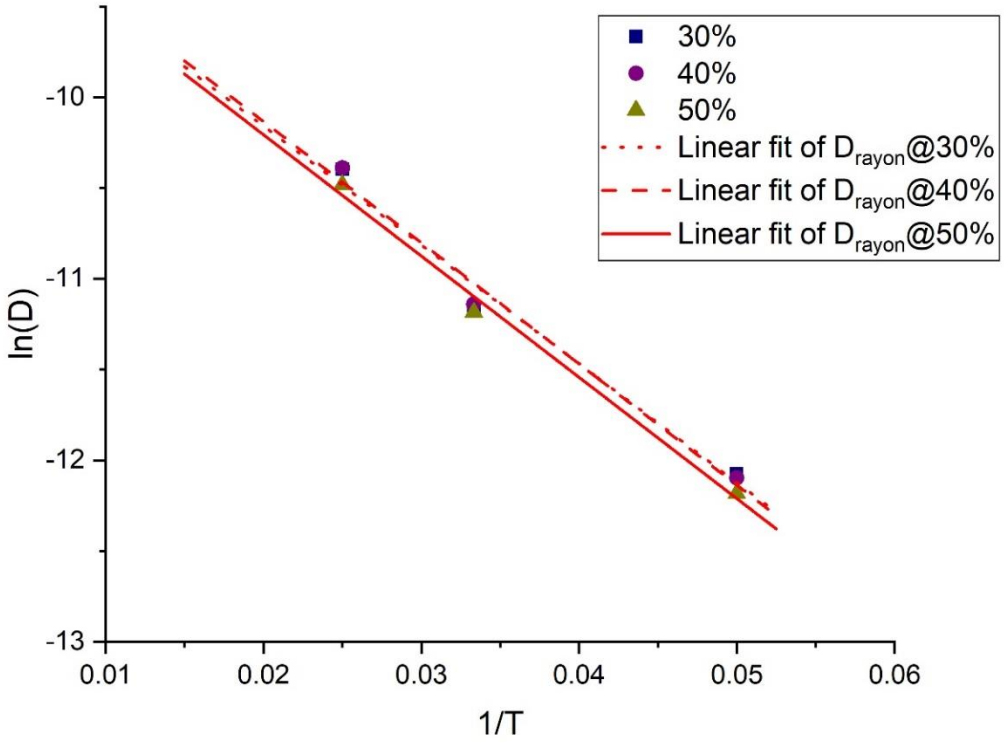

Figure 5.4: Model fitting of diffusion coefficient according to Arrhenius dependence

The diffusion coefficient D at 20 ℃, 30 ℃, 40 ℃, 30%, 40% and 50% relative humidity listed in Table 5.1 are placed in Figure 5.4. According to Espert et.al., the diffusion coefficient D is approximate to follow a linear Arrhenius dependence with temperature (Equation 2.17)[102]. Thus, the plot is linearly fitted and extrapolated as shown in Figure 5.4. The fitting curve indicates the relation between diffusion coefficients and the temperature. The diffusion coefficient at other temperatures e.g. 50 ℃ can be estimated from this curve and can be used in the verification of the model by extending the curve.

Figure 5.5 shows the verification of the model. The red curve is the simulation curve which produced by the model with estimated diffusion coefficient. From the verification the R-square values, 0.956 indicates that the model fits the data well. The model-fitting in the

linear stage is slightly higher than the experimental curve and shows a slower velocity in the curvature. The prediction of the saturation moisture content is accurate.

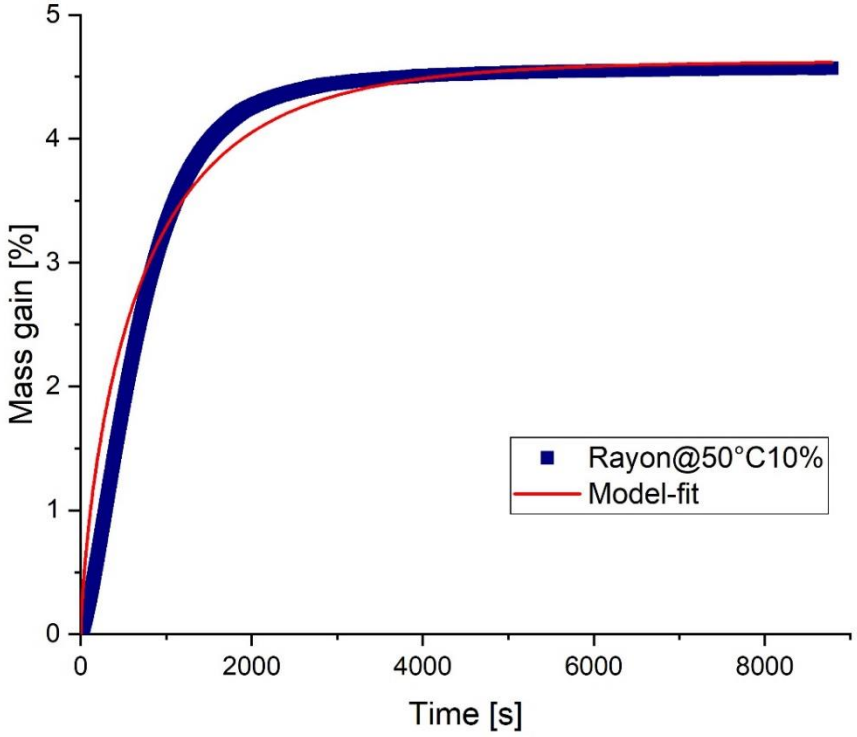

Figure 5.5: Model fitting verification using the estimated diffusion coefficient

5.1.1.2 Modelling on nylon cords

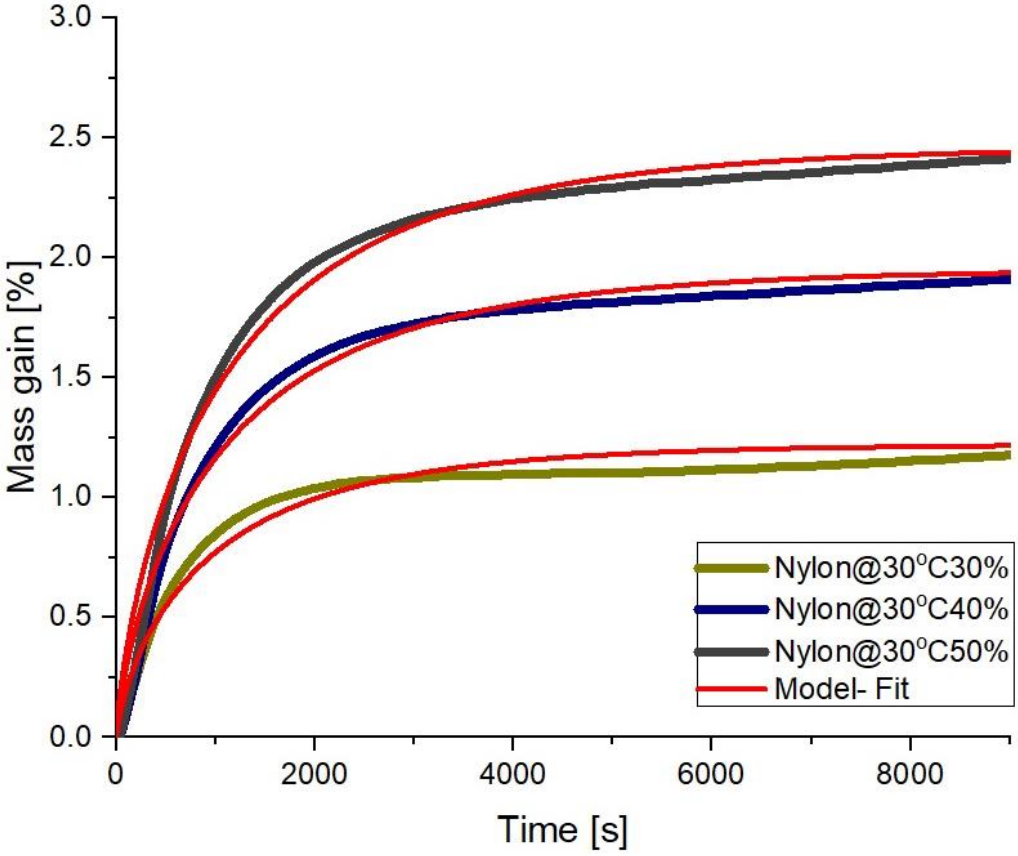

Figure 5.6: Model fitting on the result of Sorption TGA measurements on nylon cords at 30%-50% and 30 °C

The model fitting method is applied on nylon cords to determine the diffusion coefficient. The same strategy as for rayon cords is considered. The diffusion coefficient *D* at 20 °C, 30 °C and 40 °C, 30%, 40% and 50% relative humidity are determined with the model fitting method as shown in Figure 5.6, respectively. The relative humidity of 50% at 40 °C was not measured with Sorption TGA since it was found that the condition lies outside the climate range of the Sorption TGA.

All the coefficients are placed in new coordinate systems to get the relation between temperature, humidity and the diffusion coefficient. As discussed in last section and shown in Figure 5.7 the Arrhenius dependence of the temperature and the diffusion coefficient *D* is illustrated. Further coefficients under other temperature can be estimated through the linear fit.

In analogy to the rayon cords, the determined diffusion coefficient D of nylon cords can also be utilised to verify the model under other environment conditions. In Figure 5.8, the diffusion coefficient of nylon cords at 50 °C estimated from the model-fitting is applied to verify the model with the experimental data measured at 50 °C and 10% relative humidity.

The model has a slight lower velocity in the curvature. The accuracy on predicting the saturation is quite well.

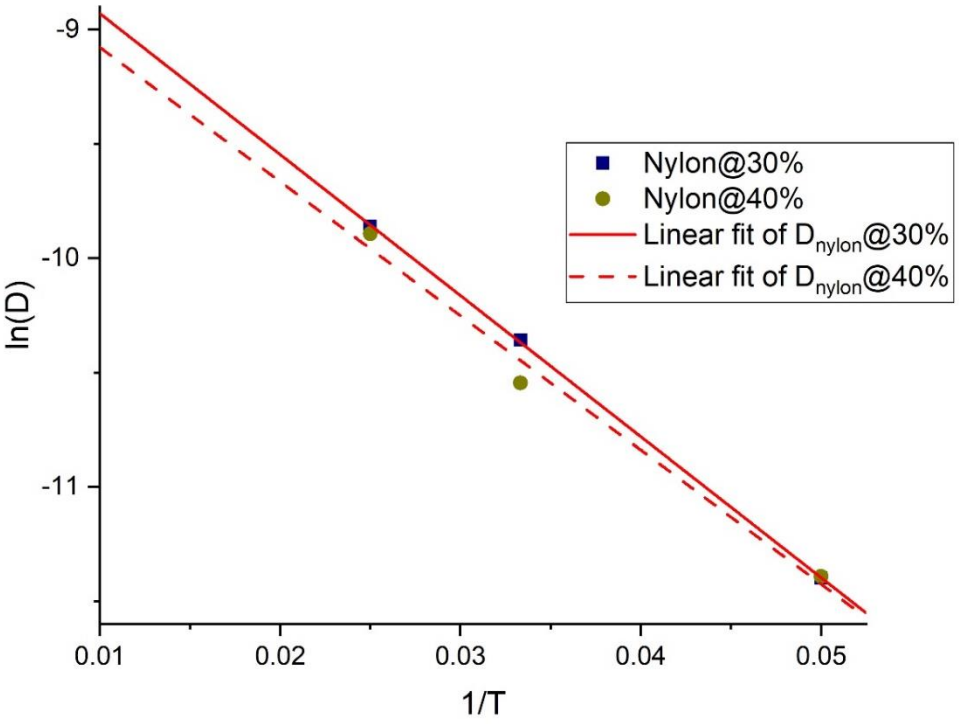

Figure 5.7: Model fitting of the relation between diffusion coefficient of nylon cords and temperature

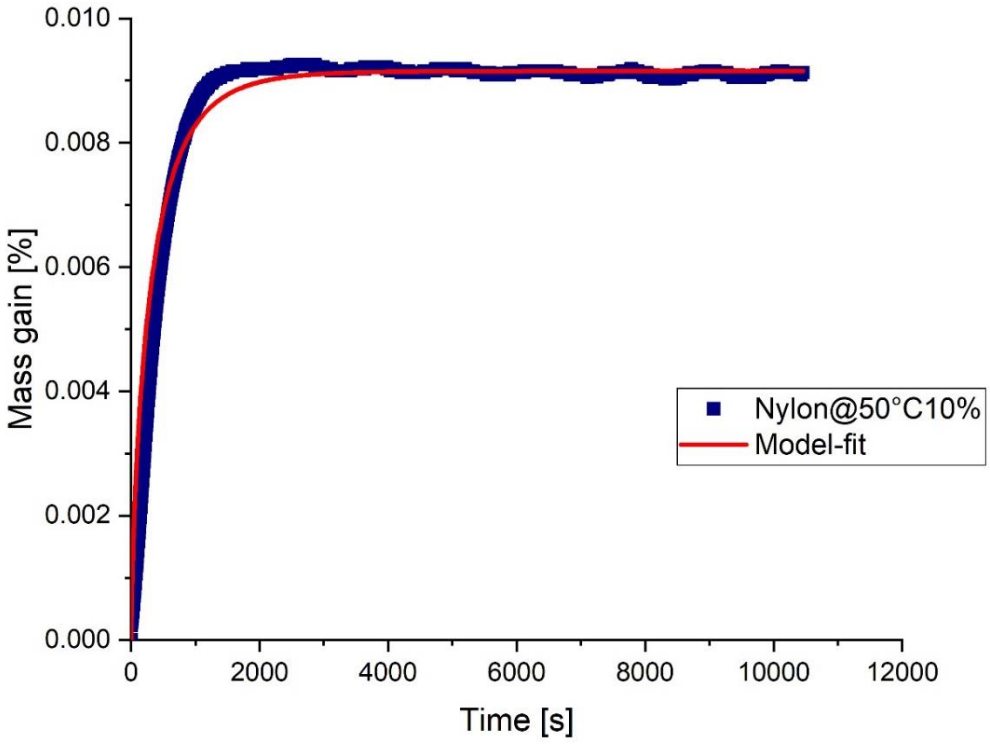

Figure 5.8: Model fitting verification using the estimated diffusion coefficient

5.2 Mathematical modelling on moisture uptake behaviour of textile reinforced rubber material

According to C. Shen et al., the diffusion coefficient of a rubber composite D_c can be estimated from the coefficient of rubber D_r and the fibre volume fraction V_f using *Equation 5.3* [97]. Since the rubberized fabric cords are surrounded by rubber, the diffusion coefficient of rubber dominates therefore the sorption process of the composite material.

The rubber composite is cut from the calendered sheet, and therefore, has a cross section in rectangular shape with length *l* and width *w*. The textile cord can be regarded as cylindrical with a diameter *d*. The fibre volume fraction can be calculated through *Equation 5.4*. The sample of rubber composite is coplanar to the upper surface. Therefore, the orientation of the fibre with respect to x axe is 90° ($\boldsymbol{\alpha} = 90°$).

$D_c = D_r \left[\left(\mathbf{1} - V_f\right) cos^2 \boldsymbol{\alpha} + \left(\mathbf{1} - \mathbf{2}\sqrt{\frac{V_f}{\boldsymbol{\pi}}} sin^2 \boldsymbol{\alpha} \right) \right]$	*Where*	D_c *: Diffusion coefficient of composite material* D_r *: Diffusion coefficient of rubber material* V_f*: fibre volume fraction* $\boldsymbol{\alpha}$*: fibre orientation with respect to x axe*	*Equation 5.3*
$V_f = \frac{\pi d^2}{4lw}$	*Where*	d *: diameter of the cord* l *: length of the sample cross section* *w: width of the sample cross section* V_f*: fibre volume fraction*	*Equation 5.4*

The rubber matrix was not measured in the Sorption TGA systematically, but only tested at specific environment conditions to support the modelling. The diffusion coefficient can be estimated using the model and the strategy as explained in the last section, as shown in Figure 5.9. Thus, all the parameters are collected to be able to calculate the coefficient D_c .

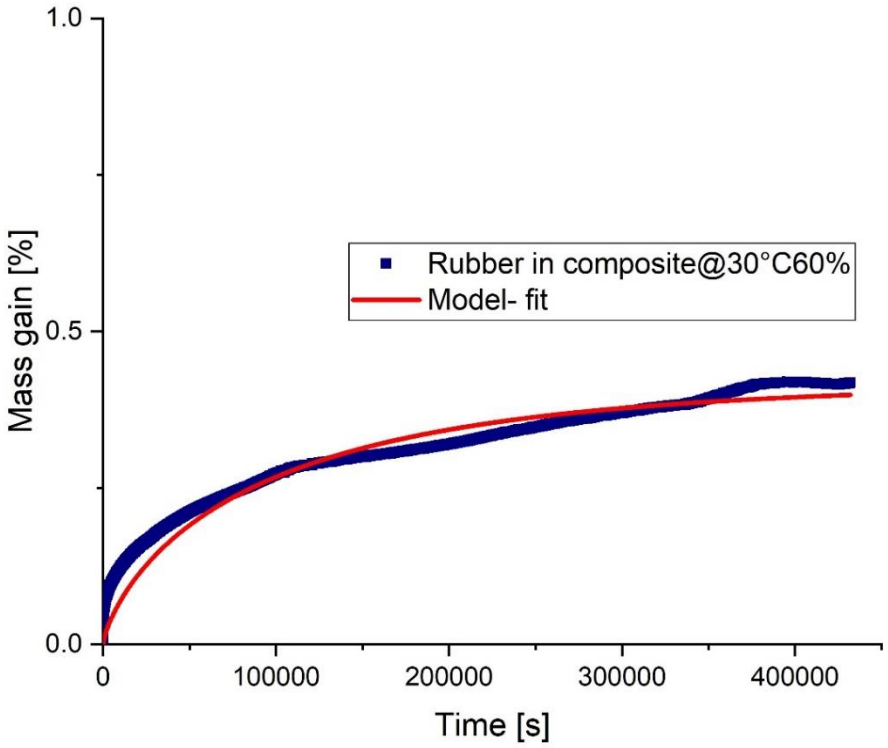

Figure 5.9: Model fit to estimate the diffusion coefficient of the rubber matrix

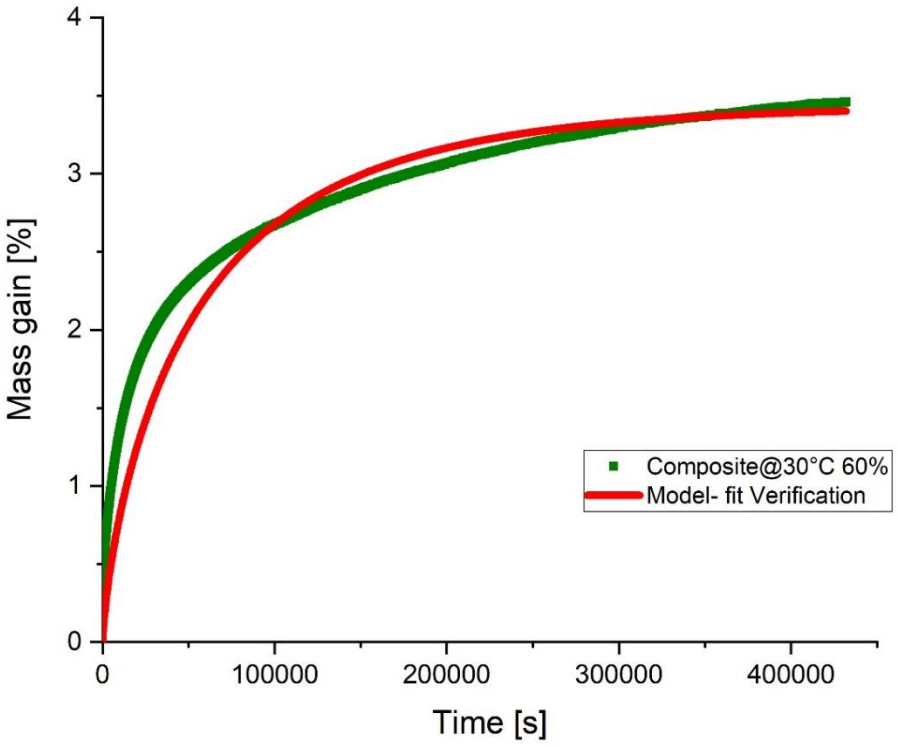

Figure 5.10: Model-fitting verification on data measured at 30 °C and 60% of rubber composite material using the estimated diffusion coefficient

The verification using the estimated diffusion coefficient is illustrated in Figure 5.10. The predictive curve shows also a Fickian behaviour and is closed to the experimental, with an R-square of the result about 0.92 which is acceptable. The measurement on rubber

composite consumed too much time. Due to the stability performance of the instruments, the effort for achieving reproducibility is too big. To optimise the model, more data and experiments for parameter determination are necessary.

5.3 Summary

In this chapter, the mathematical modelling was performed based on the results of the Sorption TGA measurement on different textile cords and rubber composites. The main contribution of this chapter can be summarised as follows:

1. According to the microscopical results of the cross sections, the shape of the textile samples can be regarded as cylindrical. The length of the sample investigated by Sorption TGA on textile cords are obviously much larger than the diameter of the sample. Thus, the problem can be considered as one dimensional. The model based on Fick's law can be applied to the data.

2. The diffusion coefficient *D* under different environment conditions are estimated with the method of model fitting. The fitting process shows high levels of correlation shown by the R-square value, especially for the data of rayon cords. The diffusion coefficient *D* estimated from the model fitting are placed into new coordinate systems in order to determine the relation between the coefficient and the temperature, which is approximately linear according to the Arrhenius dependence. The plot is linearly fitted again to estimate the diffusion coefficient *D* at other environment conditions not included into the parameter group for first model fitting. The simulation curve for mass changes is built using the coefficient estimated by the model to fit the data from the experiment. The data produced by the simulation curve is close to the experimental verification. The same strategy is applied on the nylon cords. The model can reproduce the experimental uptake curves in most cases. The estimated diffusion coefficient can be verified with the experiments at the other conditions. However, the model cannot properly fit the experiment at some extreme environment conditions because of restrictions during the experiment.

3. For the textile reinforced rubber, the diffusion coefficient can be estimated with help of different parameters such as the diffusion coefficient of the rubber matrix, fibre orientation and the fibre volume fraction. These parameters can be determined with experimental methods or estimated with model-fitting method. With a similar strategy as for the textile cords, further model-fitting methods are applied on the diffusion coefficient of the rubber composites to obtain the relation between the coefficient and the temperature. The diffusion coefficient at further environment conditions can be predicted. The prediction result is used to produce the simulation curve which is verified through model fitting with the experimental results. The verification shows with the estimated parameters the simulation curve can reproduce the experimental data.

4. The model can be used to predict the moisture uptake behaviour of textile cords and the textile reinforced rubber, which follows a Fickian diffusion. However, the work on modelling is still on a preliminary stage. Further work, such as the transport of the moisture in the corresponding longitudinal direction of the textile cords, the capillary effects along the cords, and the effect of laminate structures, is still needed to improve the accuracy of the prediction.

6 Influence of moisture on properties

The relationship between environment conditions and the absorbed moisture content is already clarified in chapter 4. To achieve the next objective, namely the influence of absorbed moisture on mechanical properties, the relationship should be extended to environment conditions and mechanical properties.

In this chapter, the influence of moisture absorbed from the environment on different properties of the materials is demonstrated. As an example of application, nylon is chosen as the research target since it is widely applied as reinforcing material in the rubber industry and it shows hydrophilic properties.

The static mechanical property is measured using the load-elongation test, which is extended with environment functionalities. The dynamic-mechanical properties are tested with a DMA supported by a humidity generator to simulate the environment condition in the DMA chamber. With microscopical methods and the classical peel test, the adhesion between rubber matrix and the nylon cords is characterised.

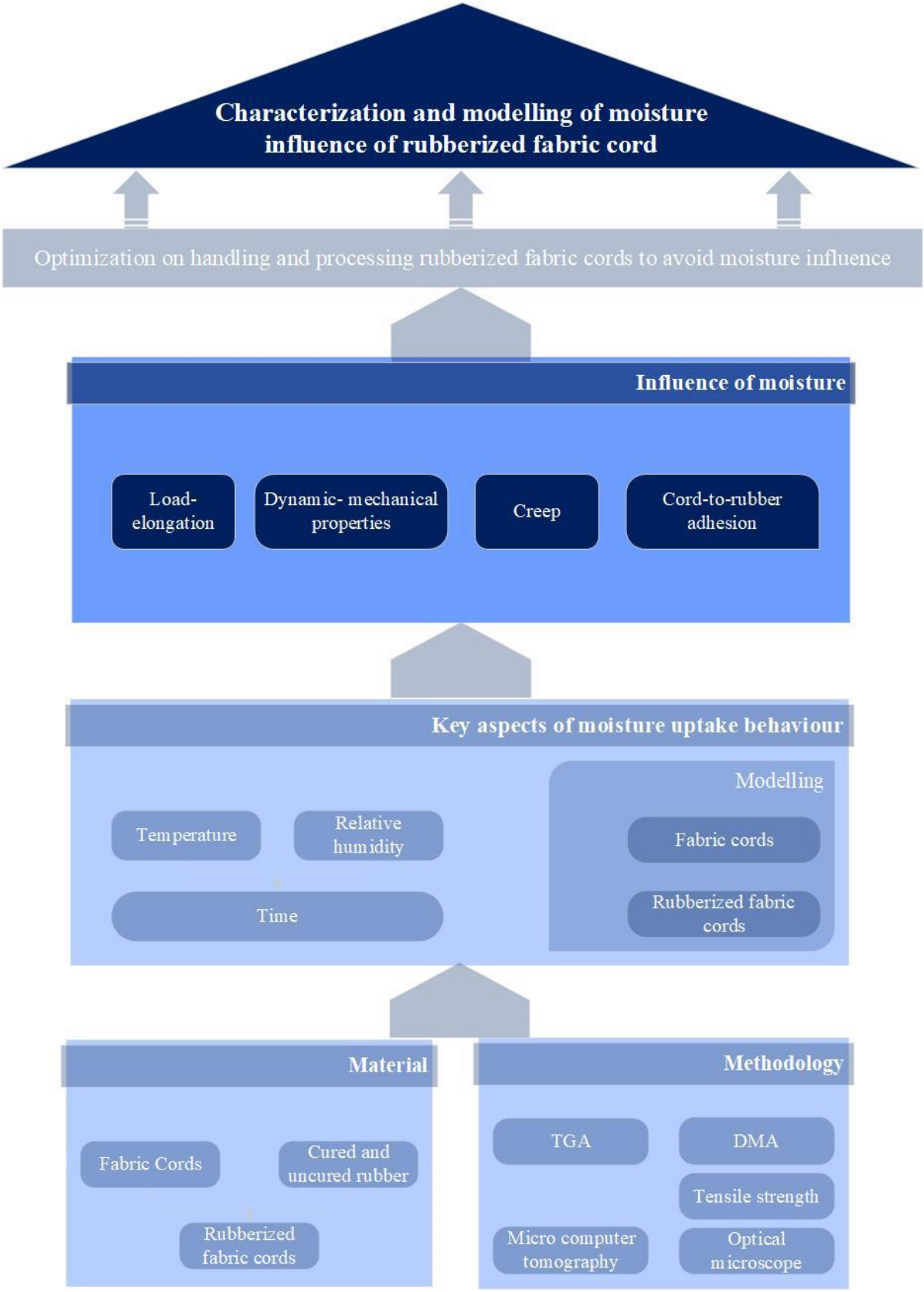
Characterization and modelling of moisture influence of rubberized fabric cord
Optimization on handling and processing rubberized fabric cords to avoid moisture influence
Influence of moisture
Load-elongation
Dynamic- mechanical properties
Creep
Cord-to-rubber adhesion
Key aspects of moisture uptake behaviour
Temperature
Relative humidity
Time
Modelling
Fabric cords
Rubberized fabric cords
Material
Fabric Cords
Cured and uncured rubber
Rubberized fabric cords
Methodology
TGA
DMA
Tensile strength
Micro computer tomography
Optical microscope

6.1 Static -mechanical properties

According to ASTM D855 and DIN 53815, the relation between tensile force and elongation is tested with the load-elongation test [107, 108]. In order to investigate the influence of moisture on this relation, the standard test is adjusted as described in section 3.2.2.1.2 and performed on a servo-hydraulic load frame with an environmental chamber from MTS Systems Corporation, Minnesota, USA.

6.1.1 Load- elongation test on rayon cords

Based on the results of the Sorption TGA measurements demonstrated and discussed in Chapter 4, a databank is built, and the relation is obtained between moisture content in rayon cords, environment condition (temperature and relative humidity) and the storage time. The rayon cords can absorb up to 6% moisture within a time interval of 20 minutes. Since the environment chamber offers the possibility to provide humidity during the experiment, the storage time under 40 ℃ and 30% relative humidity is chosen as the experiment conditions. The reason is that after the chamber is opened for the placement of the sample, a drop of temperature and humidity can be observed. Since the whole process of the sample placement is finished in 20 seconds, the influence on temperature is relative slight and the 40 ℃ can be regained quickly. But, the relative humidity drops to the level of room humidity in that short time, so that the 30% is chosen since it is similar to the room condition in the laboratory.

Table 6.1: Environment conditions for the load-elongation test on rayon cords

moisture adsorbed%	1%	2%	3%	4%	5%
storage time [s]	101	232	388	590	880

According to the result of the Sorption TGA measurement under 40 ℃ and 30% relative humidity, the samples are stored under the conditions for a certain time to get the 1% -5% moisture content absorbed (Table 6.1). The load-elongation test starts after that time immediately.

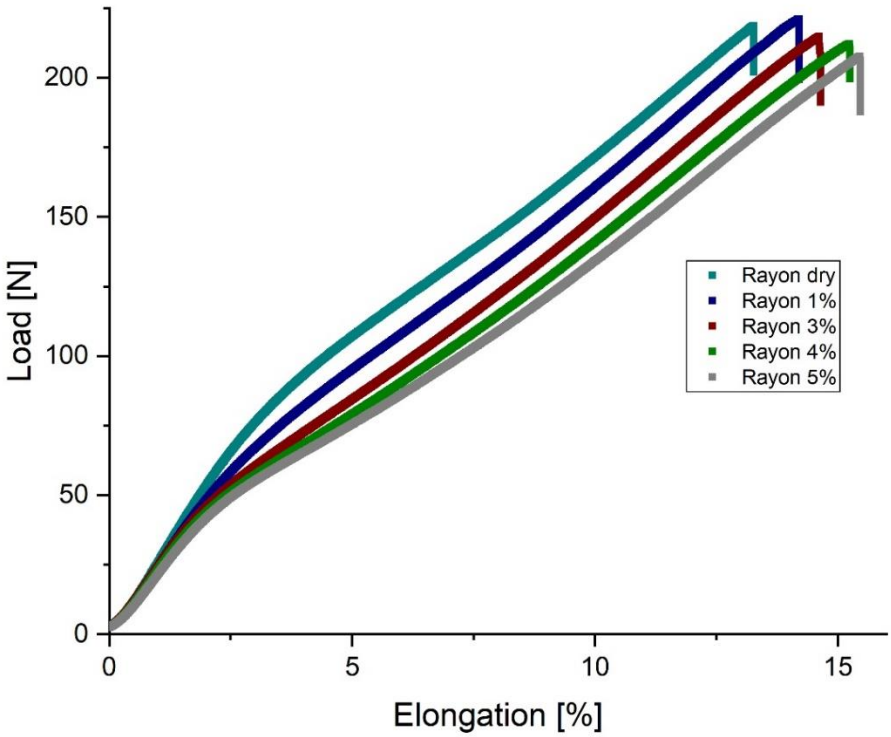

Figure 6.1: Load-elongation testing of rayon cords with different moisture content in accordance to ASTM D885 and DIN 53815

The result of the load-elongation test on rayon is illustrated in Figure 6.1. The load with elongation up to 2% is nearly the same for all the samples with different moisture content. This means there is nearly no influence from the moisture on the load below the elongation of 2%.

After that, the load of the samples with moisture begins to grow with a dropping velocity until the elongation reaches 5%. The curve rises after 5% elongation with similar slope up to the breaking elongation. This indicates the influence of moisture starts becoming visible above the elongation of 2% and the effect on the load is related to the moisture content.

As shown in Figure 2.4 and Figure 2.10, the hydroxyl groups of the cellulose fibre, from which rayon is made, is the main reason for the moisture absorption. In the molecular structure of rayon, there are both intramolecular hydrogen bonds and intermolecular hydrogen bonds. The hydrogen bonds are dissociated because of the moisture uptake behaviour. The properties of the sample are therefore impacted through this dissociation. Since the intramolecular hydrogen bonds may influence the molecule structure such as the angel of molecules, the influence of the dissociation of the intramolecular hydrogen bonds is related to the phenomena in the beginning stage of the load elongation test.

The intermolecular hydrogen bonds, which are occurring between cellulose molecules, are loss to be found between cellulose and water molecules after the dissociation. Thus, the flexibility of cellulose molecules chains is increased. The flexibility is related to the grade of the dissociation which is combined with the moisture content in the sample. The grade of dissociation happened in the samples with higher moisture content is greater than in the samples with lower moisture. Thus, the influence of moisture is also more obvious on these samples.

The breaking force, which reflects the breaking strength, can also be found in Figure 6.1. The values of the force at the breaking time lie very close to each other, which indicates the influence of moisture on the breaking force is very limited. However, the broad dispersion of breaking elongation is obvious. The sample with higher moisture content can easier reach a larger elongation under the same load due to the flexibility and an opened elongated network of molecular chains. Since the breaking loads are similar, the breaking elongation of the sample with higher moisture content is also bigger than the one of the drier samples. Moisture is acting here as a softener which changes the strength of the material.

6.1.2 Load-elongation test on nylon cords

Unlike the rayon cords, it takes more time for the nylon cords to absorb moisture from the environment. According to results from section 4.1.2, nylon cords can absorb up to 2% moisture within 20 minutes, which is insufficient to obtain a reproducible result by mechanical experiments. In order to reach 3% moisture, more than 2 hours storage time in the MTS chamber are required before each measurement. It consumes too much time if the method stays the same as by measuring rayon. Thus, the samples of nylon cords are stored under different environment condition until equilibrium and placed then into the MTS chamber to be measured. Since the placement takes only about 15 seconds time and 10 seconds for the experiment, there should not be a significant difference on moisture content in the sample. The storage conditions can be found in Table 6.2.

Table 6.2: Storage conditions and the moisture content of nylon cords before load-elongation test

Storage conditions/ moisture quota (%)	*Dry*	*23°C 55%*	*30 °C 80%*
Nylon cords	*0.8%*	*2.5%*	*3.6%*

The results of the load-elongation tests on nylon cords are illustrated in Figure 6.2. Different from the result of rayon cords, the load on nylon cords with different moisture content begins to vary after an elongation of about 10%. At the beginning of the test, all the curves rise with nearly same slope. The curve of the sample with highest moisture content, 3.6%, start

to rise with a decreasing slope after 10% elongation. The sample with 2.5% moisture stays with the sample with 0.8% moisture together until an elongation of 15% is reached.

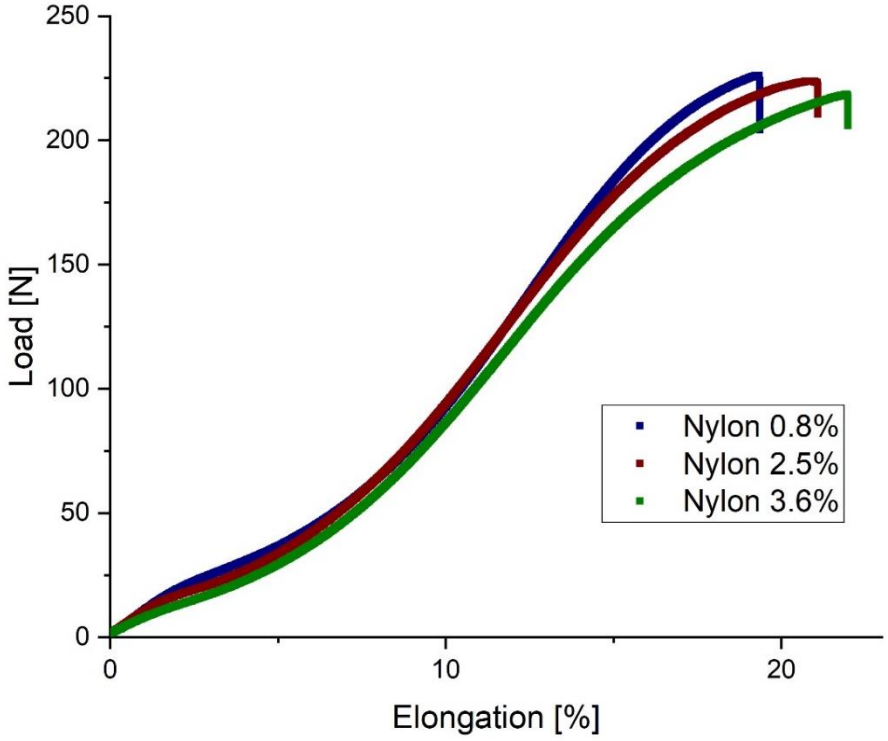

Figure 6.2: Load-elongation testing of nylon cords with different moisture content in accordance to ASTM D885 and DIN 53815

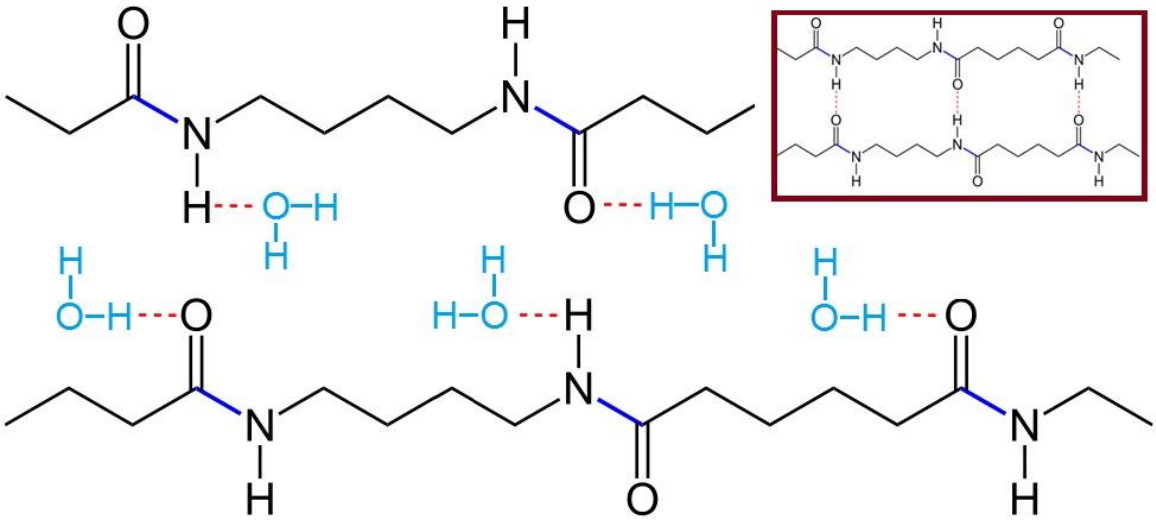

Figure 6.3: Dissociation of hydrogen bonds from polyamide under moisture

The reason of the variation can be described in the same way as for the rayon cords. According to Figure 2.5 and Figure 2.11, the molecular chain of polyamide 6.6 contains hydrogen bonds. As shown in Figure 6.3, the hydrogen bonds are dissociated and replaced by water molecules, which means the molecular chains are not connected by hydrogen

bonds with other chains anymore, but with water molecules. Therefore, the molecular chain segments of polyamide 6.6 become flexible through the dissociation of hydrogen bonds. The sliding between molecular chains can be occurred more easily. The grade of the flexibility is related to the grade of dissociation, which is determined by the moisture content in the sample. Thus, the sample tends to get higher elongation under the same external load than the sample with lower moisture content. From another perspective, the sample with higher moisture needs a lower external load to get the same elongation than the drier samples. That is the reason why the curve with higher moisture content lies under the curve drier sample.

The breaking elongation and breaking force show also regularities like the rayon cords. The breaking forces are very close to each other. The breaking elongations are relatively far from each other because of the flexibility of the molecular chain segments of the sample due to the dissociation of hydrogen bonds.

The influence of the moisture in the sample on the static-mechanical properties can be observed in both rayon and nylon cords. The load-elongation properties of rayon cords are already affected at a small elongation of 2%. On nylon cords, the effect becomes evident at the elongation above 5%. The same tendency is shown in both materials for the results regarding force and elongation. The breaking elongation becomes larger under the influence of moisture, while the breaking force stays nearly the same under the environment conditions. It is therefore worthy to pay attention to the moisture influence on the dimension stability of the cord under load.

6.2 Dynamic-mechanical properties

As described in section 3.2.2.1.3 and section 3.2.2.1.4, the dynamic-mechanical analysis with humidity function is utilised to measure the influence of moisture on the creep relaxation and the dynamic-mechanical properties. For the purpose of exemplification, nylon cords are chosen as the investigation target.

6.2.1 Creep relaxation

To describe the relaxation of polymer material which is contributed by its viscoelastic behaviour, the massless mechanical models are used. The viscous and elastic characteristics of polymeric materials can be represented by a dashpot and a spring respectively. In the Maxwell-Model, the dashpot and the spring are connected in series and in Kevin-Voigt-Model they are joint in parallel as shown in Figure 6.4 and Figure 6.5. The Kevin-Voigt-Model is usually used to describe the creep behaviour and the Maxwell-Model is more suitable for understanding the stress relaxation behaviour[122, 123].

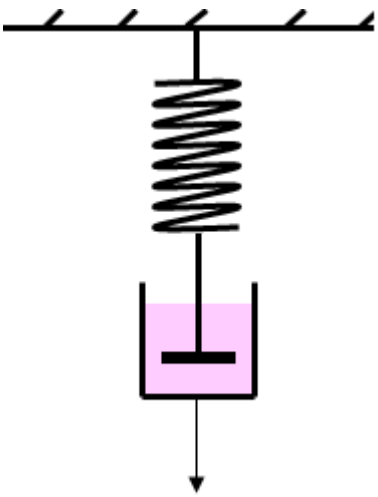

Figure 6.4: Maxwell-Model [122]

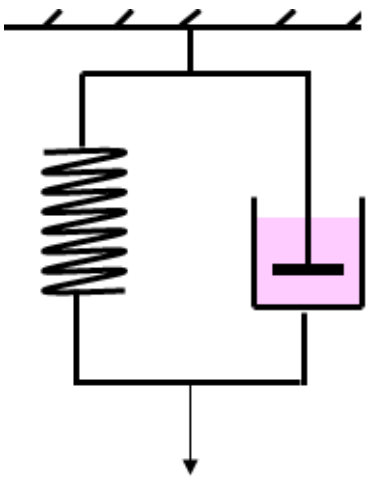

Figure 6.5: Kevin-Voigt-Model [122]

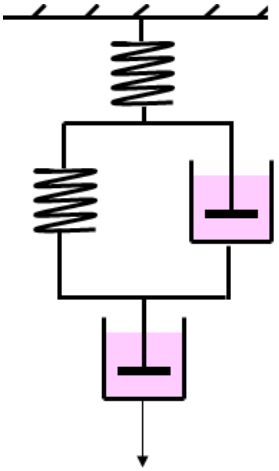

Figure 6.6: 4-Element-Model [122]

In fact, the Kevin-Voigt-Model is insufficient to describe the creeps in polymeric materials. A 4-Element-Model consisting of one Maxwell element and one Kevin-Voigt elements is more suitable to be used to describe the polymeric creep behaviour, as shown in Figure 6.6[122, 123].

The creep relaxation is measured using the method illustrated in Figure 3.19. The experiments are done firstly as pre-test to get an overview of the performance of the different cords regarding the influence of moisture on creep relaxation. Results are shown in Figure 6.7 and Figure 6.8.

According to the results of Sorption TGA measurements in Chapter 4, the rayon cord absorbs at 40 °C and 40% relative humidity about 7% moisture within the 30 minutes experiment time, while the values of nylon are about 2.5% and below 0.5% for polyester. After the comparison of the curves of each cord type, the influence of moisture on nylon is about 3.7%, 1.3% for rayon and 1.65% for polyester. Therefore, nylon is chosen as the investigation target in the creep test since the mechanical effects are more accentuated to show the principal aspects of relaxation under moisture.

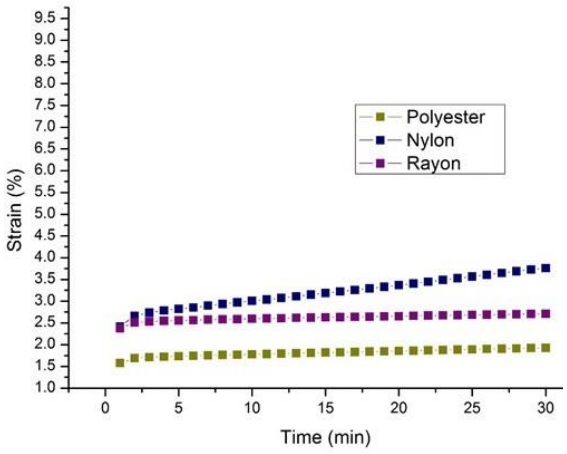

Figure 6.7: Creep relaxation of 3 cords without moisture under 60 MPa

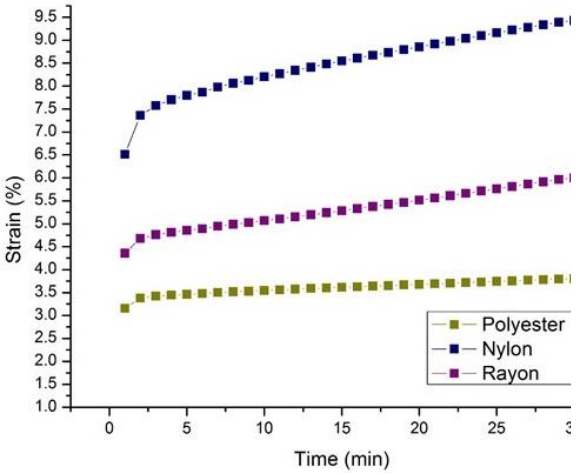

Figure 6.8: Creep relaxation of 3 cords under 40 °C and 40% relative humidity under 60 MPa

From the results shown in Figure 6.9, the influence of moisture on the creep relaxation of nylon cords can be observed. At the beginning of the experiment, the sample immediately responds to the load with a strain that increases linearly. In this stage, there is nearly no difference to be observed between samples at different levels of moisture with this pure elastic behaviour. The strain in the first stage is caused by the instant response of the network or tinny deformation which is due to the change of the length and angle of the chemical bonds. These aspects are not affected by absorbed moisture, therefor there is no obvious difference between the samples under different environment conditions.

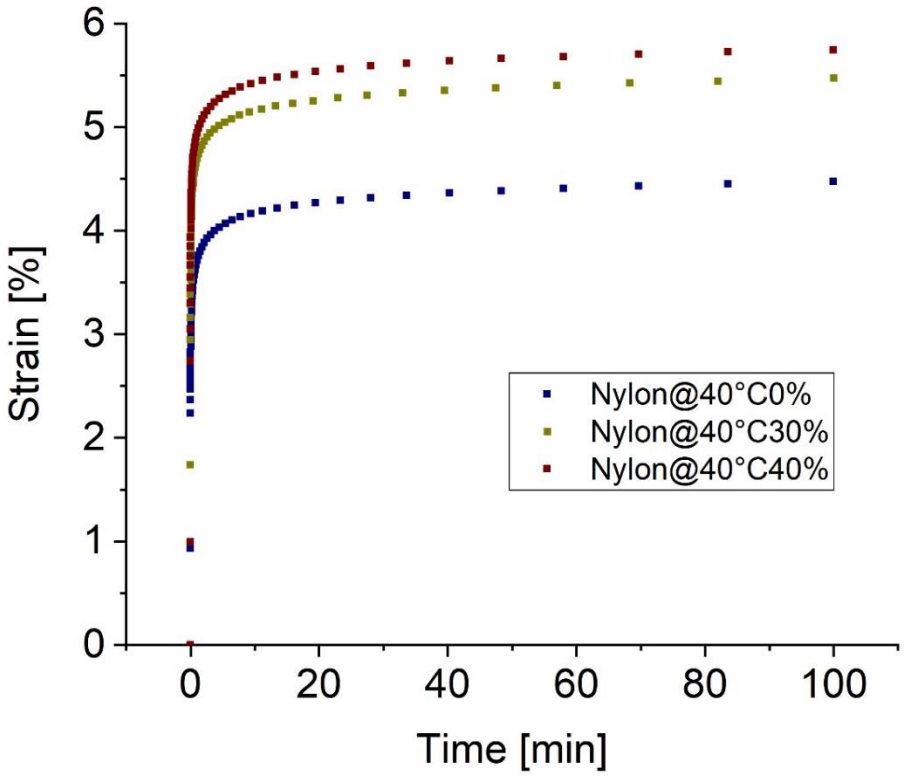

Figure 6.9: Creep relaxation of nylon cords under 0%, 30% and 40% relative humidity, 40 °C

After the stage with instantaneous strain, the rate of deformation starts to decrease rapidly with time. This deformation changes with time is called creep. The creep in this stage is caused by viscoelastic response, which is related to the motion of the molecular chain segments. The high elastic part of the viscoelastic behaviour can be described with the Kevin-Voigt-Model as shown in Figure 6.5. As described in last section, the main aspect of moisture absorption by nylon cords is the availability of hydroxyl groups. The dissociation of hydrogen bonds during the moisture uptake process gives rise to more flexibility of the chain segment. According to the result from section 4.1.2, the moisture content in the nylon cords at same temperature is proportional to the level of humidity. The chain segments of the sample at higher humidity are therefore more flexible than those at lower humidity. This flexibility of chain segments reflects as a higher strain under the same load on the sample. Thus, the curve at higher humidity lies above the one at lower humidity.

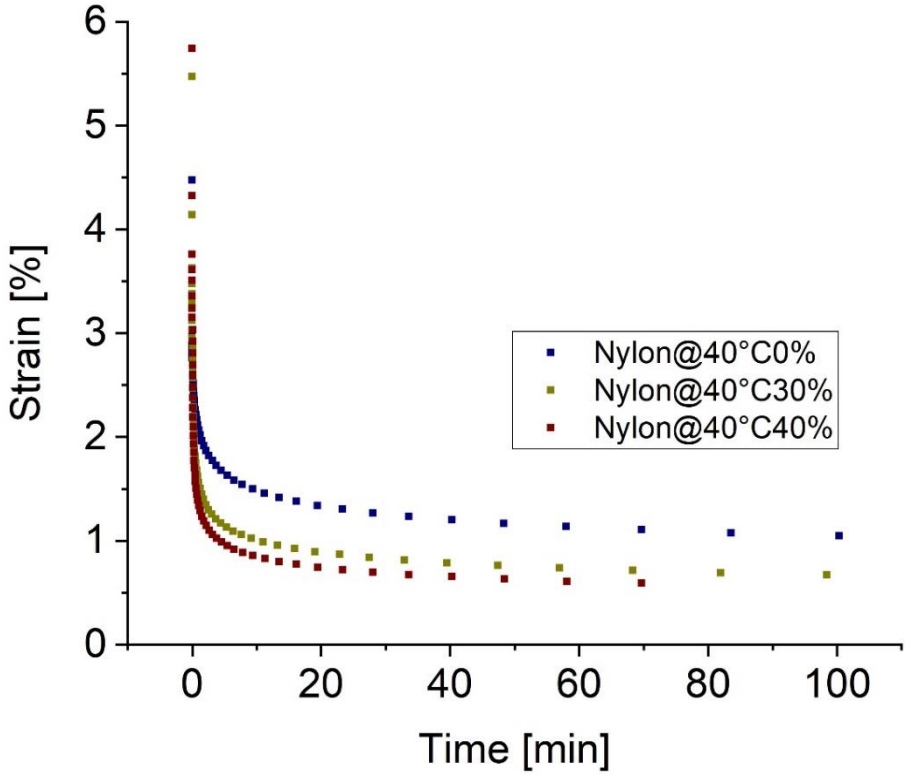

Figure 6.10: Recovery after the displacement in creep relaxation test of nylon cords under 0%, 30% and 40% relative humidity, 40 °C

As shown in Figure 6.10, the strain of the sample starts immediately decreasing at when the load is relieved. This can be explained using the same theory in the load displacement phase. The immediate recovery can be related to the instant response of the material. Since there is nearly no influence of moisture on these aspects, the curves of recovery are observed as overlapped.

The strain of the sample continues decreasing after the first stage until a residual strain. The main aspect affecting this process is the motion of chain segment, or the flexibility of the chain segment in another way. Since the recovery in this stage is caused by the viscoelastic response, the decrement of the strain is a gradual process. The sample at higher humidity absorbs more moisture and can get a more significant retraction in this stage. The deformation set is caused by the viscos flow is shown in Figure 6.11. This deformation set and the immediate response in at the beginning of the displacement- and recovery phase can be better described with the 4-Element-Model as shown in Figure 6.6. The nylon cords with higher moisture content has the lowest plastic deformation. Since the sample can get the most retraction in the recovery.

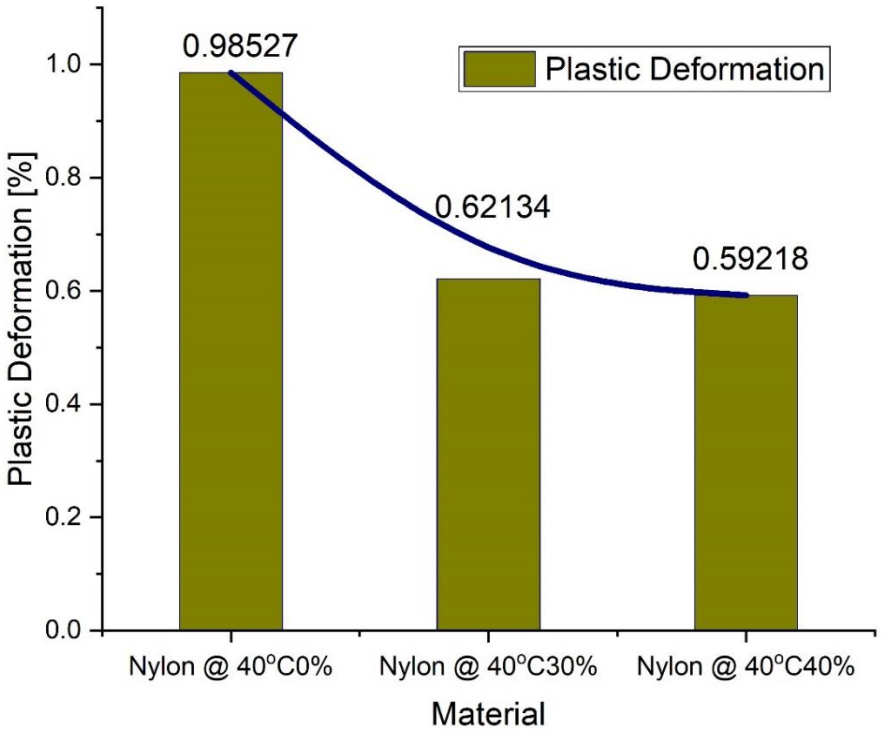

Figure 6.11: The plastic deformation of the sample at different humidity

6.2.2 Frequency sweep

As explained in section 2.2.1.1, the absolute moisture content in the air at the same pressure is related to the temperature. The temperature sweep test measured at different temperatures is therefore not appropriate as the moisture in the sample is difficult to be determined. The frequency sweep is applied to identify the influence of moisture on the dynamic-mechanical property of the nylon cord and the rubber reinforced with nylon.

The sample of nylon cords is placed into the chamber of the DMA and stored there for enough time before the test starts to get the equilibrium state, so that no more change of moisture content of the sample is happening during the experiment. Since the key aspects affecting the result of the frequency tests are the temperature, the strain and the frequency itself, all the experiments are performed at same temperature.

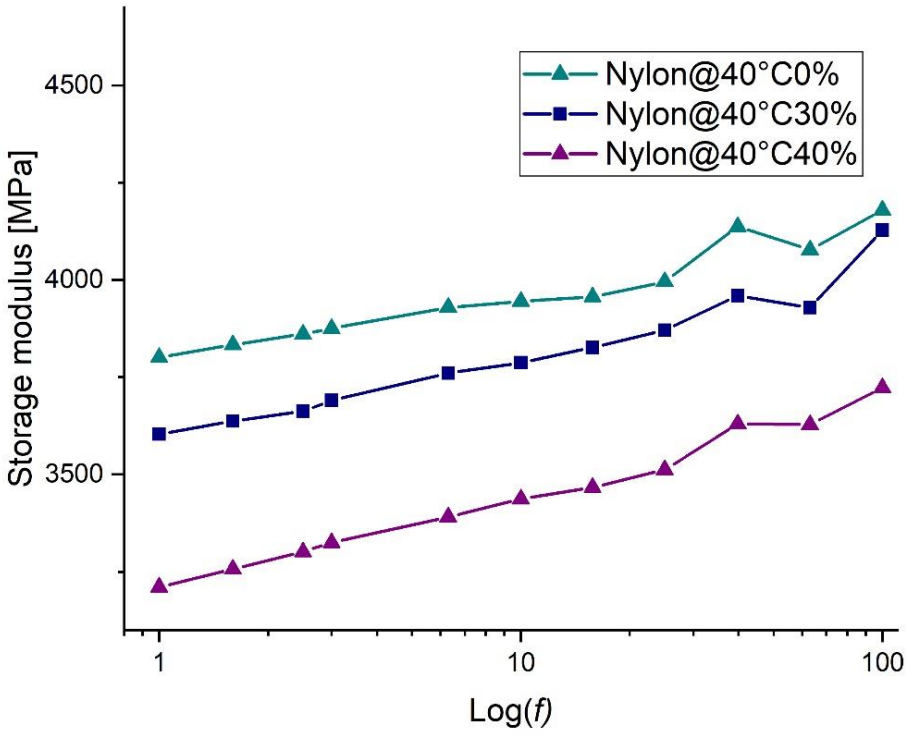

Figure 6.12: Influence of moisture of nylon cords on the storage modulus as a function of frequency at 0%, 30% and 40% relative humidity and 40 °C

As shown in Figure 6.12, the storage modulus of the sample is lower with the higher storage humidity. Since all the samples are in the equilibrium state, in which the maximum of moisture content at the environment condition is reached, the sample at higher humidity contains more moisture, according to the results from chapter 4. Thus, the sample with higher moisture content has a lower storage modulus. The influence of moisture on the storage modulus can be reflected from the state of the chain segment. In the chemical structure of nylon cord, the flexibility of chain segment is restricted by the bonding between the molecular chains. The hydrogen bonds which connect the chains are dissociated because of the moisture absorption and the chain segments can become more flexible. The motion of chain segments is the main reason of the drop of the storage modulus.

Through the observation of the curves in the area of lower frequency (below 30Hz), the slope of the curve shows a linear relationship between the storage modulus and log(f). The curve slope is also detected to increase slightly together with the frequency. This increase of slope indicates the increasing of dependency from storage modulus on the frequency. The reason can be backtracked to the time–temperature equivalence principle. The influence of the high frequency is equivalent to the influence of low temperature. From the perspective of chain segment motion, if the load lasts shorter than the response time the segment needs,

the segment will not perform any movement. This effect is in analogy to the effect at low temperature which results in an increment on modulus. In contrast, the chain segment has enough time at low frequency to respond the load, and therefore, the segment motion will be performed which brings a decrement on modulus.

Besides, the slope of the curve shows a slightly increment at higher moisture content. The hydrogen bonds between molecular chains are replaced by a new hydrogen bond between the molecular chains and the water molecules. Those hydrogen bonds are weaker than the bonds between the chains of nylon. Thus, the possibility that the bonds are destroyed during the loading at the lower frequency which is equivalent to a higher temperature is higher with more moisture content in the sample. That leads a slope increment at higher humidity.

The influence of moisture absorbed from the environment on the loss factor can be observed in Figure 6.13. The loss factor of the sample with higher moisture content lies above the curve representing the sample with lower moisture content. Since the loss factor describes the mechanical energy loss of the material when dynamical load is applied on it, the distribution of the curves can be recognized as relation between moisture content and the mechanical energy loss of the material.

As discussed in last section, the chain segment performs no motion if the time of load application is much shorter than the response time. In this case there will not be any mechanical loss. Because of the dissociation of hydrogen bonds caused by moisture absorption, the restriction on the chain segments is decreased. Besides, new hydrogen bonds are built between the water molecules and the molecular chains of polyamide. The distance between polyamide chains are therefore enlarged, which also makes the motion of chain segment easier. The segment motion is increased, which means that there will be more energy dissipated as heat compared to the material with less segment motion. The more moisture the sample absorbs, the more hydrogen bonds are dissociated. Thus, the sample with more moisture has a lower loss factor than the sample with less moisture (40 °C).

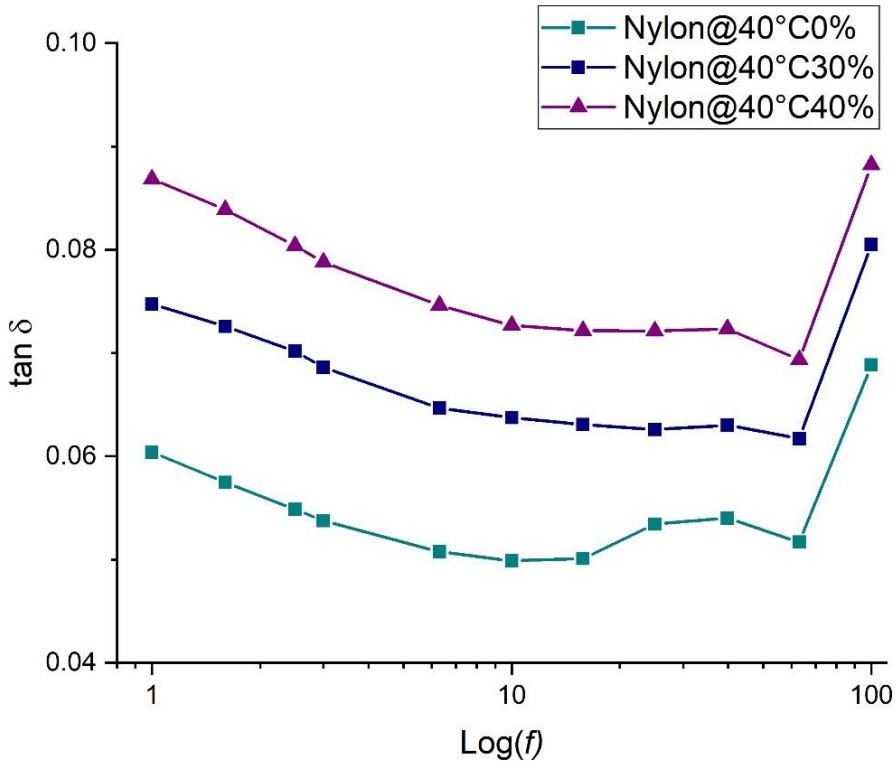

Figure 6.13: Influence of the moisture of nylon cords on the loss factor (tan (δ)) as a function of frequency at 0%, 30% and 40% relative humidity and 40 °C

Furthermore, it can be observed that the loss factor decreases with increasing frequency change. It can also be explained by the motion of chain segments. The motion at high frequency is restricted since the response time the material needs is longer than the time in which the load is applied. With lower flexibility the mechanical loss is also decreased.

Based on the result from section 4.3, the procedure of the frequency sweep test on the textile reinforced rubber is adjusted. The sample of rubber composite needs several days to reach its equilibrium state. Since it consumes too much time and energy, it is not feasible to place the sample in the DMA chamber and let it get the moisture there for such a long time. Besides, both the velocity of moisture absorption process and desorption process are slow. If the frequency sweep can be performed in a short time, the moisture content in the sample will not variate much. Thus, all the samples of rubber composites are stored in the climate chamber under the environment condition until they reach their saturation state. The frequency sweep test is performed immediately after the samples are taken out of the climate chamber.

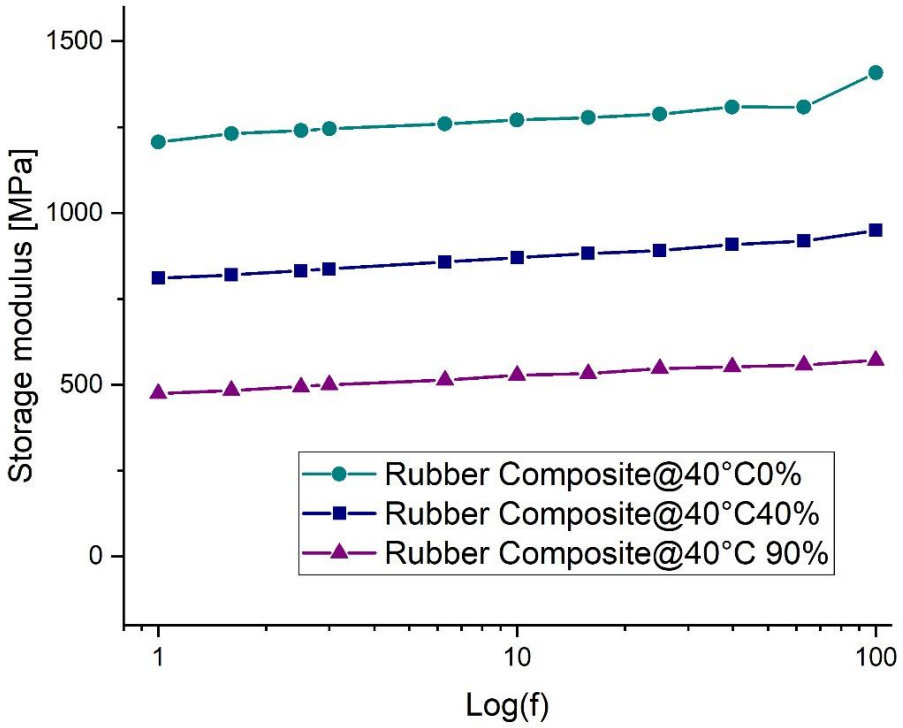

Figure 6.14: Influence of moisture on storage modulus from frequency sweep test on rubber composite materials with nylon fibre at different environment conditions

The influence of moisture on storage modulus is depicted in Figure 6.14. In analogy to the results of nylon cords, the curve from the sample with less moisture lies above the curve from the sample with more moisture. The dissociation of the hydrogen bonds plays here an important part. With the effect from the hydrogen bonds dissociation, the flexibility of chain segment is increased. The more moisture the sample absorbs, the more flexibility its chain segments have. The segments motion affects the storage modulus. Therefore, the storage modulus of the rubber composite is proportional to the moisture content in the sample.

The difference between the curves of the rubber composites and the nylon cords is obvious. The curve slope of the nylon cords is higher to be observed (Figure 6.12). The curves of rubber composites are much flatter. Since the storage modulus of the rubber composite is resulted from the cords and the rubber matrix together. The combined effect of the cord and matrix can be observed at the value of storage modulus, which is much higher than the storage modulus from rubber but also much lower than that from nylon cord. The rubber matrix shares a part of the strain on the system so that the strain applied on nylon cord becomes less. Since the moisture content in rubber is very low, the influence of moisture can be ignored. And the rubber will stay in the high-elastic state under the test frequency. The storage modulus of rubber shows no dependency on the test frequency; therefore, the slope of the curve tends to zero.

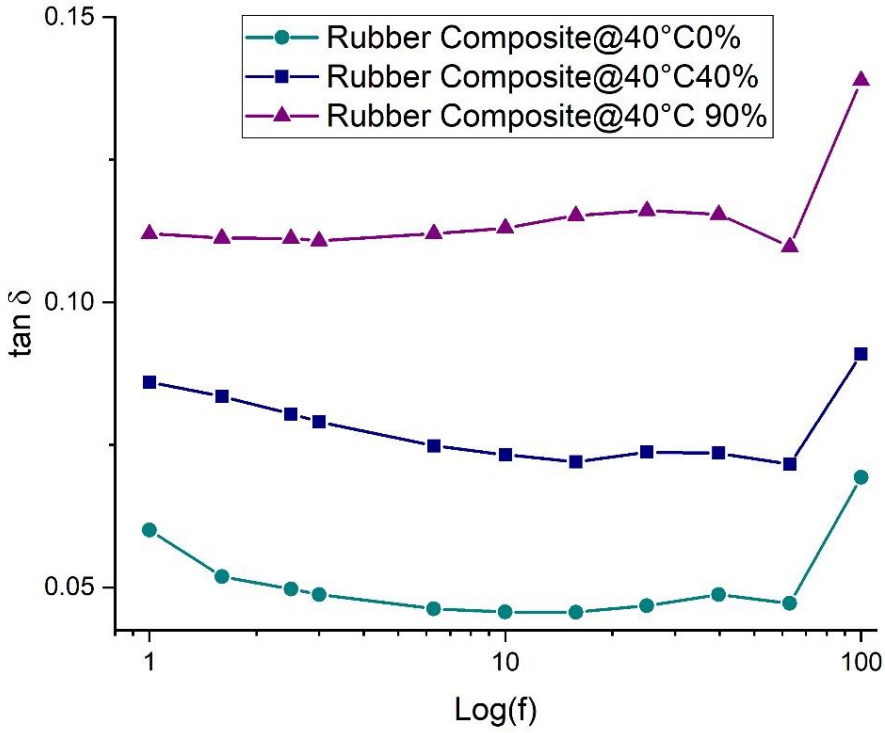

Figure 6.15: Influence of moisture on loss modulus from frequency sweep test on rubber composite materials with nylon fibre at different environment conditions

The influence of moisture on the loss factor of rubber composite material can be found in Figure 6.15. In analogy to the nylon cords, the loss factor is inversely proportional to the moisture content. The main reason of the energy dissipation is the motion of chain segments of the cords which brings more frictions between the segments. The chain segments get more flexibility through the dissociation of hydrogen bonds between the chains which happens by moisture uptake. They can better respond the load which is applied on them frequently. Thus, the possibility of a motion from chain segment become larger and more energy is dissipated to heat.

In analogy to the nylon cords, the loss factor of rubber composite has larger dependency on the change of frequency, especially in the area of low frequency. This phenomenon is more obvious by the sample saturated under relative lower humidity. This can also be related to the chain segment motion. Since the chain segments of nylon can better respond to the load applied at lower frequency, there will be more segment motion than at high frequency. The loss factor is higher with more segment motion. If the dissociation of hydrogen bonds is high enough, the chain segments can also give response to the load at high frequency. The difference of loss factor will be reduced.

6.3 Cord-to-rubber adhesion

According to the result from last section, especially the difference between the result of nylon cord and nylon reinforced rubber, it can be assumed that the interaction between nylon cord and the rubber matrix plays an important part in defining the mechanical properties. In this section, experiments are performed to observe the influence of the moisture on the cord-to-rubber adhesion. Firstly. microscopical methods are used to identify if there is any influence of moisture on the resorcinol-formaldehyde-rubber latex system (RFL), which is utilised to enhance the cord-to-rubber adhesion. As the second step, the adhesion force between cord and rubber is determined to clarify the influence of moisture.

6.3.1 Influence of moisture on the resorcinol-formaldehyde-rubber latex system (RFL)

As described in section 3.2.2.2.1 the test is performed with help of optic microscopy. The result is shown in Figure 6.16. On the left side, images of the nylon cord at a nominal magnification of 300 times show the macro structure of the cords. Since the humidity conditioning happens in a climate chamber without light, its influence can be ignored. On the structure of the cord there is no mark of moisture influence to be found. After a storage of 72 hours at 40 °C and 90% relative humidity, the structure of the cord stays the same as in the initial state.

It is difficult to find the same position under the microscope at a nominal image magnification of 1000 times, although the position is pre-marked. With help of characteristic features of the cords, the image still can be compared. At the image magnification of 1000x, all the details of the cords and the RFL dip can be clearly observed. There is no defect or damage point caused by moisture to be found after the comparison of the images. The influence of moisture can be assumed as minor on the resorcinol-formaldehyde-rubber latex system.

a1) 300x image magnifications, initial state

b1) 1000x image magnifications, initial state

a2) 300x image magnifications, 24 hours

b2) 1000x image magnifications, 24 hours

a3)300x image magnifications, 72 hours

b3)1000x image magnifications, 72 hours

Figure 6.16: Nylon cord with different storage time at 40 °C and 90% relative humidity under the optical microscope

6.3.2 Influence of moisture on the cord-to-rubber adhesion

The best and classical method to determine the cord-to-rubber adhesion is the mechanical experiment, in which the cord and rubber matrix are separated, and the force is recorded to evaluate the adhesion. Besides, the sample after the experiments can also be evaluated optically to classify the quality of adhesion from another perspective, as introduced in section 3.2.2.2.3 and 3.2.2.2.4.

As described in section 3.2.2.2.2, before the destructive methods are applied, morphological methods such as X-Ray micro-computed tomography (micro CT) can be used to obtain information about the internal failures within the sample.

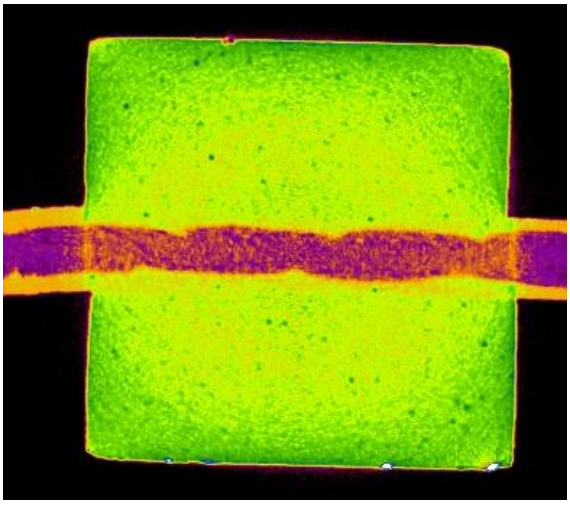

Figure 6.17: X-Ray micro-computed tomography on adried sample for pull-out test

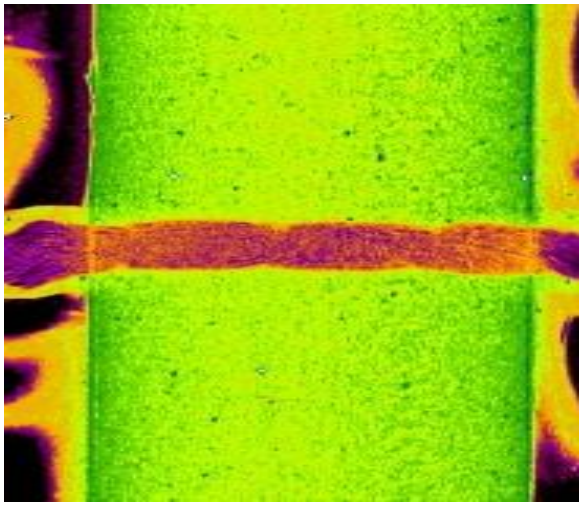

Figure 6.18: X-Ray micro-computed tomography on a sample saturated at 40 °C and 90% humidity for pull-out test

6.3.2.1 Pull-out test

The samples for the pull-out test are observed under the micro CT before the destructive test. Figure 6.17 shows the result of a sample which is prepared with cord dried in the desiccator. The rainbow colour map is used to indicate the density of the sample with the lower values are in yellow and the higher values in the reds. As shown in the result, the cord goes through the rubber has a different density. The part outside the rubber has a deeper colour which indicates the influence of moisture. The boundary is clear to be observed with different colour depth, which means the protection effect of rubber against moisture. Although there is still moisture in the cord under this protection, the amount is much lower than the outer part.

In Figure 6.18 the similar result can be found. The protection effect can easily be observed. But compared to Figure 6.17, the effect of the drying process before the sample preparation

is not obvious. According to the section 3.2.2.2.3, the cord used in the sample is conditioned in the climate chamber until its saturation at 40 °C and 90%. After the conditioning process, the cord is embedded into a rubber block with the form and vulcanized at 170 °C. Since the embedded part has only a length of 5mm, the absorbed moisture is assumed to escape from the sample during the vulcanization. Therefore, the moisture observed by micro CT in the sample stored at environment condition is not different from the dried one.

Table 6.3: Result of pull-out test

St. Adh. Textile RT	*Unit*	*Sample Dry*	*Sample 40 °C 90%*
Pull-out Force MEAN	*N*	*116.4*	*116.39*
Pull-out Force STDV	*N*	*5.39*	*2.86*
Pull-out Force MIN	*N*	*109.2*	*111.74*
Pull-out Force MAX	*N*	*124.4*	*119.78*

The results of the pull-out test confirm the assumption according to the micro CT test that the influence of moisture is minimal under the specific conditions of this test. Since the moisture content in the sample is strongly influenced by the sample preparation, another method is chosen to determine the cord-to-rubber adhesion.

6.3.2.2 Peel test

The limitation of the pull-out lies on the sample preparation, in which the moisture in the cord may escape because of the small embedding length. In the peel test, a sample with a strip form will be tested, which has a bigger adhesion area than in the pull-out test.

In analogy to the pull-out test, the micro CT is utilised to determine any internal failure before the destructive test. In order to ensure the moisture content for the peel test, pre-tests are done with samples made with calendered material and samples made in the laboratory from the same nylon cords and rubber. The results obtained by both methods show that the preparation process still has an influence on the moisture content since the sample must be vulcanized in the form under 160 °C and there is some moisture escaping through the edge of the sample. Therefore, the peel test cannot help to determine the relation between the moisture amount and the cord-to-rubber adhesion quantitatively.

The results are shown in Figure 6.19 and Figure 6.20. For both samples, the calendered materials are used in the inner layers to avoid the influence by preparing the sample with individual cords and rubbers. In Figure 6.19 the sample was stored at 23°C and 55% relative humidity, which is the room condition in the laboratory. It can be observed that there is moisture absorbed along the cord direction. The moisture has a slight aggregation at the twisted position because of the lower stress of the cord and the small free space. The dip

coating is obviously not influenced by moisture. Besides, the moisture amount in the middle of the samples is a bit more than on the boundaries.

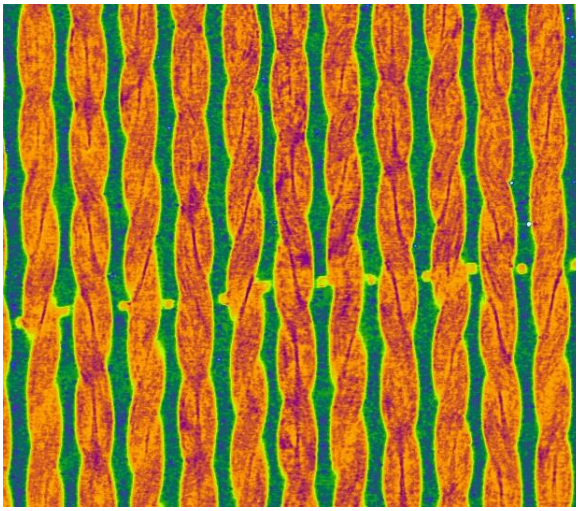

Figure 6.19: X-Ray micro-computed tomography of the sample saturated under 23℃ and 55% for peel test

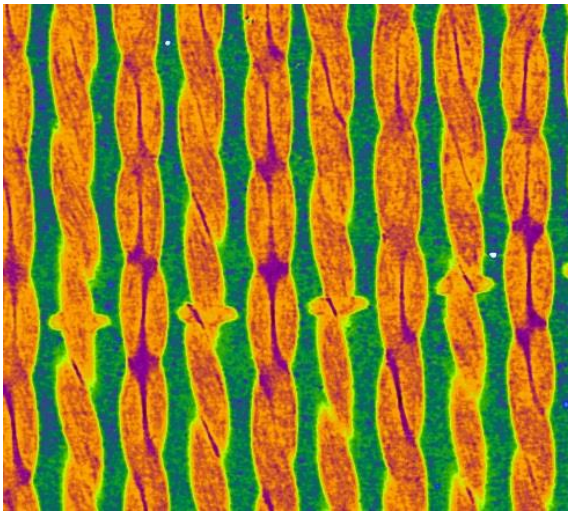

Figure 6.20: X-Ray micro-computed tomography of the sample saturated under 40 ℃ and 90% for peel test

The moisture in Figure 6.20 is similar as in Figure 6.19. The moisture distributes along the direction of the cord and aggregates at the position where the twist is. Since the cord can absorb more moisture at 40 ℃ and 90% than at room condition, the moisture can be observed clearer than in Figure 6.19. The colour and the area of moisture indicate that the moisture content in the sample is higher than in another one. However, the dip coatings in the sample are also not influenced since no obvious damage is found.

Table 6.4: Result of peel test

Peel test Textile	*Unit*	*23 ℃ 55*	*30 ℃ 70%*	*30 ℃ 90%*
Adhesion of Median MEAN	*N/25mm*	*123.61*	*121.13*	*121.51*
Adhesion of Median STDV	*N/25mm*	*3.51*	*3.44*	*1.86*
Adhesion of Median MIN	*N/25mm*	*121.33*	*117.39*	*120.08*
Adhesion of Median MAX	*N/25mm*	*127.65*	*124.15*	*123.61*

The result of the peel test is listed in Table 6.4. The adhesion mean indicates the static strip adhesion of rubberized textile fabrics evaluated through the separating forces. The adhesion of the sample stored at room temperature is only a bit higher than the other samples with higher moisture content. In analogy to the pull-out test, the standard deviation is also decreased with increased moisture content. This impact also the maximum value of adhesion during the test. Thus, it can be assumed that the influence of moisture has impact on the cord-to-rubber adhesion. But due to the small amount of moisture involved, which stays in the sample after the sample preparation, the impact is very limited.

To validate the assumption, a special sample is prepared using a sheet of calendered material which is immersed under water for a short time. The sample is then prepared and tested according to the same method described in this section in order to magnify the effects.

Table 6.5: Result of peel test on the sample immersed in water

Peel test Textile	*Unit*	*23 °C dry*	*23 °C wet*
Adhesion of Median MEAN	*N/25mm*	*166.69*	*153.47*
Adhesion of Median STDV	*N/25mm*	*6.12*	*0.6*
Adhesion of Median MIN	*N/25mm*	*160.22*	*152.78*
Adhesion of Median MAX	*N/25mm*	*172.4*	*153.88*

The result of the influence of water on the adhesion is clear. There is a decrease of about 8% on the mean value of separating forces. There is a large decrement on standard deviation which can be related to the drop of the maximum adhesion. The test under critical condition can validate the assumption that the moisture does have influence on the adhesion and the influence is proportional to the moisture amount in the sample.

6.4 Summary

In this chapter, the influence of moisture on different properties of components from rubber composite materials used in the tyre industry was investigated. The investigations were based on the results from Chapter 4. The main contribution of this chapter can be summarised as follows:

1. Based on the results from Sorption TGA measurements under different environment conditions on textile reinforcements, the rubber and the textile reinforced rubber, different mechanical tests are performed. With the contribution of the results from chapter 4, the moisture content in the cords can be predicted, so that the relation between mechanical properties and the environment conditions can be transferred to the problem between the properties and the moisture content. The amount of the necessary experiments is therefore strongly reduced.

2. The rayon cords under different environment conditions perform similar in the load-elongation test up to an elongation of 2%. Above that, the elongation of the sample with higher moisture grows more slowly than the one with lower moisture up to the elongation of 5% because of the dissociation of the intramolecular hydrogen bonds. Above this value, the curves have similar slope through to the breaking elongation. The difference of the slope indicates that the velocity of the elongation is caused by the dissociation of the intermolecular hydrogen bonds which gives the chain segments more flexibility to move. The points of breaking force are not far from each other on the same level. But the breaking elongation is proportional to the moisture content in the sample.

   Nylon cords performs different than rayon in the load- elongation test. Since the dissociation of the intermolecular hydrogen bonds is the main reason for a different performance, the sample performs similarly in the test under the elongation of 10%. From then on, the velocity of the elongation increment from the sample with higher moisture begins to drop until the end of the experiment. The sample with higher moisture content has an earlier drop point than the one with less moisture. Since the flexibility causing the segment motion under the elongation is related to the grade of dissociation. The breaking force and the breaking elongation have similar regularities as the rayon cords. The influence of moisture on dimensional stability is obvious and worth to pay attention on it.

3. In the creep tests, the influence of moisture on different cords are investigated. Nylon cords is chosen as the main target because the influence on nylon is more evident. The sample with higher moisture content creeps with lower velocity after a very

short time, since in the first stage of immediate deformation, the aspects affecting the deformation are not influenced by moisture. But, after the creep starts in the second stage, the rate of deformation starts to decrease with time. The deformation in this stage can be related to the chain segments motion which is accelerated through the dissociation of the hydrogen bonds. This dissociation is proportional to the moisture content which can be related to the environment condition with help from the result of chapter 4.

In the phase of recovery, the deformation of the sample decreases because of the instant response of the material. Since the key aspects influence the instant response are not affected by moisture, no differences are found in this stage. After the first stage, the recovery rate of the sample starts to decrease. The more moisture the sample contains, the lower is the decrement rate. The reason can also be related to the chain segments motion. The plastic deformations are calculated at the end of the experiment, and the sample with higher moisture content can get more retraction in the recovery.

4. The storage modulus of nylon cords is inversely proportional to the moisture content. It can be related to the dissociation of hydrogen bonds, which restrict the segment motion. The result shows also a dependency of the storage modulus on the frequency. According to the time–temperature equivalence principle, the segment motion at higher frequency is equivalent to the segment motion at lower temperature, where the motion of segments is restricted. Thus, the storage modulus is higher in the area of higher frequency. Besides, it can be observed that the slope of the curve with higher moisture content is higher than the other one. The reason can be backtracked to the dissociation of the hydrogen bonds, in which the hydrogen bonds between chains are replaced by new hydrogen bonds between chains and water molecules. At lower frequency, which is equivalent to higher temperature, these hydrogen bonds with water are easier to be destroyed. That may lead to the increment of the slope.

   The loss factor of the nylon sample tends to increase with increasing moisture content. The motion is affected by the dissociation of the hydrogen bonds, which is proportional to the moisture content. The possibility of segment motion is therefore higher in the sample with more moisture. That leads to a higher mechanical loss. The motion at higher frequency is decreased because the response time of the material may not be as short as the time the load is applied on it, which can lead to a decrease of segment motion. Hence, the loss factor at low frequency is higher than at high frequency.

The nylon reinforced rubber performs in analogy to the nylon cord. The storage modulus of rubber composite is proportional to the moisture content in the sample. The storage modulus of the rubber composite is resulted from the cords and the rubber matrix together. The rubber matrix shares a part of the load applied on the system, so that the load acting on the nylon cord becomes less. Rubber stays in the high-elastic state under the test frequency and there is no dependency of the storage modulus on the test frequency, therefore the curves of rubber composites are flatter.

The rubber composite material performs also in analogy to the nylon cord on loss factor, which is inversely proportional to the moisture content. The reason is the friction caused by more segment motion. The motion also influences the loss factor, so that there is a difference at low and at high frequency. The loss factor is higher at low frequency since the possibility of segment motion is higher.

5. Through the observation of the sample made of nylon cord with different conditioning time under the optical microscope, no obvious change on the surface of the resorcinol-formaldehyde-rubber latex system can be found. The influence of moisture on the RFL system can be assumed as minor.

6. The X-Ray micro-computed tomography is utilised to identify internal failures of the sample before the destructive tests such as the pull-out test and the peel test, which are classically used to determine the cord-to-rubber adhesion. From the result of the micro CT tests, no influence or presence of moisture in the sample for the pull-out test can be observed. However, the influence of the moisture is more obvious under the micro CT in the sample prepared for the peel test. The results are validated by the mechanical tests. The pull-out force of the sample conditioned before the test is nearly the same as for the dry sample. On the other hand, there is a slight difference between the adhesion value from the peel test on wet and dry samples. Due to the small amount in the sample, both tests do not show an obvious influence of moisture on adhesion. But the standard deviation tends to be smaller with higher moisture content, which can be found in both pull-out and peel tests. In the experiment with a sample humidified under critical conditions, more obvious differences can be found under the micro CT and the mechanical test. The results show that the influence of moisture on adhesion does exist and is dependent on the moisture amount.

Table 6.6: Influence of moisture on different properties of textile cords and rubberised cords

	Proportional to moisture	**Inversely proportional to moisture content**	**No influence**
Load- elongation test	Elongation under same load, breaking elongation	Load under same elongation	Breaking force, load and elongation in first stage
Creep test	Creep, recovery	Plastic deformation	Deformation and recovery in instant elastic state
Frequency sweep	Loss factor	Storage modulus, dependency on log(f),	-
Optical microscope	-	-	RFL System
Pull-out test	-	Standard deviation of pull-out force	Pull-out force
Peel test	-	Cord-to–rubber adhesion, standard deviation of adhesion	-

7 Summary and outlook

7.1 Optimization on handling and processing rubberized cord

The results of the Sorption TGA measurements which aims to get analyse the mechanism of moisture uptake behaviour of the fabric cords show that the rayon and nylon cords absorb plenty of moisture from the environment within short time. This behaviour shorts the storage time window for the fabric cords before the processing. According to the standard specification of the fabric cords, the maximum moisture content should lie below 1% at the time of processing. As it is known that rayon is more sensitive to the moisture in the air, the rayon cords are better protected from the supplier against the moisture. The protection on nylon cords is often considered as not so important as in the case of rayon, and therefore, it is not sufficient, usually consisting of only an outer package.

From the results in section 4.1, the time needed for the two kinds of fabric cords to absorb 1% moisture can be easily obtained. The rayon cord absorbs the 1% in about 300 seconds at 20 ℃, which is a very low environment condition. If the environment condition is set to be a bit more critical, e.g. 40 ℃, the time will be halved. Rayon cord needs only about 120 seconds at 40 ℃ to absorb 1% moisture from the environment, which means the time window for the application is limited to two minutes. The nylon cords perform better than rayon cords, indeed. It takes 340 seconds for nylon cords to get the 1% mass increment through moisture absorption at 40 ℃. The absorption time at 20 ℃ is 660 seconds, which is doubled than the time at 40 ℃.

From the perspective of the equilibrium, the moisture content at saturation of rayon cords at 20 ℃ and 90% relative humidity is more than 20%. Even at a very dry condition, e.g. 10% relative humidity, the rayon cord can still absorb more than 4% moisture on its own mass. For nylon cords, which are not so carefully protected before processing, the moisture content by saturation at 20 ℃ and 90% relative humidity is about 5.2%. The saturation point of nylon is below 1% only if the humidity is under 15% which is hardly to be ensured in the storage or processing, especially in summer.

As discussed in section 3.2.1, the moisture uptake behaviour of both rayon and nylon cord is a physical phenomenon which is reversible through a drying process. As shown in Figure 3.5 and Figure 3.6, the drying process has no influence on the cord. An example of such drying process is illustrated in Figure 7.1. The rayon cords are saturated at 40 ℃, 30%, 40% and 50% relative humidity, respectively. The drying process is immediately applied on the

cords after the absorption process. The storage temperature is adjusted from 40 ℃ to 60 ℃ and the humidity is set to 0%. The reason for choosing 60 ℃ is due to the restriction of the humidity sensor in the heat chamber. In the standard drying method, the temperature can be set up to 105 ℃. According to the plots, the rayon cords are dried in about 600 seconds from the equilibrium state to a moisture content below 1%. Since the rayon cords are mostly protected by methods such as using a protection film, and therefore, with a low probability of saturation, a process with similar conditions or higher temperatures for about 300 seconds might be sufficient for drying the cords before processing.

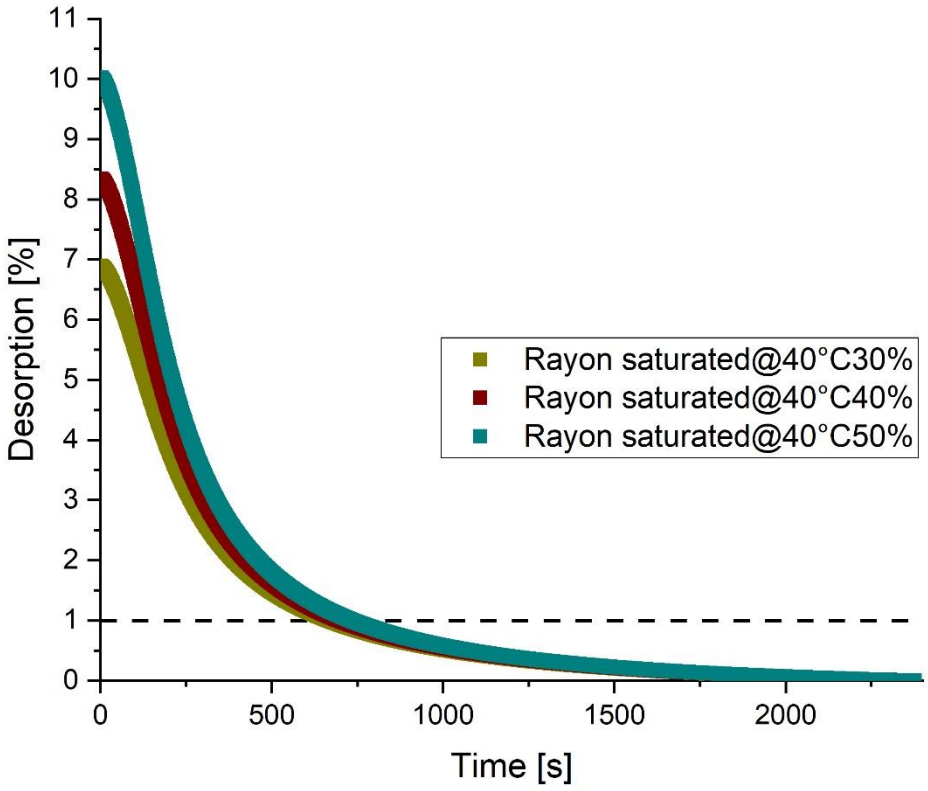

Figure 7.1: Desorption process of saturated rayon cords which were saturated under 60 ℃

The nylon cord normally stored with less protection might absorb a certain amount of additional moisture, especially under high relative humidity. A drying process can also be set up for nylon cords. However, depending on the saturation point and the diffusion coefficient *D* of nylon cords, it takes also not such a long time to dry them. According to the plot in Figure 7.2, it takes about 120 seconds to dry nylon cords from saturation to the moisture content below 1%, which can be realized in factory easily. In order to use the method of the drying process, the influence of the high temperature should be considered. Since the moisture content by equilibrium is not very high, the method using only gas to dry the cord should also be enough.

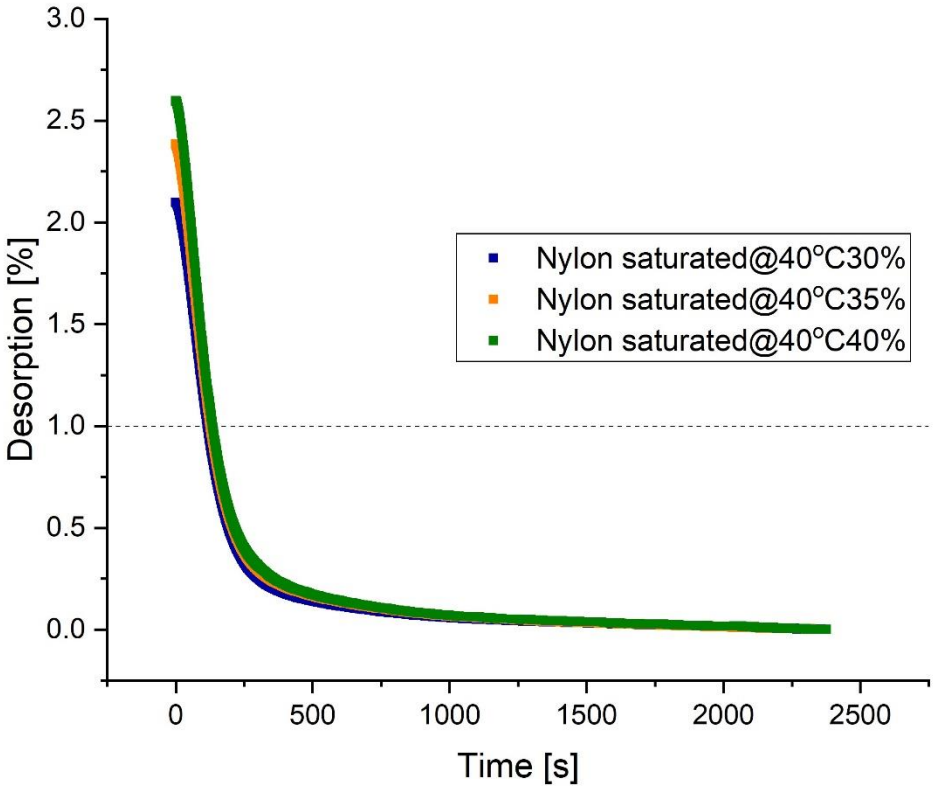

Figure 7.2: Desorption process of saturated rayon cords which were saturated under 60 °C

According to section 4.2 and 4.3, the rubber used as matrix in the composite absorbs only a small amount of moisture. Applying high temperature to dry the uncured rubber compound or uncured calendered material might cause problems such as premature crosslinking. Therefore, moisture desorption requires controlling the environment conditions in the storage area. The dry air can be used to reduce the moisture content at least on the surface of the material in question, since it consumes much energy and takes longer time to get only a limited effect.

7.2 Conclusions

Fabric cords are one of the most important components in rubber industry to supply the products with their strength. Due to their microstructure, some textile cords are sensitive to moisture. These cords absorb moisture from the environment during the process and the storage. The absorbed moisture might have impact on the properties of the cords and then the performance of the final product.

Objectives of this research is to analyse and discuss the mechanism of moisture uptake behaviour of the fabric cords, the rubbers and the rubberized textile cords, to model the moisture uptake behaviour and to determine the influence of absorbed moisture on different properties of the materials. The optimization can be suggested based on the analysis of the results achieved from different experiments and the mathematical model.

Characterisation of moisture uptake behaviour

The thermos-gravimetric analysis which is enhanced by the humidity generator was utilised to monitor the mass changes of the sample during the storage at a certain environment condition. Against the classical method, the measurement with Sorption TGA has obvious advantage on test accuracy. With this method, the moisture uptake behaviour of fabric cords, the rubber which is typically used as matrix in the composite and the rubberized textile cords were investigated systematically.

The result of Sorption TGA measurement reveals that all the three types of cords: rayon, nylon and polyester, have similar performance on moisture uptake behaviour. All of the cords absorb moisture with a high, linear velocity at the beginning of the experiments. The second stage begins after a certain time related to the environment condition, in which the cords absorb further moisture with a decreasing velocity until they reach the steady state. The time point at which the cord leaves the linear stage in depending on the temperature and relative humidity. The sample at same temperature but lower relative humidity leaves the first stage earlier with its absorption speed starts to decrease.

The moisture amount which is often described using the moisture content at the saturation state is related to the relative humidity under the specific temperature. The fabric cords can absorb more moisture at higher relative humidity under same temperature and has a higher moisture content at the equilibrium. The rayon cord has a mass increment of about 20% after the experiment at 20 °C and 90% relative humidity. The value after the experiment with same storage time at 20 °C and 30% relative humidity is only about 6.8%. The values of nylon cord under same environment conditions are 5.4% and 1.6%, for polyester cord 1% and 0.26%, respectively. The velocity of the moisture absorption depends on the

temperature under same relative humidity. The time needed from samples under higher temperature to reach the equilibrium state is shorter than the sample under lower temperature.

The other one of the most important aspect which influents the moisture uptake behaviour especially the absorbed moisture amount is the chemical structure. Rayon cord can absorb obviously more moisture than the other cords due to the chemical structure of cellulose from which rayon is made. Sample example can be made using the data above: Rayon absorbs about 20% at 20 °C and 90% relative humidity, at the same time only 5% for nylon because of the hydroxyl groups of polyamides. Polyester can absorb only 1% moisture until its saturation under the same environment condition and therefore is recognised as not moisture sensitive compared with rayon and nylon cord.

Sorption TGA measurements with similar settings but a longer experiment time were performed to investigate the moisture behaviour of rubber which is used as matrix. The results show similar trends and distribution under different environment conditions as by textile cords. The rubber compound is a complicate system which consists of many ingredients. To determine the influence of the ingredients, different recipes were used to process the rubber compounds and vulcanizates. Results show that the moisture uptake behaviour of sample with different type of carbon black does not vary. The carbon black amount has influence because with lower carbon black content, the amount of other hydrophilic ingredients will be increased so that the total absorbed moisture is higher than rubber with higher filler content. Resorcinol and HMMM resin have also influence on the moisture uptake behaviour because of their hydroxyl groups. Since they are only used as enhancement on cord-to-rubber adhesion, with the tinny absolute amount the influence of them is limited.

The rubberized textile cords were also tested with Sorption TGA. The sample was prepared from calendered material consisting of rubber matrix and textile reinforcements. The performance of Sorption TGA experiments are similar to the single components. The rubber matrix affects the moisture absorption by slowing down the process compared to the pure textile cords. This effect results in the failure of most samples to reach their saturation state within the 5 days experiment time. The influence of the open ends of the textile materials were also investigated. Through comparison of the results from measurement with opened and closed ends, the moisture amount absorbed from the open ends is calculated. For sample which has a limited length, the influence of open ends is obvious.

The textile cords, especially the moisture sensitive types, can absorb much moisture from the environment within very short time compared with their whole storage time before processing. The rubber matrix is not as sensitive as the textile cords but the effect of some ingredients during the processing should not be ignored. With the “protection effect” of

rubber matrix, the velocity of moisture absorption from rubberise cords are dramatically decreased. But the influence of the open ends needs to be considered.

Modelling of moisture uptake behaviour

Based on the results of Sorption TGA measurements, mathematical modelling was performed to predict the moisture uptake behaviour of textile cords and the rubberized cords. The model of Fick's law is considered as most suitable for solving the moisture absorption problem. According to the observation under optical microscope, the cross section of the fabric cords can be regarded as round. That means the shape of fabric cords can be assumed as cylindrical with a diameter which is much smaller than the length. Thus, the moisture absorption can be considered as one dimensional.

The diffusion coefficient *D* is to be estimated by using the model- fitting method on the experimental data. The fitting process is evaluated as very good through the R-square value for the fabric cords. The relation between the diffusion coefficient, the temperature and the relative humidity can be determined by linear fitting the plot distribution of diffusion coefficient as approximated in the coordinate system with temperature or humidity. With help of the Arrhenius-relation, further diffusion coefficient *D* can be estimated. With the estimated value, the new simulation curve is plotted and used to fit the experimental data to get the simulation verified. The data produced by the simulation curve is close to the experimental by the verification which indicates the verification as successful. Same procedure was applied on nylon cords and the model can reproduce the experimental uptake curves in most of the cases. For some other conditions the model- fitting method cannot be finished because of some fluctuation during the experiment which related to the performance of the instrument.

The diffusion coefficient *D* of rubberised textile cord can be 0estimated with presence of different parameters such as the diffusion coefficient of the rubber matrix, the fibre orientation and the fibre volume fraction. The parameters can be determined with experimental methods or estimated with model- fitting method. With similar strategy as the textile cords, further model- fitting methods are applied on the diffusion coefficient of the rubber composite to get the relation between the coefficient, the relative humidity and the temperature. The diffusion coefficient D can be therefore predicted, and the prediction can be evaluated by fitting the simulation curve with the experimental. The result shows the simulation curve with the estimated parameters can reproduce the experimental data.

The result of the verification shows that the model can be used to predict the moisture uptake behaviour of textile cords and the textile reinforced rubbers, which follows a Fickian

diffusion. However, the work on modelling is still on the preliminary stage. The accuracy of the prediction needs to be enhanced.

Influence of moisture on properties

The influence of moisture on different mechanical properties can be identified as a problem to clarify the relation between environment condition and mechanical properties. With the contribution of the Sorption TGA results this problem can be transferred to the relation between moisture content in the sample and the change on mechanical properties, since the moisture content in the sample can be determined from the Sorption TGA results or predicted with the mathematical model. Thus, the amount of measurements is strongly reduced.

In the load- elongation test, rayon cords with different moisture content have similar performance under the elongation of 2%. The elongation of the sample with higher moisture content increases slower than the drier samples from 2% to 5%, which is caused by the dissociation of the intramolecular hydrogen bonds. The curves have then similar slope through to the breaking elongation. In this stage, the velocity of the elongation is caused by the dissociation of the intermolecular hydrogen bonds which gives the chain segments more flexibility to move. The breaking forces of all the sample are similar but the breaking elongation is proportional to the sample moisture content.

The nylon cords perform different than rayon in the load- elongation test. The sample with different moisture content performs similar until the elongation reaches 10%. From then on, the velocity of the elongation increment from the sample with higher moisture begins to drop until the end of the experiment, the higher the moisture content the earlier the velocity starts dropping. The main reason for the drop is the segment motion caused by dissociation of the intermolecular hydrogen bonds, and this segment motion under the elongation is related to the grade of dissociation. The influence of moisture on breaking force and breaking elongation is similar as by rayon cords. The impact on the dimensional stability of the textile cords is very obvious.

Nylon was chosen as the investigation target after the first executing of the creep test since the influences are more obvious. In the first stage of immediate deformation, the aspects which may affect the deformation are not influenced by moisture. In the second stage where the creep happens, the rate of deformation starts to decrease with time. The deformation of sample in this stage is caused by viscoelastic response which is related to the chain segment motion. The dissociation grade of hydrogen bonds which influents the motion is proportional to the moisture content in the sample. Thus, the nylon cord with higher moisture content has larger creep in this stage. In the first phase of the recovery stage, the

instance deformation doesn't differ since the key aspects which may impact the response are not affected from moisture. The sample with more moisture amount has a smaller decrement on recovery velocity than the dryer sample, means the sample with higher moisture content has a higher recovery. This can be related also to the segment motion, which is easier for the sample with higher moisture content. Thus, the sample with higher moisture content has also a lower plastic deformation.

The storage modulus of nylon cords is inversely proportional to the moisture content. The dissociation of hydrogen bonds is responsible for the drop of the storage modulus. The result shows also a dependency from the storage modulus on the frequency which can be explained with the time–temperature equivalence principle. The chain segments at higher frequency are equivalent to the segments under lower temperature, where their mobility is restricted. Thus, the storage modulus is higher in the area of high frequency. Besides, it can be observed that the slope of the curve with higher moisture content is slightly higher than the other. The hydrogen bonds between chains are replaced by new hydrogen bonds between chain and water molecule. At lower frequency which is equivalent to higher temperature these hydrogen bonds with water are easier to be destroyed. That may lead the increment of the slope.

The loss factor of the nylon cord tends to increase with increasing moisture content. The mechanical loss is caused by segment motion, which is more probably in the sample with higher dissociation grade of hydrogen bonds. The grade of dissociation is proportional to the moisture content. Thus, the cord with higher moisture content has also higher loss factor. The segment motion decreases with frequency since at higher frequency, the segment tends to have more difficulty to be able to response the load applied on it. Less mobility of the segment leads to decreasing of loss factor.

The nylon reinforced rubber performs analogy to the nylon cord because of the skeleton effect of the cord. The curve of rubberised nylon cord is flatter compared to the nylon cord, since the rubber matrix shared a part of the strain and the rubber stays in high-elastic state under the test frequency so there is no dependency of the storage modulus on the frequency. The loss factor of rubber composite material is inversely proportional to the moisture content. The material with more moisture has more flexibility on segment motion which brings more frictions between segment and leads to higher energy dissipated to heat. The loss factor of rubber composite has dependency on the change of frequency, especially in the area of low frequency. This phenomenon is more obvious by the sample saturated under relative lower humidity whose chain segments can better respond to the load applied at lower frequency. More segment motion leads to more mechanical loss. If the dissociation grade is high enough, so that the chain segments can give response to the load at high

frequency. The difference of loss factor will be reduced. Thus, the curve of rubber composite with more moisture is more even.

According to the results of DMA test, the influence of moisture on cord-to–rubber adhesion has been assumed. Through the observation under the optic microscope on the sample made of nylon cord with different conditioning time no obvious change on the surface of the resorcinol-formaldehyde-rubber latex system can be found. The influence of moisture can be assumed as minor on the RFL system.

The classical method to determine the adhesion between rubber matrix and the cord is the pull-out test and the peel test. The micro computed tomography was applied to identify the internal failure of the sample before the destructive test. On the sample for pull-out test there is no obvious failure to be found. However, the influence of moisture can be observed on the sample for peel test. Both results are validated through the mechanical tests. The result of pull-out test on conditioned sample and the dry sample show no obvious difference. On the other hand, the difference between adhesion of the wet and dry samples from peel test is only slight. Since the moisture amount in the sample is limited because of the sample preparation, both tests do not show obvious influence of moisture on the adhesion. The results from the experiment with sample which is humidified under critical condition show that the influence of moisture on adhesion do exists and is depended on the moisture amount.

7.3 Outlook

While the moisture uptake behaviour of fabric cords, the rubber matrix materials and the rubberised textile cords are systematically investigated, there are still some noteworthy aspects for the future work.

Characterisation of moisture uptake behaviour

The investigation on moisture uptake behaviour of fabric cords recovered most of the environment conditions which the instrument allows. Because of the high probability of condensation under high temperature, the experiments were done mostly under 40 °C or only low relative humidity at 40 °C. The upper limit of the experimental setting is 40 °C and 50% relative humidity. Some of the critical conditions might appear during the processing such as 40 °C and 80% cannot be reached. These critical conditions should be precisely the key point of the research. It is therefore necessary to be able to extend the research to more critical conditions. The classical methods can be considered if the limitation of the instrument cannot be avoided.

The studies on rubber matrix and rubberised cords are not as comprehensive as on the textile cords. The Sorption TGA measurements consumes much time and energy to be performed because of the longer extended experiment time. Thus, many potential interesting aspects are not analysed. One of the most importance ingredients of rubber matrix is silica filler which is known as moisture sensitive. The research in this thesis shows already that the carbon black has no influence on moisture uptake behaviour of rubber matrix. The investigation on rubber matrix needs the study on silica filler to be full systematically.

More experimental data on different environment conditions is indispensable for improving the accuracy of the simulation. To perform Sorption TGA measurement under further conditions may supply the mathematical model with more possibilities of verification. Further research on multi-layer structure might also be interesting for serial production in a factory.

Besides, the accuracy of the mathematical model could be improved. More contribution factors to the moisture uptake such as capillary effect, which might account for initial moisture uptake, can be considered.

The range of investigation on the influence of moisture on different properties of the materials is very wide. The studies in this thesis is only at a preliminary stage. The influence of moisture on rubber has been assumed to be minor because of the small moisture amount absorbed from rubber in the Sorption TGA test. Some detailed measurements on rubber as

verification would be probably interesting. Furthermore, nylon cords were chosen as the investigation target in most of experiments. For a more comprehensive research, rayon and polyester cords should also be studied.

Cord-to-rubber adhesion was an important target of this thesis, the moisture is considered to strongly impact the adhesion in both rubber matrix and textile cords. The pull-out test and peel test show different results in terms of adhesion behaviour. The absorbed moisture was easily released from the sample during the vulcanisation process under high temperature and pressure because of the small size of the sample. The rubberised cord is closed by tire building before the tire vulcanisation so that not all the moisture can be released from the cord. Thus, it is still reasonable to do future investigations on the influence of moisture on cord-to-rubber adhesion with new methods which might retain the moisture in the sample.

References

[1] A. Ciesielski, An introduction to rubber technology. iSmithers Rapra Publishing, 1999.

[2] W. Davis, One river: Explorations and discoveries in the Amazon rain forest. Random House, 2014.

[3] M. Morton, Rubber technology. Springer Science & Business Media, 2013.

[4] L. R. G. Treloar, The physics of rubber elasticity. Oxford University Press, USA, 1975.

[5] A. N. Gent, Engineering with rubber: how to design rubber components. Carl Hanser Verlag GmbH Co KG, 2012.

[6] B. Weinstein, The Amazon rubber boom, 1850-1920. Stanford University Press, 1983.

[7] C. Goodyear, "US Patent# 3,633," June, vol. 15, p. 1844, 1844.

[8] P. J. Flory, Principles of polymer chemistry. Cornell University Press, 1953.

[9] J. E. Mark, B. Erman, and M. Roland, The science and technology of rubber. Academic press, 2013.

[10] J. Busfield, C. Deeprasertkul, and A. Thomas, "The effect of liquids on the dynamic properties of carbon black filled natural rubber as a function of pre-strain," Polymer, vol. 41, no. 26, pp. 9219-9225, 2000.

[11] C. Nah, J. Y. Lim, B. H. Cho, C. K. Hong, and A. N. Gent, "Reinforcing rubber with carbon nanotubes," Journal of applied polymer science, vol. 118, no. 3, pp. 1574-1581, 2010.

[12] K. Tsunoda, J. Busfield, C. Davies, and A. Thomas, "Effect of materials variables on the tear behaviour of a non-crystallising elastomer," Journal of Materials Science, vol. 35, no. 20, pp. 5187-5198, 2000.

[13] G. R. Hamed, "Reinforcement of rubber," Rubber chemistry and technology, vol. 73, no. 3, pp. 524-533, 2000.

[14] D. Edwards, "Polymer-filler interactions in rubber reinforcement," Journal of Materials Science, vol. 25, no. 10, pp. 4175-4185, 1990.

[15] J. Fröhlich, W. Niedermeier, and H.-D. Luginsland, "The effect of filler–filler and filler–elastomer interaction on rubber reinforcement," Composites Part A: Applied Science and Manufacturing, vol. 36, no. 4, pp. 449-460, 2005.

[16] C. R. D. GmbH. "Tire production." https://www.continental-tires.com/car/tire-knowledge/tire-basics/tire-production (accessed 2020).

[17] J. Tully, The devil's milk: A social history of rubber. NYU Press, 2011.

[18] J. D. Walter, "Cord—Rubber Tire Composites: Theory and Applications," Rubber Chemistry and Technology, vol. 51, no. 3, pp. 524-576, 1978.

[19] F. J. Kovac, "Tire technology," 1973.

[20] L. Job and R. Joseph, "Studies on rubber-to-nylon tire cord bonding," Journal of applied polymer science, vol. 71, no. 7, pp. 1197-1202, 1999.

[21] G. V. Research, "Tire Cord Fabrics Market Size, Share & Trends Analysis Report By Material (Nylon, Polyester), By Tire Type, By Vehicle Type (Passenger Car, Commercial Vehicles), By Application, By Region, And Segment Forecasts, 2020 - 2027," GVR-4-68038-596-0, 2020.

[22] J. B. Maginnis, "The Effect of Moisture on Twisted Yarns," Textile research journal, vol. 20, no. 3, pp. 165-171, 1950.

[23] D. Ashpole, "The moisture relations of textile fibres at high humidities," Proceedings of the Royal Society of London. Series A. Mathematical and Physical Sciences, vol. 212, no. 1108, pp. 112-123, 1952.
[24] A. K. Naskar, A. Mukherjee, and R. Mukhopadhyay, "Studies on tyre cords: degradation of polyester due to fatigue," Polymer Degradation and Stability, vol. 83, no. 1, pp. 173-180, 2004.
[25] A. Aytaç, M. Şen, V. Deniz, and O. Güven, "Effect of gamma irradiation on the properties of tyre cords," Nuclear Instruments and Methods in Physics Research Section B: Beam Interactions with Materials and Atoms, vol. 265, no. 1, pp. 271-275, 2007.
[26] J. Giridhar, Kishore, and R. Rao, "Moisture absorption characteristics of natural fibre composites," Journal of reinforced plastics and composites, vol. 5, no. 2, pp. 141-150, 1986.
[27] J. Montalvo, T. Von Hoven, and M. S. Cintron, "Evaluation of Karl Fischer titration vial closure integrity for extended storage of cotton test specimens," AATCC Journal of Research, vol. 5, no. 1, pp. 7-20, 2018.
[28] C. Chow, X. Xing, and R. Li, "Moisture absorption studies of sisal fibre reinforced polypropylene composites," Composites science and technology, vol. 67, no. 2, pp. 306-313, 2007.
[29] M. Tajvidi and G. Ebrahimi, "Water uptake and mechanical characteristics of natural filler–polypropylene composites," Journal of Applied Polymer Science, vol. 88, no. 4, pp. 941-946, 2003.
[30] Continental Reifen Deutschland GmbH. "Materials used in a tyre." http://blobs.continental-tires.com/www8/servlet/blob/606132/d2e4d4663a7c79ca81011ab47715e911/download-tire-basics-data.pdf (accessed.
[31] Continental Reifen Deutschland GmbH. "Tire mixture." https://www.continental-tires.com/car/tire-knowledge/tire-basics/tire-mixture (accessed 2020).
[32] E. McDonel, "Tire cord and cord-to-rubber bonding," The pneumatic tire, p. 80, 2006.
[33] Continental Reifen Deutschland GmbH. "Tire components." https://www.continental-tires.com/car/tire-knowledge/tire-basics/tire-components (accessed 2020).
[34] T. Gries, D. Veit, and B. Wulfhorst, Textile Fertigungsverfahren: Eine Einführung. Carl Hanser Verlag GmbH Co KG, 2018.
[35] G. B. Kauffman, "Rayon: the first semi-synthetic fiber product," Journal of chemical education, vol. 70, no. 11, p. 887, 1993.
[36] T. Takeyama and J. Matsui, "Recent developments with tire cords and cord-to-rubber bonding," Rubber Chemistry and Technology, vol. 42, no. 1, pp. 159-256, 1969.
[37] S.-m. Choi and C. Kim, "Radial tire for automobile," ed: Google Patents, 2004.
[38] J.-F. Fritsch, P. Rugraff, and J. A. Funderburk, "Hybrid cabled cord and a method to make it," ed: Google Patents, 2003.
[39] R. Adams, "Wallace Hume Carothers," National Academy of Sciences, Biographical memoirs, vol. 20, pp. 293-309, 1939.
[40] G. B. Kauffman, "Wallace Hume Carothers and nylon, the first completely synthetic fiber," Journal of Chemical Education, vol. 65, no. 9, p. 803, 1988.
[41] H. P. Kiran Pulidindi, "Tire Cord And Tire Fabrics Market Size By Product , By Vehicle Type , Industry Analysis Report, Regional Outlook, Application

Growth Potential, Price Trends, Competitive Market Share & Forecast, 2019 – 2026," 2019. [Online]. Available: https://www.gminsights.com/industry-analysis/tire-cord-and-tire-fabrics-market?utm_source=GoogleAds&utm_medium=Adwords&utm_campaign=Polymer-PPC&gclid=Cj0KCQjwnqH7BRDdARIsACTSAdvXo67sKAaTsD3VajvjOpAO32wYJtpTb1_p-Qvp2UB_0WOv1j8t6swaAqEZEALw_wcB

[42] B. P. Federation, . "Nylons (Polyamide)." https://www.bpf.co.uk/plastipedia/polymers/polyamides.aspx (accessed 2020).

[43] W. J. Rex and D. J. Tennant, "Improvements rela· ting to the Manufacture of Highly Polymeric Substances," ed.

[44] L. N. Ji, "Study on preparation process and properties of polyethylene terephthalate (PET)," in Applied Mechanics and Materials, 2013, vol. 312: Trans Tech Publ, pp. 406-410.

[45] J. S. Amneus, "Weaving polyester fiber fabrics," ed: Google Patents, 1969.

[46] J. Rath, T. Chaki, and D. Khastgir, "Effect of thermal treatment on structure and properties of polyester tire cords," Journal of applied polymer science, vol. 124, no. 1, pp. 266-274, 2012.

[47] T. Solomon, "Systems for tire cord-rubber adhesion," Rubber chemistry and technology, vol. 58, no. 3, pp. 561-576, 1985.

[48] H. Watanabe, S. Makino, and T. Kuroda, "Process for producing an adhesive-treated polyester fiber cord," ed: Google Patents, 2003.

[49] www.lexico.com "moisture." https://www.lexico.com/definition/moisture (accessed 2020).

[50] J. M. Wallace and P. V. Hobbs, Atmospheric science: an introductory survey. Elsevier, 2006.

[51] S. S. Wyer, A Treatise on Producer-gas and Gas-producers. Engineering and mining journal, 1907.

[52] T. I. S. o. t. G. I. Association. " "Climate/humidity table"." https://www.tis-gdv.de/tis_e/misc/klima.htm/ (accessed 2020).

[53] E.Britannica."Climate- Humidity indexes." https://www.britannica.com/science/climate-meteorology/Humidity-indexes (accessed 2020).

[54] G. Crini and P.-M. Badot, Sorption processes and pollution: Conventional and non-conventional sorbents for pollutant removal from wastemasters. Presses Univ. Franche-Comté, 2011.

[55] H. Kayser, "Ueber die Verdichtung von Gasen an Oberflächen in ihrer Abhängigkeit von Druck und Temperatur," Annalen der Physik, vol. 250, no. 11, pp. 450-468, 1881.

[56] T.B.a.L.R.T.S.Center, . "“Glossary”." http://www.brownfieldstsc.org/glossary.cfm?q=1 (accessed 2020).

[57] L. Ferrari, J. Kaufmann, F. Winnefeld, and J. Plank, "Interaction of cement model systems with superplasticizers investigated by atomic force microscopy, zeta potential, and adsorption measurements," Journal of colloid and interface science, vol. 347, no. 1, pp. 15-24, 2010.

[58] M. W. Dictionary/Thesaurus, . ""absorption (chemistry)"." https://web.archive.org/web/20181005080455/http://www.memidex.com/absorption+chemistry (accessed 2020).

[59] J. McMurry and E. Simanek, "Fundamentals of organic chemistry," Thomson Brooks/Cole, California, 2003.
[60] P. W. Atkins, Julio De Paula, and James Keeler., Atkins' Physical chemistry. Oxford, United Kingdom ; New York, NY : Oxford University Press, , 2018.
[61] J. McMurry, , A. McDonald., Ed. Fundamentals of Organic Chemistry (Fifth ed.). 2003.
[62] C. T. Lewis and C. Short, "A Latin dictionary: founded on Andrew's ed. of Freund's Latin dictionary," 1966.
[63] J. Crank, The mathematics of diffusion. Oxford university press, 1979.
[64] P. Shewmon, Diffusion in solids. Springer, 2016.
[65] J. Philibert, "One and a half century of diffusion: Fick, Einstein before and beyond," 2006.
[66] E. J. Kontturi, "Surface chemistry of cellulose," Espoo, Finland, p. 145, 2005.
[67] E. L. Lindh, "Cellulose-water interaction: a spectroscopic study," KTH Royal Institute of Technology, 2016.
[68] J. Credou and T. Berthelot, "Cellulose: from biocompatible to bioactive material," Journal of Materials Chemistry B, vol. 2, no. 30, pp. 4767-4788, 2014.
[69] D. Klemm, B. Heublein, H. P. Fink, and A. Bohn, "Cellulose: fascinating biopolymer and sustainable raw material," Angewandte chemie international edition, vol. 44, no. 22, pp. 3358-3393, 2005.
[70] W. Wennekes, R. Datta, J. W. Noordermeer, and F. Elkink, "Fiber adhesion to rubber compounds," Rubber chemistry and technology, vol. 81, no. 3, pp. 523-540, 2008.
[71] M. Jawaid, S. M. Sapuan, and O. Y. Alothman, Green Biocomposites: Manufacturing and Properties. Springer, 2016.
[72] S.-S. Choi and O.-B. Kim, "Influence of rubber and fabric cord on deformation of a fabric cord-inserted rubber composite by thermal aging," Journal of Industrial and Engineering Chemistry, vol. 19, no. 2, pp. 650-654, 2013.
[73] J. Karlsson, M. Andersson, P. Berntsson, T. Chihani, and P. Gatenholm, "Swelling behavior of stimuli-responsive cellulose fibers," Polymer, vol. 39, no. 16, pp. 3589-3595, 1998.
[74] L. Pupure, N. Doroudgarian, and R. Joffe, "Moisture uptake and resulting mechanical response of biobased composites. I. constituents," Polymer composites, vol. 35, no. 6, pp. 1150-1159, 2014.
[75] E. Cotterill, "Relative Humidity and Rayon," Journal of the Textile Institute Proceedings, vol. 41, no. 1, pp. P9-P15, 1950.
[76] W. Camacho, A. Vallés-Lluch, A. Ribes-Greus, and S. Karlsson, "Determination of moisture content in nylon 6, 6 by near-infrared spectroscopy and chemometrics," Journal of applied polymer science, vol. 87, no. 13, pp. 2165-2170, 2003.
[77] I. San Diego Plastics. "Nylon." http://www.sdplastics.com/nylon.html (accessed 2020).
[78] P. Ghosh, Polymer science and technology. Tata McGraw-Hill Education, 1990.
[79] M. Arroyo and O. Olabisi, "Handbook of thermoplastics," ed: Ed. Marcel Dekker, New York, 1997.
[80] C. P. Kuda-Malwathumullage and G. W. Small, "Determination of moisture content of polyamide 66 directly from combination region near-infrared spectra," Journal of Applied Polymer Science, vol. 131, no. 16, 2014.

[81] P. Bruttel and R. Schlink, "Water determination by Karl Fischer titration," Metrohm monograph, vol. 8, no. 026, p. 50003, 2003.
[82] G. Lachenal, "Dispersive and Fourier transform near-infrared spectroscopy of polymeric materials," Vibrational Spectroscopy, vol. 9, no. 1, pp. 93-100, 1995.
[83] P. Kenins, "Influence of fiber type and moisture on measured fabric-to-skin friction," Textile Research Journal, vol. 64, no. 12, pp. 722-728, 1994.
[84] D. Negru, I. DULGHERIU, L. BUHU, A. BUHU, and E. LOGHIN, "Absorption and moisture transfer through knitted fabrics made of natural and man-made fibers," Comparative analysis of siro yarn properties spun on ring and pneumatic compact spinning systems, p. 268, 2017.
[85] K. Kohata, M. Miyagawa, A. Takaoka, and H. Kawai, "FUNDAMENTAL STUDIES ON THE INTERACTION BETWEEN MOISTURE AND TEXTILES," Sen'i Gakkaishi, vol. 42, no. 3, pp. T136-T154, 1986.
[86] R. Waller, K. Bass, and W. Roseveare, "Degradation of rayon tire yarn at elevated temperatures," Industrial & Engineering Chemistry, vol. 40, no. 1, pp. 138-143, 1948.
[87] J. Dillon and I. Prettyman, "The Effects of Temperature and Humidity on the Physical Properties of Tire Cords," Journal of Applied Physics, vol. 16, no. 3, pp. 159-172, 1945.
[88] E. Honold and H. Wakeham, "Hysteresis, Elastic Modulus, and Growth of Tire Cords under Comparable Loads," Industrial & Engineering Chemistry, vol. 40, no. 1, pp. 131-134, 1948.
[89] P. Willett, "Viscoelastic properties of tire cords," Journal of Applied Polymer Science, vol. 19, no. 7, pp. 2005-2014, 1975.
[90] S. RAMEZANI, "Effect of moisture on mechanical properties and adhesion strength of nylon 6 and 66 cords/RFL/rubber systems," 2010.
[91] W. Claxton, M. Forster, J. Robertson, and G. Thurman, "Correlation of Nylon Tirecord Properties with Tire Flatspotting," Textile Research Journal, vol. 36, no. 10, pp. 903-914, 1966.
[92] E. Gardner, "The Effect of Moisture On Some Textile-Rubber Composites," Journal of Coated Fibrous Materials, vol. 2, no. 1, pp. 24-35, 1972.
[93] Z. Li, J. Wan, L. Zhang, J. Cui, and S. Zhao, "Effects of heat and moisture on characteristics, tensile properties of RFL-coated rayon cords, and their adhesion with NR/SBR matrix," Journal of Applied Polymer Science, vol. 134, no. 48, p. 45559, 2017.
[94] B. Standard and B. ISO, "Plastics-determination of water absorption," British Standard, United Kingdom, 1999.
[95] D. ASTM, "570-98. Standard test method for water absorption of plastics," ASTM International, 1998.
[96] P. Neogi, Diffusion in polymers. CRC Press, 1996.
[97] C.-H. Shen and G. S. Springer, "Moisture absorption and desorption of composite materials," Journal of composite materials, vol. 10, no. 1, pp. 2-20, 1976.
[98] Y. Wan, H. Luo, F. He, H. Liang, Y. Huang, and X. Li, "Mechanical, moisture absorption, and biodegradation behaviours of bacterial cellulose fibre-reinforced starch biocomposites," Composites Science and Technology, vol. 69, no. 7-8, pp. 1212-1217, 2009.
[99] W. Loh, A. Crocombe, M. A. Wahab, and I. Ashcroft, "Modelling anomalous moisture uptake, swelling and thermal characteristics of a rubber toughened

epoxy adhesive," International journal of adhesion and adhesives, vol. 25, no. 1, pp. 1-12, 2005.
[100] H. G. Carter and K. G. Kibler, "Langmuir-type model for anomalous moisture diffusion in composite resins," Journal of Composite Materials, vol. 12, no. 2, pp. 118-131, 1978.
[101] A. Célino, S. Fréour, F. Jacquemin, and P. Casari, "Characterization and modeling of the moisture diffusion behavior of natural fibers," Journal of Applied Polymer Science, vol. 130, no. 1, pp. 297-306, 2013.
[102] A. Espert, F. Vilaplana, and S. Karlsson, "Comparison of water absorption in natural cellulosic fibres from wood and one-year crops in polypropylene composites and its influence on their mechanical properties," Composites Part A: Applied science and manufacturing, vol. 35, no. 11, pp. 1267-1276, 2004.
[103] V. Sinija and H. Mishra, "FTNIR spectroscopic method for determination of moisture content in green tea granules," Food and Bioprocess Technology, vol. 4, no. 1, pp. 136-141, 2011.
[104] ProUmid. "MHG32 – Controlled Humidity." https://proumid.com/en/humidity-generator/controlled-humidity-mhg32/ (accessed 2020).
[105] Mettler-Toledo. "Simultaneous Thermal Analysis (TGA/DSC)." https://www.mt.com/de/en/home/products/Laboratory_Analytics_Browse/TA_Family_Browse/TGA_DSC.html#overviewpl (accessed 2020).
[106] M. S. Corporation, "Serie 370 product information," ed, 2008.
[107] "ASTM D885 / D885M-10a(2014), Standard Test Methods for Tire Cords, Tire Cord Fabrics, and Industrial Filament Yarns Made from Manufactured Organic-Base Fibers, ASTM International, West Conshohocken, PA, 2014, www.astm.org," ed.
[108] DIN 53815, Testing of textiles; definitions for the simple tensile test, 1989.
[109] DIN 51220, Materials testing machines - Generals for requirements and for verification and calibration of materials testing machines, 2003.
[110] T. Instruments. "Q800 DMA." https://www.tainstruments.com/q800-dma/ (accessed 2020).
[111] Keyence, "Superior analysis through clearer observation, VHX digital microscope," ed, 2017.
[112] P. X.-R. GmbH. "CT- Compact." https://www.procon-x-ray.de/ct-micro-2-2-2/ (accessed 2020).
[113] N. S. S.L. "Radiography & Micro-CT." http://www.novadep.com/radiography-micro-ct/ (accessed 2020).
[114] ZwickRoell. "ProLine for Standardized Tests." https://www.zwickroell.com/en/universal-testing-machines/proline (accessed 2020).
[115] "ASTM D1871-04(2014), Standard Test Method for Adhesion Between Tire Bead Wire and Rubber, ASTM International, West Conshohocken, PA, 2014, www.astm.org," ed.
[116] ASTM D2229-10(2014), Standard Test Method for Adhesion Between Steel Tire Cords and Rubber, ASTM International, West Conshohocken, PA, 2014, www.astm.org.
[117] DIN 53530:1981-02,Testing of organic materials; Separation test on fabric plies bonded together, D. I. f. Normung, 1981.
[118] DIN ISO 6133, Rubber and plastics - Analysis of multi-peak traces obtained in determinations of tear strength and adhesion strength (ISO 6133:2015), 2017.

[119] ISO 36， Rubber, vulcanized or thermoplastic — Determination of adhesion to textile fabrics, 2020.
[120] L. C. Silva, "Iso-moisture: a new concept to predict moisture content in rayon cords and its influence on tire performance," Master of science, FEUP, 2020.
[121] J. M. Oliveira, "Characterization of Tire Reinforcement Polymers focusing on Temperature, Linear Density and Hydrophilicity," Master, 2020.
[122] A. Eggers, Doctor, TU Clausthal, 2020.
[123] J. Zhang, J. Ru, H. Chen, D. Li, and J. Lu, "Viscoelastic creep and relaxation of dielectric elastomers characterized by a Kelvin-Voigt-Maxwell model," Applied Physics Letters, vol. 110, no. 4, p. 044104, 2017.